Role of Human T Cells in Experimental Hypertension and Hypertensive Kidney Damage

Inaugural dissertation

for the attainment of the title of doctor
in the Faculty of Mathematics and Natural Sciences

at the Heinrich Heine University Düsseldorf

presented by

Masudur Rahman

from Dhaka (Bangladesh)

Düsseldorf, May 2023

from the Department of Nephrology, University Hospital of Düsseldorf

at the Heinrich Heine University Düsseldorf

Published by permission of the

Faculty of Mathematics and Natural Sciences at

Heinrich Heine University Düsseldorf

Supervisor: Professor Dr. Johannes Stegbauer

Co-supervisor: Professor Dr. Eckhard Lammert

Date of the oral examination: 22/08/2023

To My Parents

Motiur Rahman & Jennat Rahman

Statutory Declaration

I declare under oath that I have produced my thesis independently and without any undue assistance by third parties under consideration of the ‘Principles for the Safeguarding of Good Scientific Practice at Heinrich Heine University Düsseldorf”

Düsseldorf,

Masudur Rahman

List of Abbreviations

A.U: Arbitary unit

ACE: Angiotensin converting enzyme

Ang II: Angiotensin II

APC: Antigen presenting cell

ARNA- afferent renal nerve activity]

AT_1: Ang II type 1

BP: Blood pressure

BPM: Beats per minute

CCL5: CC-chemokine ligand 5

CCR2: C-C chemokine receptor 2

cDNA: Complementary DNA

CKD: Chronic kidney disease

COX: Cyclooxygenase

CTLs: Cytotoxic T lymphocytes

CXCL10: Interferon gamma induced protein 10

DAMPs: Danger associated molecular patterns

dNTPs: Deoxyribonucleotides

ECFV: Extracellular fluid volume

ENaC: Epithelial sodium channel

FFPE: Formalin-fixed paraffin embedded

GAPDH: Glyceraldehyde phosphate 3-dehydrogenase

GBD: Global burden of disease

gDNA: Genomic DNA

GFR: Glomerular filtration rate

HC: Healthy control

ICAM: Intracellular adhesion molecule

IFN: Interferon

IL: Interleukin

LANUV NRW: Landesamt fuer Natur-, Umwelt- und Verbraucherschutz NordrheinWestfalen

mAb: monoclonal antibody

MCP: Monocyte chemoattractant proteins

m-CSF: Macrophage colony-stimulating factor

MHC: Major histocompatibility complex

MSNA: Muscle sympathetic nerve activity

MTT: Thiazolyl Blue Tetrazolium Bromide

Na^+-H^+: Sodium proton exchanger

Na^+-$HCO3^-$: Sodium-bicarbonate co-transporter

Na^+K^+ ATPase: Sodium potassium ATPase

NaPi2: Sodium phosphate cotransporter

NE: Norepinephrine

NH3: Sodium-proton exchangers

NKCC2: Sodium potassium chloride co-transporter

NLRP 3: NOD-like receptor protein 3

NO: Nitric oxide

PAMPs: Pathogen associated molecular patterns

PBMCs: Peripheral mononuclear cells

PCR: Polymerase chain reaction

PRRs: Pattern recognition receptors

qPCR: Quantitative PCR

RAAS: Renin-angiotensin-aldosterone system

RIHP: Renal interstitial hydrostatic pressure

ROS: Reactive oxygen species

RPP: Renal perfusion pressure

SGK1: Serum and glucocorticoid regulated kinase 1

TCR: T cell receptor

TE: TRIS/EDTA

TEM: Effector memory T cells

TGF: Transforming growth factor

Th1: T helper 1

Th17: T helper 17

Th2: T helper 2

TLR: Toll like receptor

TNF: Tumour necrosis factor

Treg: Regulatory T cell

TRH: Therapy resistant hypertension.

VCAM: Vascular cell adhesion molecule

VSMCs: Vascular smooth muscle cells

β2AR: Beta 2 adrenergic receptors

Zusammenfassung

Bedeutung humaner T Zellen bei Hypertonie und hypertensivem Endorganschaden

Ziel: Entzündliche Prozesse beeinflussen die Entwicklung von Bluthochdruck und Hypertonie-assoziierten Endorganschäden. Tierversuche weisen darauf hin, dass die adaptive Immunität, insbesondere T-Zellen, zur Entwicklung von Bluthochdruck beitragen. Aufgrund der komplexen pathophysiologischen Wechselwirkungen zwischen Immunsystem, Gefäßsystem und Niere, ist der Einfluss von humaner T Zellen auf die Entwicklung von Hypertonie und hypertensivem Endorganschaden nicht vollständig erforscht.

Methoden: Um den Einfluss humaner T-Zellen bei Hypertonie zu untersuchen, transferierten wir T-Zellen von therapieresistenten Hypertoniker (TRH) und gesunden Kontrollpersonen in immundefiziente NOD.Cg-Prkdcscid H2-K1tm1Bpe H2-D1tm1Bpe Il2rgtm1Wjl/SzJ (NSG-(KbDb) ^{Null}) Mäuse, um ein humanisiertes Mausmodell zu etablieren. Hypertonie wurde durch eine chronische Infusion von Angiotensin (Ang)II (500 ng/kg/min) für 14 Tage induziert. Der Blutdruck wurde kontinuierlich radiotelemetrisch gemessen. Die Bewertung der T-Zell-Untergruppen erfolgte mittels Durchflusszytometrie, die Funktion der Nierengefäße mittels isoliert perfundierter Niere, die Gefäßfunktion mittels Drahtmyographie, die relative Abundanz der mRNA mittels qPCR und die Gefäßhypertrophie sowie die Infiltration durch Immunzellen wurden mittels Immunhistochemie bestimmt.

Ergebnis: T Zellen von TRH oder gesunden Kontrollen wurden in NSG-(KbDb) ^{Null} mäuse injeziert. Nachdem überprüft wurde, dass die T Zellen erfrolgreich angewachsen sind und proliferierten, wurde der Blutdruck zu Studienbeginn und unter chronischer AngII-Infusion gemessen. Unter basalen Bedingungen unterschied sich der systolische Blutdruck zwischen beiden Gruppen nicht (128 ± 5 vs. 133 ± 4 mmHg, n = 6). Nach Ang II Infusion, war der systolische Blutdruck bei NSG-(KbDb) ^{Null} mäusen, die T- Zellen von TRH erhielten, im Vergleich zu gesunden Kontrollen erhöht (Woche 1: 133 ± 6 vs. 162 ± 3 mmHg, n = 6, $P <$ 0,01; Woche 2: 141 ± 6 vs. 158 ± 7 mmHg, n = 5-6, $P < 0,05$). Darüber hinaus war die Carbachol induzierte endothelialabhängige renale Vasorelaxation in isoliert perfundierten Nieren von NSG-(KbDb) ^{Null} mäusen, die T Zellen von TRH erhielten (n=4), im Vergleich zu gesunden Kontrollen (n=5) signifikant abgeschwächt. Im Vergleich zu zu den NSG-(KbDb) ^{Null} mäusen, die T Zellen von TRH bekommen haben, war die die Zahl von Effektor-Memory-CD4 (CD4+CD45RA-CCR7-) und T-Helper 17-Zellen (CD4+CCR6+ CXCR3-) in Milz und Nieren, sowie die renale Expression von humanen proinflammatorischen Zytokinen, wie zum Beispiel huTNF-α (1,51 ± 0,22 vs. 1,00 ± 0,05 relative mRNA-Expression, $*P < 0,05$, n = 5–6),

signifikant höher als NSG-(KbDb) ^{Null} mäusen, die mit T-Zellen von Kontrollen bekommen haben. Um die Relavenz auf die Gefäßfunktion von humanem TNF-α zu bestimmen, haben wir huTNF-α übernacht mit murinen Aortenringen inkubiert. Dabei zeigte sich, dass die Inkubation mit huTNF-α eine signifikant reduzierte endothelabahängige Vasorelaxation auf Carbachol im Vergleich zu unbehandelten Aortenringen (maximale Relaxation: 41 ± 10 vs. 22 ± 7 %, **P*< 0,01, n=3-5) bewirkt. Als Proof of Concept, wurden NSG-(KbDb) ^{Null} Mäuse, denen T-Zellen von TRH transplantiert worden waren, mit dem TNF-α-Inhibitor Etanercept behandelt. Die TNF-α-Inhibitor Behandlung führte zu einer signifikant abgeschwächten hypertensiven systolischen Blutdruckantwort auf Ang II im Vergleich zu den unbehandelten Tieren führte (132 ± 1 vs 2 mmHg, **P*<0,01 n=6).

Zusammenfassung: Die vorliegenden Ergebnisse deuten darauf hin, dass insbesondere TNF-α als wichtiges entzündungsförderndes Zytokin, welches von humanen T-Zellen von Patienten mit TRH freigesetzt wird, die Entwicklung von Hypertonie direkt beeinflussen kann. Diese Arbeit zeigt eine mögliche pathophysiologische Relevanz von humanen T Zellen bei der Entstehung von Hypertonie auf.

1 Abstract

Role of human T cells in experimental hypertension and hypertensive kidney damage

Objective: Inflammatory processes seem to influence the development of hypertension and hypertensive endorgan damage. Animal studies suggest that adaptive immunity, in particular T cells contribute to the development and extent of hypertension. However, due to the complex pathophysiological interactions between immune response, vasculature and kidney, the impact of human T cells in the development of hypertension and hypertensive endorgan damage is still not known.

Methods: To investigate the impact of human T cells in hypertension and end organ damage, we established mice a humanized mouse model. Therefore, we transferred T cells from treatment resistant hypertensive patients (TRH) and healthy controls into immunodeficient NOD.Cg-Prkdcscid H2-K1tm1Bpe H2-D1tm1Bpe Il2rgtm1Wjl/SzJ (NSG-(KbDb) ^{null}) mice. Hypertension was induced by chronic angiotensin (Ang) II (500ng/kg/min) infusion for 14 days. Blood pressure was continuously measured by radiotelemetry. Assessment of T cell subsets performed by flow cytometry, renal vascular function by isolated perfused kidney, vascular function by wire myography, relative abundance of mRNA by qPCR and vascular hypertrophy and immune cell infiltration were determined by immunohistochemistry.

Results: T cells from TRH or healthy controls were transferred into NSG-(KbDb) ^{null} mice. After ensuring proper T cell engraftment, blood pressure was measured at baseline and under chronic AngII infusion. Systolic blood pressure did not differ at baseline between both groups (128 ± 5 vs. 133 ± 4 mmHg, n=6). However, systolic blood pressure in response to AngII was increased in NSG-(KbDb) ^{null} mice receiving PBMCs from TRH compared to healthy controls (week 1: 133 ± 6 vs. 162 ± 3 mmHg, n=6, P<0.01; week 2: 141 ± 6 vs. 158 ± 7 mmHg, n=5-6, P<0.05). Moreover, endothelial-dependant renal vasorelaxation induced by carbachol was significantly attenuated in isolated perfused kidneys of NSG-(KbDb) ^{null} mice receiving PBMCs from TRH (n=4) compared to healthy controls (n=5). In addition, proportions of effector memory CD4 (CD4+CD45RA-CCR7-) and T helper 17 cells (CD4+CCR6+ CXCR3-) in the spleens and kidneys of NSG-(KbDb) ^{null} mice engrafted with PBMCs from TRH were significantly higher compare to controls. Furthermore, renal expression of human T cell derived pro-inflammatory cytokines such as huTNF-α (1.51 ± 0.22 vs. 1.00 ± 0.05 relative mRNA expression, *P<0.05, n=5-6), huIFN-γ (1.67 ± 0.37 vs. 1.00 ± 0.13 relative mRNA expression, P=0.07, n=8-5), and huIL-17a (3.71 ± 1.69 vs. 1.00 ± 0.15 relative mRNA expression, P=0.07,

n=6-4) as well as perivascular T cell infiltration were relatively higher in NSG-(KbDb) ^{null} mice engrafted with PBMCs from TRH compared to controls. To determine whether human TNF-α deteriorates endothelial function, overnight incubation of aortic rings with human TNF-α shows significantly reduced maximal relaxing response (E_{max}) to carbachol compared with untreated aortic rings (41 ± 10 vs 22 ± 7%, **P*<0.01, n=3-5). As a proof of concept, NSG-(KbDb) ^{null} mice engrafted with PBMC from TRH were treated with TNF-α inhibitor etanercept resulting significantly blunted systolic blood pressure in response to Ang II compared to untreated mice (132 ± 1 vs. 160 ± 2 mmHg, **P*<0.01 n=6).

Conclusion: The present results suggest that TNF-α in particular, as an important proinflammatory cytokine released by human T cells from patients with TRH, may directly influence the development of hypertension. This work highlights a possible pathophysiological relevance of human T cells in the development of hypertension.

2 Introduction

Hypertension affects over one billion people all over the world and is one of the major modifiable causes of premature death (Nguyen et al., 2021). According to a report from global burden of disease (GBD) study, hypertension is one of the leading risk factors for global attributable deaths, pushing behind high plasma glucose, high LDL cholesterol alcohol and malnutrition (Fig-1) (GBD et al., 2020).

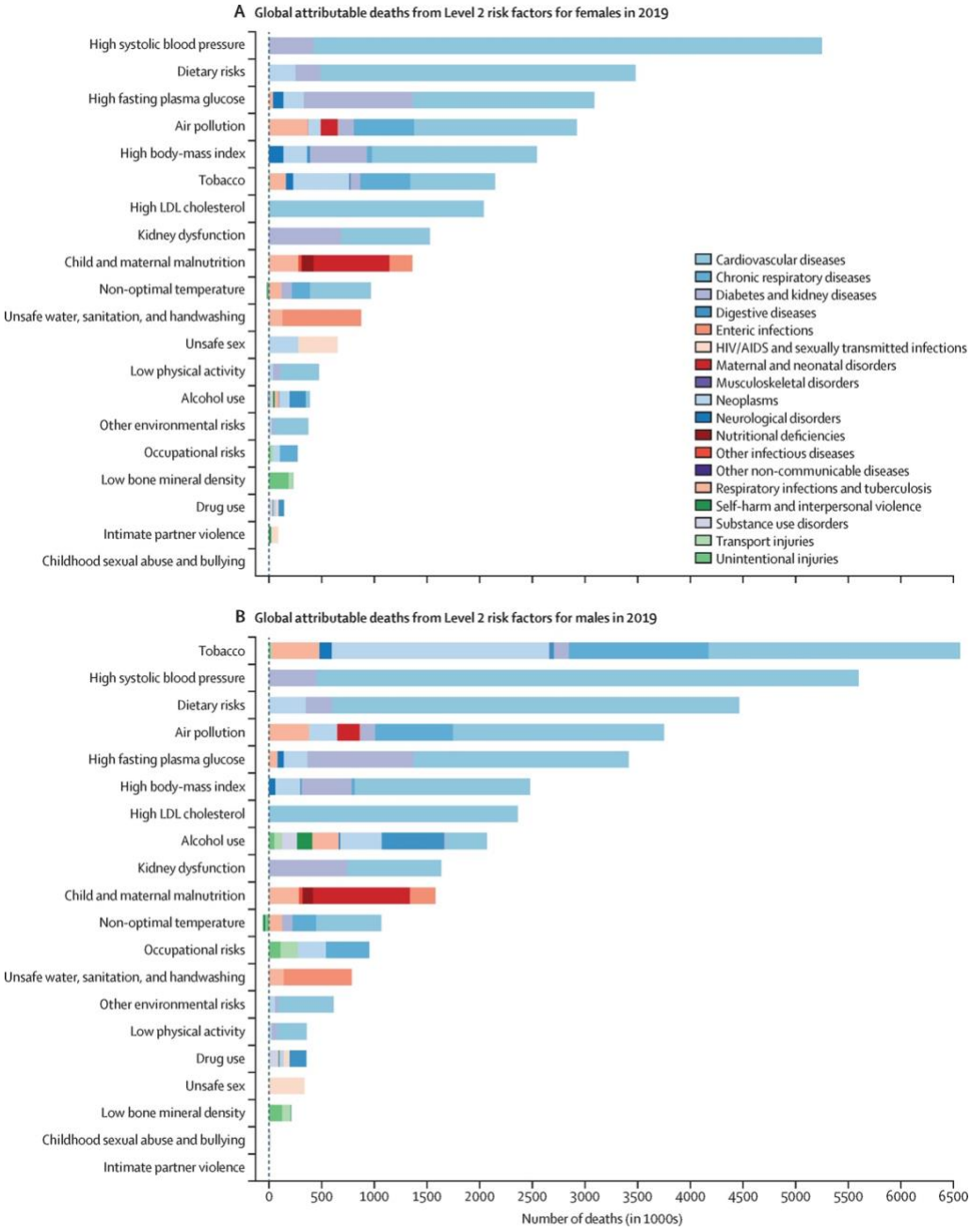

Figure 1: High systolic blood pressure is the leading risk factors for global attributable deaths for both males and females (GBD et al., 2020).

Hypertension associated complications such as stroke, atherosclerosis, heart failure, intracerebral haemorrhage, cardiac hypertrophy; chronic kidney disease and kidney failure are the leading causes for cardiovascular morbidity and mortality (Singh et al., 2014). Though growing awareness and huge number of available antihypertensive drugs, less than 50% of hypertensive patients are able to achieve optimum blood pressure (BP). An increasing number of these events called therapy resistant hypertension (TRH). TRH can be defined as BP above 140/90mmHg when patients are receiving three or more antihypertensive drugs including a diuretic (Braam et al., 2017). Based on prescribed pharmaceutical agents, TRH can be classified into two categories such as uncontrolled TRH and controlled TRH. Uncontrolled TRH is diagnosed when office BP of a patient is above the goal despite of having thre different antihypertensive drugs including a diuretic whereas controlled TRH can be defined when patient receives four or more antihypertensive drugs to attain targeted BP (Alsharari et al., 2022). According to NHANES report, 8-12% of adult hypertensive patients are diagnosed with THR. TRH is widespread in patients who are above 55 years of age, ethnically black, have high body mass index, diabetes or chronic kidney disease (CKD) (Sarafidis et al., 2013). In the majority of the cases, the inability to identify the exact reasons or mechanism of hypertension development compounds to the poor outcome. It has been shown that sympathetic nervous system overactivity, increased renin-angiotensin-aldosterone system (RAAS) activity, inflammation or impaired nitric oxide (NO)/cGMP cascade are the major contributors of development and progression of hypertension, thus complex interaction between the immune system, vasculature and kidney play a pivotal role in the pathogenesis of hypertension and hypertension associated end-organ damage. (Mennuni et al., 2014; Drummond et al., 2019; Rodriguez-Iturbe et al., 2017)

Kidney is a culprit and a victim of hypertension

BP can be defined as a product of cardiac output and total peripheral resistance whereas cardiac output is the product of stroke volume and heart rate (Ivy et al., 2014). The kidney plays a central role in the homeostasis of blood pressure (Wadei et al., 2012). It maintains blood pressure by regulating extracellular fluid volume (ECFV) through sodium and water balance. However, increased sodium and water consumption causing higher blood volume and cardiac output that lead to increased renal perfusion pressure (RPP) (Van Beusecum et al., 2015). Consequently, increased RPP causes elevated renal interstitial hydrostatic pressure (RIHP) resulting increased excretion of sodium and water leading to reduced ECFV and blood pressure. This phenomenon is referred as ‘pressure natriuresis’ (Ivy et al., 2014; Khraibi et al., 2002). On the contrary, when the blood pressure drops, nephrons of the kidney increase the reabsorption

of sodium and water to elevate ECFV thus increasing blood pressure (Van Beusecum et al., 2015). The renin angiotensin aldosterone system (RAAS) is one of the main modulators of pressure natriuresis and salt balance. In normotensive condition, salt intake is inversely related to RAAS activation. According to multiple studies, low salt consumption stimulates RAAS activity and facilitates sodium reabsorption whereas high salt load significantly suppresses RAAS activity and accelerate sodium excretion (Schweda et al., 2015). Moreover, increased RIHP causes rapid redistribution of sodium-proton exchangers (NH3) and sodium phosphate cotransporter (NaPi2) at apical proximal tubule and inhibits sodium potassium (Na^+K^+) ATPase activity resulting increased sodium excretion. In addition, increased RPP is associated with increased renal nitric oxide (NO) formation that mediate pressure natriuresis by inhibiting sodium potassium chloride co-transporter (NKCC2) (Baek et al., 2021). Therefore, the relationship between RPP and pressure natriuresis are vital for regulation of blood pressure and impairment of this relationship leads to genesis and progression of hypertension (Ivy et al., 2014).

Moreover, the kidney is highly innervated with sympathetic nerves and exaggerated renal sympathetic outflow plays a significant role in the pathophysiology of hypertension (Leong et al., 2006; McDonough et al., 2010; Kim et al., 2013; Amann et al., 2000). Recent human and animal studies demonstrated that denervation of renal sympathetic nerves attenuates blood pressure and reduce renal damage (Azizi et al., 2018; Mahfoud et al., 2013). However, chronic untreated high blood pressure causes injury to the integral vasculature of the kidney, which prompts activation of the RAAS and increased renal sympathetic nerve activity (RSNA) leading to vasoconstriction, reduced renal blood flow, increased renin secretion (further RAAS activation) and reabsorption of salt and water resulting in augmented hypertension and an exaggerated kidney damage. Thus, the kidney plays the role of a culprit as well as a victim of hypertension (Fig- 2) (Mennuni et al., 2014; Kamat et al., 2015; Sparks et al., 2015).

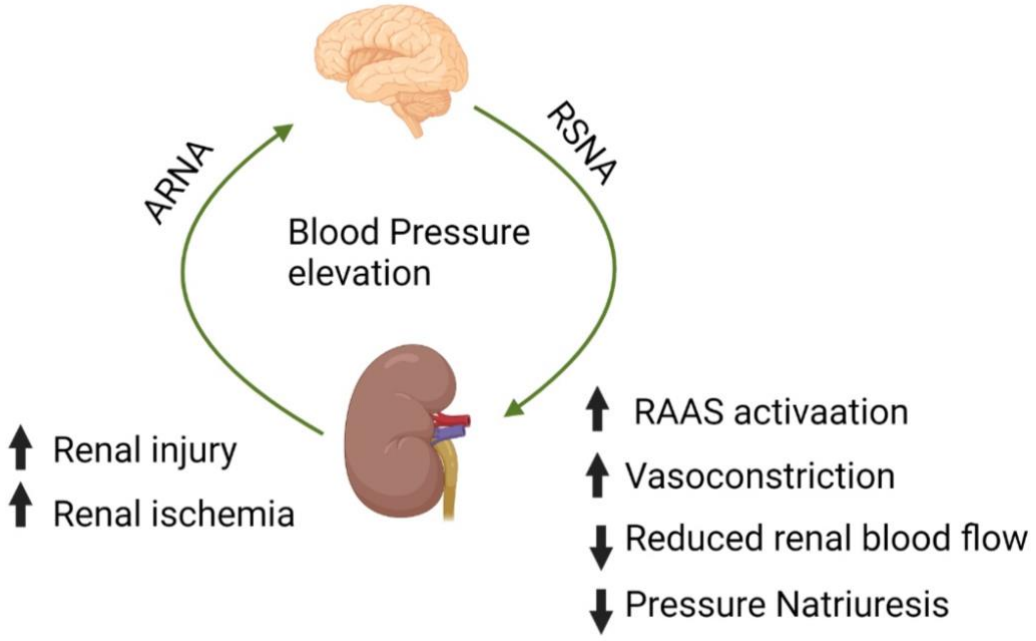

Figure 2: Kidney is a culprit and a victim of hypertension (Adopted from McDonough et al., 2010; Mennuni et al., 2014; Fountain et al., 2022).

Renin angiotensin aldosterone system (RAAS)

RAAS is a complex mixture of an endocrine, paracrine, and autocrine system associated with diverse physiological functions as well as inflammation, fibrosis, and target organ damage. One of the main components of the RAAS is renin, a 340 amino acid long protein released by the juxtaglomerular apparatus in the kidney. Prorenin is the precursor of renin, which is proteolytically activated by cathepsin B in the kidney and non-proteolytically by renin receptors in many tissues. Renin also acts as hormone due to its signalling function. It is expressed in response to reduced RPP, low sodium load or activation of beta (β) 1 adrenoceptors of sympathetic nervous system. Renin hydrolyses 118 amino acid long serum globulin protein named angiotensinogen and convert them into angiotensin I. Angiotensinogen is an enzyme inhibitor produced by liver and a member of serpin family. Thyroid hormone, corticosteroid, angiotensin II, estrogen levels can influence the plasma concentration of angiotensinogen. Angiotensin I is a decapeptide, further metabolized by dipeptidyl carboxypeptidase enzyme called angiotensin converting enzyme (ACE) in endothelial cells, lung capillaries and epithelial cells of kidney and produce angiotensin II (Ang II) (Romero et al., 2015; Patel et al., 2017).

Ang II is a biologically active hormone of RAAS and directly or indirectly involves in blood pressure modulation. It binds with its specific cell surface receptors on different tissues and

exerts various biological actions (Fig- 3) (Fountain et al., 2013; Manrique et al., 2009). Ang II binds to Ang II type 1 (AT_1) receptors on the vascular smooth muscle cells of renal afferent and efferent arterioles causing vasoconstriction which results increased pressure of glomerular capillaries, reduced renal blood flow and glomerular filtration rate (GFR) (Mennuni et al., 2014). Ang II also activates different sodium transporters, such as sodium-bicarbonate (Na^+-$HCO3^-$) co-transporter and (Na^+-H^+) exchanger at proximal tubules and epithelial sodium channel (ENaC) at distal nephron to increase sodium reabsorption leading to a shift of fluid into extracellular space thus increasing arterial pressure (Fountain et al., 2022; Sparks et al., 2014; Zaika et al., 2013). Moreover, Ang II stimulates aldosterone secretion by interacting with the adrenal gland. Aldosterone is a hormone that binds to mineralocorticoid receptors and increases sodium reabsorption and potassium excretion at the site of the renal distal tubule and collecting duct thereby increasing ECFV and blood pressure (Mennuni et al., 2014; Fountain et al., 2022). In addition, Ang II accelerates inflammation that prompts vascular damage in various mechanisms. It promotes infiltration of immune cell in the vascular tissue by increasing vascular permeability. Ang II stimulates expression of adhesion molecules such as VCAM (vascular cell adhesion molecule)-1, selectins to promote adhesion of immune cells to the vascular tissues thus remodelling the extracellular matrix. Moreover, Ang II involves in the polarization of monocytes into macrophages and promotes expression of monocyte chemoattractant proteins (MCP)-1(Ruiz-Ortega et al. 2000). It also induces vascular NADH oxidase thus stimulating reactive oxygen species (ROS) production. Increased ROS contributes to vascular hypertrophy by increased synthesis and proliferation of collagen as well as tissue remodelling by increased proliferation of interstitial fibroblasts and reduced apoptosis of local interstitial cells (Fig-3) (Touyz et al., 2005; Mennuni et al., 2014).

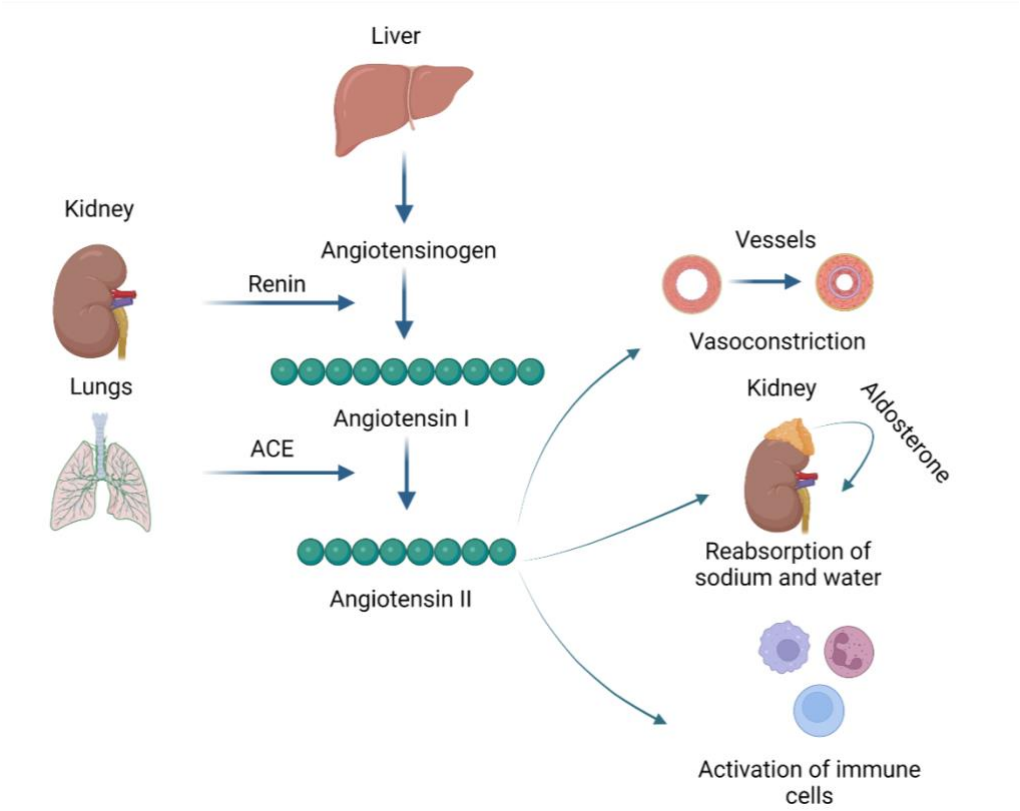

Figure 3: Renin angiotensin aldosterone system in high blood pressure (Adopted from Mennuni et al., 2014; Fountain et al., 2022).

Role of immune system in blood pressure regulation

The immune system plays a significant role in the pathogenesis of hypertension and end organ damage. Many clinical and pre-clinical studies suggest that hypertension is associated with prolonged activation of innate and adaptive immune response driven by various cellular elements such as monocytes/macrophages, natural killer cells, dendritic cells, B and T lymphocytes (Drummond et al., 2019).

Innate immunity

Innate immunity is a cascade of immediate responses against certain molecular signals such as pathogen associated molecular patterns (PAMPs) or danger associated molecular patterns (DAMPs). Pattern recognition receptors (PRRs) detects these signals and initiate assembly of complexes named inflammasomes. Inflammasomes are responsible for synthesis and secretion of various pro-inflammatory cytokines, which neutralize the harmful elements and trigger 'pyroptosis'- a regulated process of cell death. NOD-like receptor protein (NLRP) 3 is one of four inflammasomes directly associated with hypertension. NLRP3 releases pro-inflammatory cytokines interleukin (IL)-1ß and IL-18 via caspase 1 dependant pathway resulting vascular inflammation and hypertension (Rodriguez-Iturbe et al., 2017). Moreover, current evidence

suggests that Toll like receptor (TLR) - 4, a specific PRR involves in the activation of NLRP-3 and inhibition of TLR-4 lead to downregulation of NLRP-3, IL-1ß, and IL-18 (Qi et al., 2021). Recent studies showed that TLR4 is relatively higher in hypertensive patients and pharmacological or genetic blockade of TLR4 showed significant reduction in inflammation, blood pressure, cardiac and renal injury (Drummond et al., 2019).

Monocytes and macrophages

In addition, there are evidence that innate immune cells like monocytes and macrophages are also playing an important role in the pathogenesis of hypertension. Wenzel et al., demonstrated that infiltration of pro-inflammatory monocytes and macrophages promote arterial hypertension and vascular dysfunction (Wenzel et al., 2011). Multiple hypertensive animal models demonstrated increased deposition of macrophages in the brain, heart, kidney and vasculature compared to normotensive controls (Mervaala et al., 1999; Bush et al., 2000). According to some studies, reducing infiltration of macrophages in the tissue by inhibiting monocyte chemoattractant protein (MCP) -1 or blocking of its respective receptor, C-C chemokine receptor 2 (CCR2) causes blunted hypertension induced by Ang II induced or DOCA salt (Ishibashi et al., 2004, Elmarakby et al., 2007). It has been demonstrated that macrophage colony-stimulating factor (m-CSF) deficient mice demonstrated reduced endothelial dysfunction, reactive oxygen species, vascular remodelling, thus attenuated DOCA and ANG II induced hypertension (De Ciuceis et al., 2005). Macrophages produce proinflammatory cytokines such as Tumour necrosis factor (TNF) -α and IL-1β as well as reactive oxygen species causing endothelial and epithelial dysfunction leading to impaired sodium excretion and augmented blood pressure (Rucker, et al., 2017).

Adaptive immunity

The adaptive immunity can be defined as targeted immune response towards a specific endogenous or exogenous antigen. T and B-lymphocytes are the major players of adaptive immune system. It has been demonstrated that mice lacking T and B-lymphocytes (rag1-/-) are less susceptible to Ang II induced hypertension compared to wild type mice. However, adoptive transfer of only T cells re-established Ang II induced hypertension in these mice, indicating pivotal role of T cells in the pathogenesis of experimental hypertension. T cells induce hypertension by augmented oxidative stress, increased immune cell infiltration in perivascular tissue, impairment of vascular function, overexpression of adhesion molecules and inflammatory cytokines such TNF-α in presence of Ang II infusion (Guzik et al., 2007).

Activation of T cell is a complex process and requires two signals. First, T cell receptor (TCR) of T lymphocyte binds with a specific antigen-MHC complex presented by Antigen presenting

cell (APC) then it interacts with CD80 or CD86 molecule of APC through CD28 receptor as a co-stimulatory signal (Rodriguez-Iturbe et al., 2017). Co-stimulation is essential for activation of T cell in hypertension and deletion or blockage of this co-stimulatory pathway has shown to prevent hypertension in experimental mice (Drummond et al., 2019).

Moreover, T lymphocytes can also be activated by hypertensive stimuli such as Ang II or L-NAME with high salt resulting generation of antigen experienced T cells named 'effector memory T cells.' Even after removal of the stimuli, group of dormant effector memory T cells remain in the bone marrow which can be activated, proliferated and migrated to blood vessels and other organs after subsequent exposure to the antigen (Drummond et al., 2019). In addition, interaction between CD70 molecule of APC and CD27 molecule of T lymphocyte is essential for formation of memory T cells (Rodriguez-Iturbe et al., 2017. It has been demonstrated that after secondary stimulation, hypertension was developed by activation of memory T cells in the kidney and in the bone marrow. Moreover, it has been shown that mice without CD70 cannot produce memory T cell, thus unable to develop hypertension in response to secondary stimulation (Itani et al., 2016).

Based on the surface markers, T lymphocytes can be categorized into two types- CD4 positive cells are called helper T cells whereas CD8 positive cells are called cytotoxic T cells. Depending on the cytokine exposure, naïve CD4 cells can be polarized into T helper 1 (Th1), T helper 2 (Th2), T helper 17 (Th17) or regulatory T cell (Treg) (Zhang et al., 2015).

Th1 and Th2 cells

Th1 subset is generated when CD4 positive cells are exposed to IL-12 and interferon (IFN)-γ and prominently secrets IL-2, TNF-α, and IFN-γ (Ganta et al., 2005). It has been demonstrated that hypertensive patient have increased circulatory Th1 levels (Ji et al., 2017). According to Shao et al., Ang II induced Th1 type response exaggerates blood pressure and renal injury (Shao et al. 2003). Moreover, clinical data suggest that hypertensive patient have increased TNF-α, and IFN-γ level compared to normotensive subjects (Mirhafez et al., 2014). Multiple studies demonstrated the significant role of TNF-α in blood pressure regulation. Sriramula et al. showed that TNF-α deficit mice failed to exert high blood pressure in response to Ang II infusion, however treating these mice with recombinant TNF-α has shown to re-establish the hypertensive response to Ang II (Sriramula et al., 2008). Moreover, Elmarakby and colleagues demonstrated that development of Ang II induced hypertension in mice with high salt diet is hindered due inhibition of TNF-α by etanercept (Elmarakby et al., 2006). Elevated TNF-α inhibits eNOS production and promote generation of ROS causing reduced bioavailability of NO which leads to increased renal vasoconstriction and reduced glomerular filtration rate.

These effects are directly associated with vascular dysfunction and hypertension (Goodwin et al., 2007; Seidel et al., 2006; Zia et al., 2006; Elmarakby et al., 2006).

Moreover, IL-2 is usually important for the formation of memory T cells. (Zhu et al., 2008). Th2 requires IL-4 environment and mostly secrets IL-4 and IL-10 (Ganta et al., 2005). These cells generally exert immune response against extracellular parasites and involves in induction of allergic response. IL-4 is an important mediator of IgE production and they are involved in Th2 differentiation (Zhu et al., 2008).

Regulatory T cells (Treg)

Treg is polarized in presence of TGF-β1 and low level of IL-6 and responsible for secretion of anti-inflammatory immune factors such as IL-9, IL-10, TGF-ß and cytotoxic T lymphocyte 4 (Zhang et al., 2014). It has been demonstrated that weekly administration of Tregs can improve cardiac activity, endothelial function, oxidative stress and inflammation in Ang II or mineralocorticoid induced hypertension (Kasal et al., 2012). Moreover, higher doses of Tregs injection showed decline in immune cell infiltration along with gradual reduction in blood pressure (Kvakan et al., 2009). Mian et al. demonstrated isolation of T cells from Scurfy and wild type mice and transferred them into rag-/- mice (lack of T and B lymphocytes). Scurfy mice lack Treg due to mutated FoxP3 gene. Interestingly, rag-/- mice received T cells from Scurfy mice showed exaggerated blood pressure and vascular damage in response to Ang II thus suggesting important role of Treg in blood pressure regulation (Mian et al., 2016). Other groups showed different strategy to increase Tregs in mice infused with angiotensin II. Thus, mice were treated with immune complex IL-2/mAb (monoclonal antibody) CD25 promoting interaction of IL-2 with CD25+ cells causing rapid expansion of Treg in the spleen resulting in lower infiltration and activation of immune cell as well as reduced expression of IL-17 in the aorta (Rodriguez-Iturbe et al., 2017).

Th17 cells

Th17 cells are generated under the influence of IL-6, IL-21, IL-23, IL-1ß and transforming growth factor (TGF)-ß. Th17 predominantly generates IL-17 and IL-22. It has been shown that hypertensive patients have higher serum IL-17 level compared to normotensive controls (Madhur et al., 2010). Moreover, deletion of IL-17 in mice showed blunted hypertension and renal injury in response to Ang II infusion (Kamat et al., 2015, Norlander et al., 2016). IL-17 causes increased sodium and water retention leading to hypertension by upregulating Na^+-H^+ exchangers (NH3), Na^+ Cl^- co-transporters (NCC) and epithelial Na^+ channels (ENaC) on renal distal and proximal tubules via serum and glucocorticoid regulated kinase 1 (SGK1) dependent pathway. IL-22 causes endothelial dysfunction by interfering with the cyclooxygenase activity

of vascular wall thereby increasing vascular resistance. T regs suppresses polarization of Th17 (hou et al., 2008). Treatment with spironolactone hinders activation of Th17 and upregulates Tregs in heart and kidneys whereas anti IL-17a antibody treatment improve hypertension and reduces fibrosis in heart and kidneys (Rodriguez-Iturbe et al., 2017).

Cytotoxic T lymphocytes (CTLs) - It has been shown that CTLs are one of the key mediators of hypertension and are predominantly activated in the kidneys of the mice. Genetical or pharmacological blockade of CTLs in mice demonstrate 50 % reduction in hypertension induced by Ang II or DOCA and salt treatment (Trott et al., 2014). CTLs are the major source of TNF-α and IFN-γ, and inhibition of either of these cytokines showed reduced blood pressure and renal damage in mice under hypertensive condition. Furthermore, CLT knock out mice showed lower renal infiltration of leucocytes and less impaired endothelial function compared to wild type mice suggesting influence of CD8 cells in increased peripheral resistance (Drummond et al., 2019). Recently it has been demonstrated that CD8 cells are responsible for upregulation of Na^+ Cl^- cotransporters in the distal convoluted tubules of the kidney, resulting increased reabsorption of sodium and water in hypertensive mice (Liu et al., 2017).

Gamma-delta (γδ) T cells-

γδ T cells are specialized T cell subpopulation highly distributed in the peripheral organs (Ribot et al., 2021). It has been demonstrated that hypertensive mice have increased γδ T cell in the spleen. Moreover, deletion or inhibition of γδ T cell in mice cause attenuated hypertension and reduced endothelial dysfunction under Ang II infusion (Caillon et al., 2017). γδ T cells are responsible for inflammation associated hypertension by releasing various pro-inflammatory cytokines such as CC-chemokine ligand 5 (CCL5) , IL-17, TNF-α, IFN-γ (Drummond et al., 2019).

Interaction between immune system, RAAS and Sympathetic nervous system (SNS)

Many studies demonstrated complex interactions between immune system, RAAS, as well as SNS in hypertension. A potent component of RAAS, Ang II involves in the modulation of T cell function by interacting with AT1 receptor on its cell surface and stimulates formation of various pro-inflammatory cytokines like TNF-α, IFN-γ and IL-17. These cytokines interact with the vasculature causing vasoconstriction and also induce sodium and water reabsorption by interacting with various Na^+ channels in the nephrons of the kidney (Drummond et al., 2019; Kamat et al., 2015; Sriramula et al., 2008). Moreover, Ang II dependant hypertension leads to increased infiltration of T cell in vasculature, heart and kidney resulting in an accelerated

hypertensive end-organ damage. Furthermore, Ang II also promotes accumulation of effector memory T cell in renal and cardiovascular tissue (Crowley et al., 2010; Wu et al., 2016).

In addition, RAAS also interacts with sympathetic nervous system through Ang II that interacts with AT1 receptor on sympathetic nerve ending facilitating a release of norepinephrine (NE) (Boehm *et al*., 2002; Stegbauer et al., 2005; Rump et al., 1995). Moreover, interaction between SNS and immune system is well documented.NE interacts with immune cells via alpha and beta adrenergic receptors, thus exerting various pathophysiological effects (Bellocch et al., 2022). NE regulates mobilization of lymphocyte in the bloodstream by interacting with beta 2 adrenergic receptors (β2AR) on their cell surface (Dimitrov et al., 2009). Moreover, *in vitro* studies demonstrated that β2ARs expressed on naïve T cells promote helper T cells to differentiate towards Th1 subtypes through IFN-γ/IL-12 interaction (Sanders et al., 2012). Furthermore, NE involves in the modulation of Tregs (Wirth et al., 2014). In addition, NE stimulates secretion of inflammatory cytokines such as IL-1, IL-6, CCL2 and CXCL3 by central and effector memory CD8 cells (Fig- 4) (Slota et al., 2015).

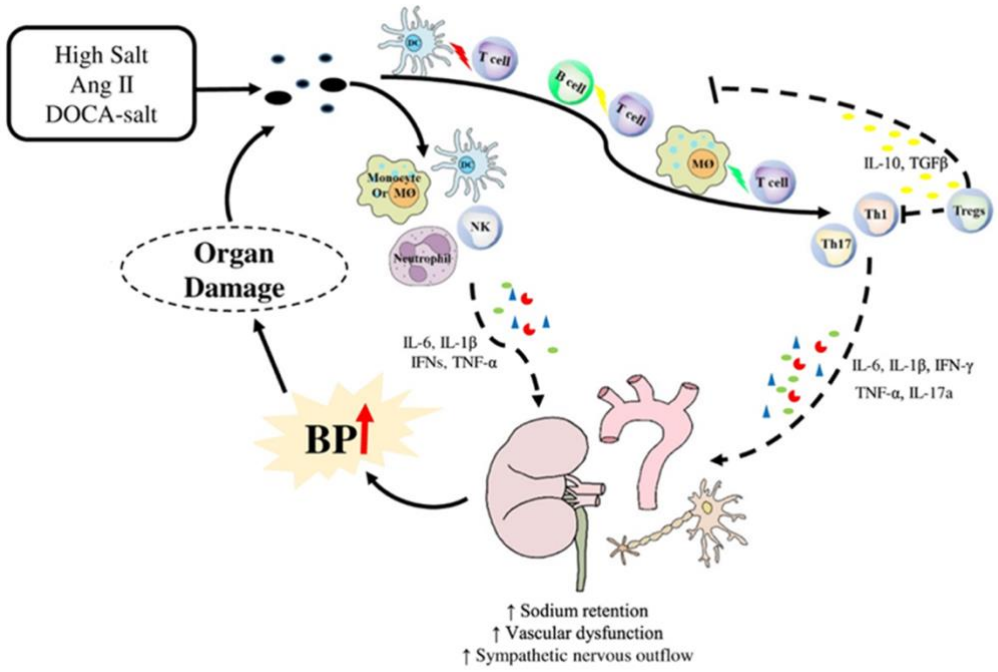

Figure 4: Increased interaction of immune system with other systems lead to exaggerated hypertension (Adopted from Lu et al. 2018).

Therapy resistant hypertension (TRH) can be characterized by excessive sympathetic nerve activity. A recent study was performed with 32 TRH patients, 35 non-resistant hypertensive patients and 19 normotensive controls. According to the study, TRH patients showed significantly higher muscle sympathetic nerve activity (MSNA) compared to compared to

normotensive controls and non-resistant hypertensive patient (Grassi et al., 2016). Another study demonstrated that renal NE spillover is significantly higher in TRH patients compared to normotensive controls and essential hypertensive patients (Grassi et al., 2015). Zaldivia et al showed that renal denervation significantly reduces sympathetic nerve activity resulting reduced blood pressure as well as inflammatory response of immune cells. (Zaldivia et al., 2017). Another study determined that renal denervation causes reduced T cell infiltration in kidneys, which results attenuated blood pressure in hypertensive mice (Xiao et al., 2015).

Based on these studies, it is plausible that increased sympathetic nerve activity of TRH patient maintains and prolongs hypertension and end organ damage partly through immune cell mediated mechanism. However, fascinating results from various animal studies suggest significant role of immune cells, particularly T cells in the development and exaggeration of hypertension and end organ damage, but in practice outcome associated with diagnosis and treatment of TRH is quite unsatisfactory. One of the possible explanations could be lack of investigation to distinguish functions of T cell subsets and associated cytokines from patient with TRH.

Aim of the study and approach

The aim of the study is to investigate whether human T cells from TRH patient cause or exaggerate hypertension. Moreover, whether certain T cell subset and pro-inflammatory cytokines are responsible for blood pressure exaggeration. To identify the underlying mechanism how T cells from patients with TRH mediates hypertension. We have used a specialized immunodeficient mouse model named NSG-(KbDb) ^{null} mice (NOD.Cg-Prkdcscid H2-K1tm1Bpe H2-D1tm1Bpe Il2rgtm1Wjl/SzJ) into which we have transferred T cells from patients and healthy controls. We induced experimental hypertension by chronic Ang II (500ng/kg/min) infusion for 2 weeks. We have analyzed the inflammatory status as well as immune cell subsets and function from patients with TRH and healthy controls. This unique experimental approach gave us for the first time the opportunity to investigate the underlying mechanisms and effects of human T cells from patients with TRH in the development and extent of hypertension and end organ damage.

3 Materials and methods

Animal experiments were conducted in accordance with the instructions from the Directive 2010/63/EU of the European Parliament on the protection of animals used for scientific purposes, were approved by the responsible federal state authority LANUV NRW (Landesamt fuer Natur-, Umwelt-, und Verbraucherschutz NordrheinWestfalen). Breeding and maintenance of the experimental mice were organized and conducted at the local animal care facility at Heinrich-Heine-Universität Düsseldorf. Mice were housed under standard conditions with free access to standard food and water ad libitum. Light to dark cycle was 12:12 hours. The living environment and condition of the mice were inspected daily

Mouse strain

A specialized immunodeficient mouse strain NSG-(K^bD^b) ^{null} (NOD.Cg-*Prkdc*^{scid} *H2-K1*^{tm1Bpe} *H2-D1*^{tm1Bpe} *Il2rg*^{tm1Wjl}/SzJ) (JAX stock #023848) was chosen for our experiments for various reasons. They lack mature T cells or B cells, they do not have functional natural killer cells and they deficit murine class I major histocompatibility complex (MHC). Thus, the incidence of graft versus host disease is very low and occurs usually after 16 weeks of immune cell transfer. Moreover, a transfer of $2x10^6$ -$5x10^6$ human peripheral blood mononuclear cells (PBMCs) is sufficient to induce a good T cell engraftment. However, irradiation or implantation of human fetal lymphatic tissue is not necessary. In our study, 6 to 8 weeks old male NSG-(K^bD^b) ^{null} mice were used. Mice were supplied with neomycin (Sigma-Aldrich Chemie GmbH, Steinheim, Germany) in the drinking water during the whole experimental period.

Study Design

PBMCs were isolated from healthy controls and therapy resistant hypertensive patients and $2x10e^6$ - $5x10^6$ PBMCs were transferred intravenously into NSG-(K^bD^b) ^{null} mice. Peripheral blood was collected and analyzed after 3 weeks of PBMCs transfer and after the sacrifice of the mice through flow cytometry to ensure successful engraftment. Successfully engrafted mouse showed >14 human CD4 cells and >500 human CD4 cells per µL of the peripheral blood after 3 weeks of PBMC injection and after the sacrifice of the mice, respectively. After successful engraftment, telemetry catheters were implanted in a subset of mice. Later, osmotic minipumps were implanted subcutaneously to induce blood pressure. After 14 days of blood pressure measurement, mice were anesthetized with the mixture of ketamine (100 mg/kg, i.p.) (Ketaset, Zoetis, New Jersey, United States) and Xylazine (5 mg/kg, i.p.) (Rompun, Bayer, Leverkusen, Germany). Then, peritoneal cavity was opened and left renal vein was cut to withdraw blood. Afterwards, euthanized of the mice were ensured by cervical dislocation. Then ice cold PBS

containing 100 U/mL heparin (B. Braun, Melsungen, Germany) was used to flush remaining blood from the circulatory system and then organs were collected for further assessment.

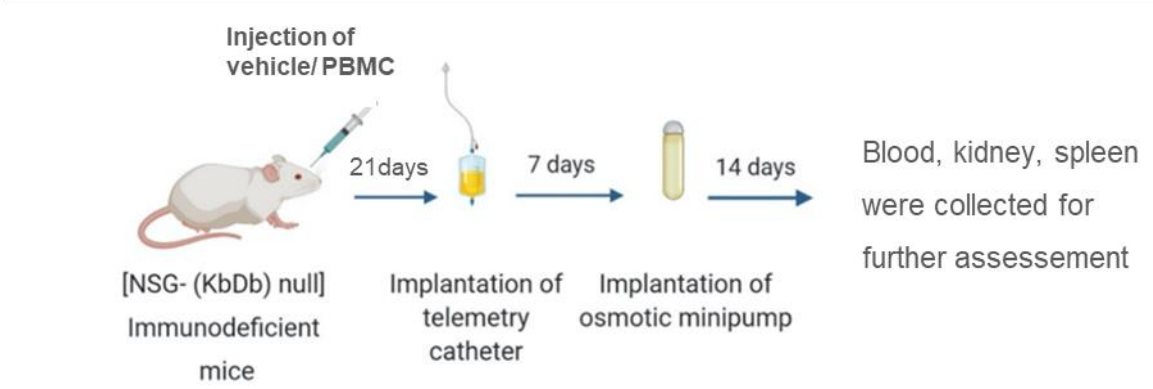

Figure 5: NSG-(K^bD^b) ^{null} mice were injected with either vehicle or PBMCs from healthy controls or hypertensive patient. After 21 days of transfer, telemetry catheters were implanted in a subset of mice. After 7 days, osmotic minipumps were implanted for 2 weeks. Afterwards, mice were euthanized.

Isolation of PBMCs

Blood samples from healthy controls and therapy resistant hypertensive patients were collected into Ficoll-Hypaque tubes (BD Vacutainer® CPT™, New Jersey, USA). Then, samples were centrifuged at 2600 rpm for 20 minutes to separate PBMCs. Afterwards, the cloudy layer of PBMCs located between ficoll and plasma was collected carefully and washed with PBS. To confirm good engraftment, we transferred intravenously $2x10e^6$ - $5x10^6$ PBMCs from healthy controls and therapy resistant hypertensive patient into NSG-(K^bD^b) ^{null} mice.

Blood pressure measurement by tail-cuff

Systolic blood pressure (SBP) was measured in conscious mice using tail-cuff plethysmography (BP-98A; Softron Co., Tokyo, Japan). Each conscious mouse was immobilized by putting it in a restrainer. Then, the mouse along with the restrainer was placed in a climatic coil that was adjusted to 37° C to provide heating. Before experiment, mice were trained for 5 consecutive days for adaptation. Later, SBP was measured by placing the cuff at the proximal end of the tail of the mouse. Daily ten measurements from each mouse were recorded and calculated as mean of all recorded values.

Blood pressure measurement by telemetry catheters

BP was measured continuously in a subset of conscious mice by radio-telemetry catheters (Data Sciences International,'s-Hertogenbosch, The Netherlands). Radio-telemetry catheters were implanted as described in Stegbauer et al., 2017; JCI Insight. Mice were anesthetized with the mixture of ketamine (100 mg/kg, i.p.) and Xylazine (5 mg/kg, i.p. Then dissection of left common carotid artery was performed followed by cannulation and advancement of the catheter until the small notch of the tubing placed at the opening of the vessel. After fixing the catheter, the transmitter was implanted subcutaneously. Afterwards, mice were allowed to recover for 7 days to restore homeostatic circadian rhythms. BP and heart rate were recorded every 20 minutes for 10-second intervals.

Preparation and implantation of osmotic minipumps

Ang II was infused via osmotic minipumps (1002, Alzet, Durcet, California, USA) into the mice to induce high blood pressure. Ang II solution was prepared by diluting lyophilized powder of Ang II (A9525, Sigma-Aldrich Chemie GmbH, Steinheim, Germany) with saline (Fresenius Kabi, Bad Homburg, Germany) to achieve a concentration so that the release rate would be 500 ng/kg/min from the minipump. To ensure complete filling of the minipumps, weight of the minipumps were measured before and after filling. Then the minipumps were incubated at 37° C overnight to achieve rapid release of Ang II after implantation. Before implantation of minipumps, mice were anesthetized with the mixture of ketamine (100 mg/kg, i.p.) and Xylazine (5 mg/kg, i.p.). To prevent dehydration of the eyes, ophthalmological cream was applied to the eyes of the mouse. Afterwards, back of the neck of the mouse was shaved and disinfected. Then a small cut was made on the shaved region of the mouse followed by preparation of a subcutaneous pocket on the flank of the mouse using a sterile scissor. Then osmotic minipump was inserted in upright position in the pocket. Later, the surgical opening was closed by single knot stiches. To ensure complete recovery, mice were observed following days after the surgical procedure.

Isolated kidney perfusion

Ex vivo isolated kidney perfusion was performed as described in Stegbauer et al., 2005, Journal of Hypertension; to investigate renal endothelial dependent vasorelaxation. Mice were anesthetized and peritoneum was opened. To prevent blood flow, a knot was made above renal artery by surgical sutures as well as caudal aorta were blocked using bent clamp. Later, abdominal aorta was exposed and a small cut was made to insert cannula. After carefully insertion of cannula, a knot was tightened around the cannula. Then, the cannula was connected

with in house made Krebs–Henseleit solution followed by rupturing of left renal vein to flush out blood from the kidneys. Composition of the Krebs–Henseleit solution as follows- 118 mM NaCl, 4.7 mM KCl, 2.5 mM $CaCl_2$, 1.03 mM KH_2PO_4, 0.45 mM $MgSO_4.7H_2O$, 11.1 mM of glucose, 0.067 mM Na_2EDTA, 0.07 mM ascorbic acid and 25 mM $NaHCO_3$. Afterwards, fat, muscle and connective tissues were carefully removed from the renal arteries. Later, two polyethylene tubing (Portex, Germany; internal diameter 0.28 mm) were inserted into two renal arteries and were tightened using sutures. Then, catheter along with the kidney was dissected and attached with the perfusion circuit. Then 60 mM KCL was perfused through the kidneys to check the viability of the kidneys followed by 30 minutes of stabilization period. Krebs–Henseleit solution was used as neutral buffer. Later, norepinephrine (1 μM; Sigma Aldrich) was used for pre- contraction of the kidneys followed by application of incremental concentration of carbachol (Sigma) to determine renal endothelial dependent vasorelaxation.

Flow cytometry

Flow cytometry analysis of PBMC from healthy controls and hypertensive patients as well as peripheral blood, single cell suspension of spleen and kidney of the experimental mice using CytoFLEX Flow Cytometer (Beckman Coulter Inc, California, USA). PBMC samples were isolated as mentioned, washed and stained with following antibodies for 30 minutes at room temperature in the dark.

Antibody	Catalog no.	Dye	Company
CD45	563717	BV650	BD bioscience, Heidelberg, Germany
CD3	563800	BV786	BD bioscience, Heidelberg, Germany
CD4	566908	BV605	BD bioscience, Heidelberg, Germany
CD8	565192	APC R700	BD bioscience, Heidelberg, Germany
CD45Ra	A82946	Pacific Blue	Beckman Coulter, , Krefeld, Germany
CCR7	562381	PE-CF 594	BD bioscience, Heidelberg, Germany
CD127	351316	APC	Biolegend, San Diego, USA
CD25	IM2646	PC5	Beckman Coulter, Krefeld, Germany
CCR6	B68132	PC7	Beckman Coulter, Krefeld, Germany
CXCR3	12183942	PE	ebioscience, San Diego, USA

CRTH2	350114	APC/cyanine7	Biolegend, San Diego, USA

Peripheral blood samples were collected and treated with lysis buffer to get rid of red blood cells. Then, the samples were centrifuged at 300 g for 5 minutes followed by aspiration of the supernatant. Later, the pellets were washed with wash buffer [0.5% bovine serum albumin (BSA) in PBS)] and similarly stained with mentioned antibody panel. After sacrificing the mice, spleen and decapsulated kidneys were collected and kept in ice cold PBS. First, spleen was fragmented into small pieces followed by washing through 100 µm filter (EASYstrainer™, Greiner bio-one, Solingen, Germany) using wash buffer. Then, spleen cell suspension was centrifuged at 300 g for 5 minutes and the supernatant was aspirated. Afterwards, the pellet was re-suspended and stained as mentioned above using the same antibody panel. However, kidney was chopped to form a cell mass using razor sharp blade then incubated in collagenase solution on a shaker for 30 minutes at 37° C. Afterwards, the cell mass was washed through 100 µm filter using wash buffer. Later, the cell suspension was centrifuged at 300 g for 5 minutes followed by aspiration of the supernatant. Then the pellet was re-suspended and stained with the same antibody panel mentioned above. After staining, each sample was washed with wash buffer and centrifuged at 300g for 5 minutes. Later, the pellet was re-suspended and analyzed by flow cytometer. The antibodies were used to characterize distinct T cell subsets such as naive CD4 T cells: CD4+CD45RA+CCR7, central memory CD4 T cells: CD4+CD45RA-CCR7+; effector memory CD4 T cells: CD4+CD45RA-CCR7-; effector CD4 T cells: CD4+CD45RA+CCR7- and the corresponding Th1 cells: CXCR3+CCR6-,CRTH2-; Th2 cells: CXCR3-, CCR6-,CRTH2+; Th17 cells: CXCR3-, CCR6+ CRTH2-; Treg cells: CD25+CD127-; naive CD8 T cells: CD8+CD45RA+CCR7+; central memory CD8 T cells: CD8+CD45RA-CCR7+; effector memory CD8 T cells: CD8+CD45RA-CCR7-; effector CD8 T cells: CD8+CD45RA+CCR7-; as described by Maecker et al., 2012.

Data analysis was performed using Kaluza® Flow Analysis Software (Beckman Coulter Inc., Krefeld, Germany). Gating Strategy for PBMCs from healthy controls and therapy resistant hypertensive patient as well as peripheral blood, spleen and kidney of experimental mice to evaluate T cell was shown in following figure 6.

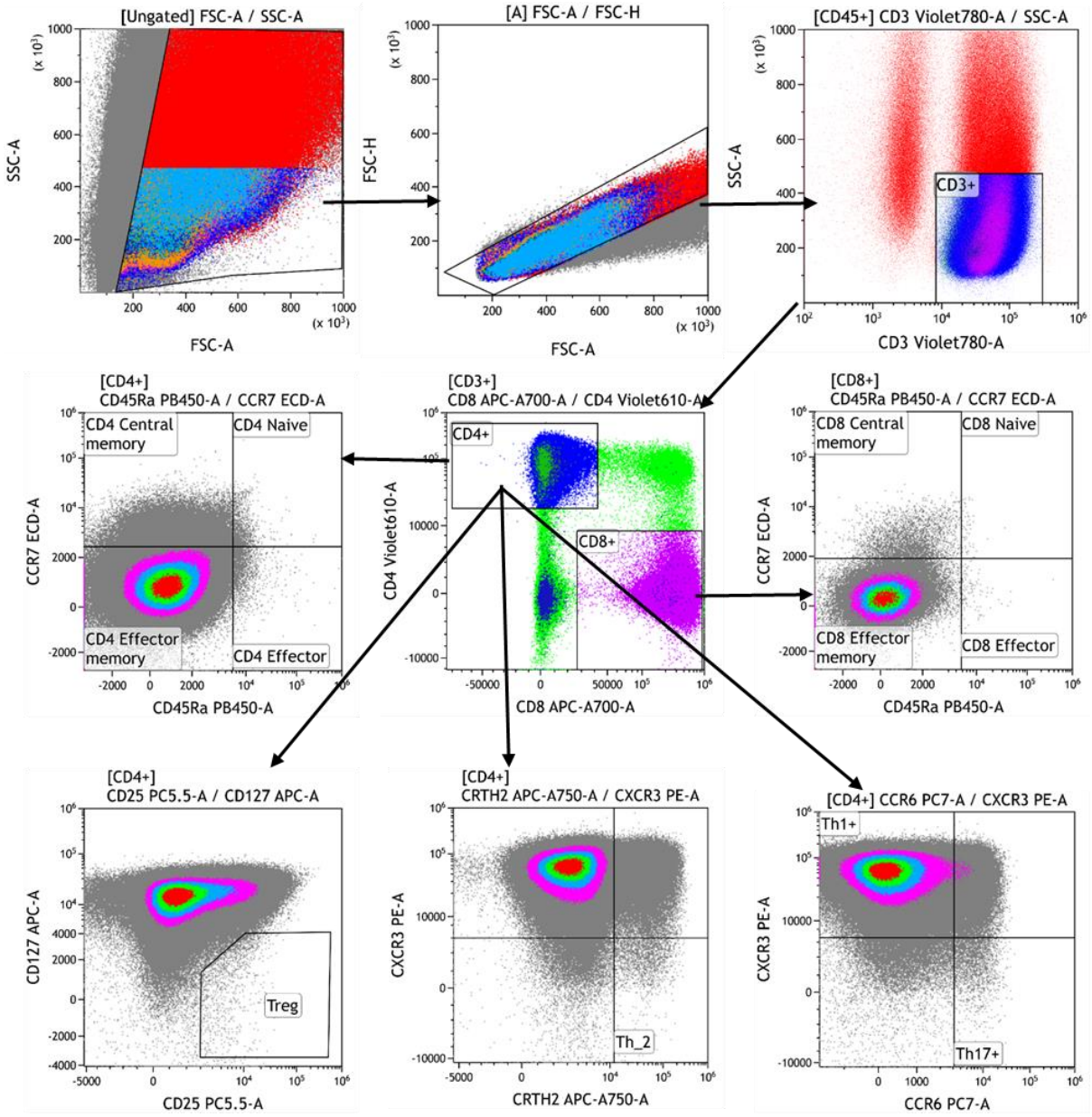

Figure 6: Gating strategy for PBMCs from healthy controls and hypertensive patients and peripheral blood, spleens and kidneys of experimental mice for assessment of T cells

Tissue viability test and *in vitro* studies of renal tissue

Mice were anesthetized and euthanized as mentioned above. Then, kidneys of the mice were decapsulated and fixed in the tissue slicer (Leica Biosystems, Nußloch, Germany) using low melting point agarose (Sigma-Aldrich Chemie GmbH, Steinheim, Germany). Later, tissue samples were cut with the thickness of 2 µm and incubated in 12 well culture plate containing Williams E medium supplemented with 2 mM L-glutamine (Sigma), 100 g/L glucose (Carl Roth GmbH, Karlsruhe, Germany) and 10 µg /ml ciprofloxacin (Sigma). Three tissue slices were incubated per plate representing specific time point such as 0 hour, 3 hours, 6 hours, 12

hours and so on. Later, 260 µl MTT (Thiazolyl Blue Tetrazolium Bromide) (Sigma) (3.5 mg /ml) solution was added to each well and incubated at 37° C for one hour. Afterwards, wet weights of the tissue slices were measured. Then, medium was aspirated and 1ml isopropanol was added in each well followed by 30 minutes of incubation on a shaker to dissolve the byproduct formazan. Viable cells are responsible for the conversion of MTT into purple colored formazan. Later, absorption of eluted formazan was measured at 560 nm. Viability of the tissue was calculated from the ratio of the absorption of dissolved formazan and weight of the tissue. After establishing viability, tissue slices were incubated in above mentioned medium additionally containing human cytokines such as human TNF-α (R&D system, Wiesbaden, Germany) (0.1 ng/mL) or human interferon-γ (R&D system, Wiesbaden, Germany) (100 U/mL) at 37° C in an oxygenated atmosphere with 5% CO2 for different time periods to investigate interaction between human cytokine and murine renal tissue.

Isolation and *in vitro* studies of aortic rings

Mice were anesthetized and euthanized as mentioned above. Then thoracic aorta was dissected and kept in PBS followed by removal of attached connective tissue and adipose tissue. Later, each thoracic aorta was cut into four rings with the length of 2 mm. Afterwards, each aortic ring was incubated in above mentioned medium either containing distilled water (vehicle) or 4 nM human TNF alpha for 22 hours at 37° C on a shaker. After incubation, the aortic rings were mounted in a wire myograph (Multi Myograph Model 610 M, Danish Myo Technology, Denmark) as described in Broekmans et al. 2016; ASPET. Thoracic aorta placed in house made Krebs-Henseleit solution with the ionic composition of 118 mM NaCl, 4.7 mM KCl, 2.5 mM $CaCl_2$, 1.03 mM KH_2PO_4, 0.45 mM $MgSO_4.7H_2O$, 11.1 mM of glucose and 25 mM $NaHCO_3$. The solution was gassed continuously with carbogen and the temperature was maintained at 37° C. Later, 5 mN resting tension was applied to the aortic rings followed by 30-40 minutes of equilibration in presence of diclofenac (3 µM) (Sigma-Aldrich Chemie GmbH, Steinheim, Germany). Then, pre-contraction was induced by norepinephrine (1 µM) (Sigma) followed by cumulative concentration response curve to carbachol (0.3 µM-300 µM) to determine endothelium dependent vasorelaxation.

Determination of the concentration of plasma cystatin C

Mouse/Rat Cystatin C Quantikine® ELISA Kit; Catalog no. - MSCTC0 (R & D system, Wiesbaden, USA).

Component	Amount
Mouse/Rat Cystatin C microplate	one polystyrene microplate with 96 wells
Mouse/Rat Cystatin C conjugate	12 mL of polyclonal antibody
Mouse/Rat Cystatin C Standard	40 ng of recombinant mouse/rat Cystatin C
Mouse/Rat Cystatin C Control	1 vial of recombinant mouse/rat Cystatin C in a buffered protein base
Assay Diluent	12 mL buffered protein solution
Calibrator Diluent	21 mL of a concentrated buffered protein base
Wash buffer Concentrate	21 mL of a 2 fold concentrated solution of buffered surfactant
Color reagent A	12 mL of stabilized hydrogen peroxide
Color reagent B	12 mL of stabilized chromogen
Stop Solution	23 mL of diluted hydrochloric acid
Plate sealer	Adhesive strips

The concentration of plasma cystatin C was determined from the blood of the mice using Mouse/Rat Cystatin C Quantikine® ELISA (Enzyme-linked immunosorbent assay) Kit in accordance to manufacturer's protocol.

Reagent Preparation

Calibrated diluent was diluted using distilled water (1:4 dilutions). Cystatin C control was reconstituted by adding 1mL of distilled water followed by thorough mixing. Cystatin C standard was reconstructed by using calibrated diluent (1:4 diluted). The concentration of the stock solution is 8000 pg/mL. Then a dilution series of cystatin C was prepared in six tubes with the concentration of 4000 pg/mL, 2000 pg/mL, 1000 pg/mL, 500 pg/mL, 250 pg/mL, 125 pg/mL, respectively. The undiluted stock solution served as high standard and calibrated diluent

served as the zero standard. Concentrated wash buffer was diluted 25 times using distilled water.

Sample preparation

Plasma samples were prepared by diluting 400 times using calibrated diluent (1:4 diluted).

Assay Procedure

After preparation steps, 50 µL of Assay diluent was pipetted into each well of the ELISA microtiter plate. Then 50 µL of standard, sample and control were pipetted into each well. After that the plate was covered with adhesive strip and incubated at room temperature for 2 hours. After the incubation period, microtiter plate was decanted to remove the solutions and washed five times with wash buffer. Then the plate was inverted and blotted against clean paper towels in order to remove remaining liquid. Afterwards 100 µL cystatin C conjugate was pipetted into each well and covered with adhesive foil followed by 2 hours of incubation. After the incubation, washing step was repeated followed by botting the plate against the clean paper towels. Later, 100 µL of substrate solution was pipetted into each well and incubated at room temperature in a dark place for 30 minutes. Then stop solution was added into each well to stop the reaction and the microtiter plate was gently tapped in order to ensure thorough mixing. A microplate reader was used to determine the optical density of each well at the wavelength of 450 nm.

Determination of concentration of urinary nitrite/nitrate content

The Nitrate/Nitrite colorimetric assay Kit (780001, Cayman Chemical, Michigan, USA) was used to determine the concentration of the urinary nitrate/nitrite content in accordance with the manufacturer's protocol.

Component	Amount
Microplate (uncoated)	one polystyrene microplate with 96 wells
Assay buffer	100 mL
Nitrate Reductase enzyme	1.2 mL
Nitrite reductase cofactor	1.2 mL
Nitrate standard	1.0 mL
Assay buffer	100 mL
Griess reagent R1	2 vials

Griess reagent R2	2 vials
Plate sealer	Adhesive strips

Reagent preparation

Contents of assay buffer was diluted with 100 mL of ultrapure water. Then, 1.2 mL of assay buffer was added to reconstitute nitrate reductase enzyme as well as nitrate reductase cofactors. Nitrate standard was reconstituted using 1 mL of assay buffer followed by thorough mixing. The concentration of the stock was 200 µM. By serial diluting the stock, standard curve was prepared.

Sample preparation

Urine samples were diluted (1:20) using assay buffer.

Assay procedure

After preparation steps, 200 µL assay buffer was added to the blank wells. Then, 80 µl of samples were added to the wells. Later, 10 µL of enzyme cofactor mixture followed by 10 µL nitrate reductase mixture were added to samples and standards. Then the plate was covered with adhesive strip and incubated for one hour at room temperature. After incubation, 50 µL of Griess reagent R1 followed by 50 µL of Griess reagent R2 were added to both samples and standards. After 10 minutes of incubation, absorbance was measured at 540-550 nm using microplate reader.

Isolation of ribonucleic acid (RNA)

RNA contents from the tissue sections of the mice were isolated using RNeasy® plus mini kit (74134, Qiagen, Germany) in accordance with the manufacturer's protocol.

First, each tissue sample was transferred into a solution of RLT buffer and 10% beta (β) mercaptoethanol. Then tissue samples were ruptured for 20-30 seconds using a homogenizer. Afterwards each solution containing the ruptured tissue was centrifuged at 21000 g for 3 minutes. Then the supernatant was transferred to genomic DNA (gDNA) eliminator column and shortly centrifuged at 8000 g in order to get rid of genomic content. Then the gDNA column was thrown away and 70% ethanol was added to the eluted solution and mixed properly. Afterwards the mixture was transferred into RNA column and shortly centrifuged at 8000 g. The eluent was thrown away and the RNA column was washed two times with 350 µL of RW1 buffer followed by short centrifugation at 8000 g in order to remove carbohydrates, proteins and other impurities. Afterwards DNAse enzyme was added to the column and incubated for 15 minutes at room temperature in order to remove any remaining genomic DNA. Then the

column was washed two times with 500 µl of RPE buffer in order to remove any kind of salt impurities. Then the column was centrifuged for 2 minutes at maximum speed in order to remove any kind of liquid from the column. Then 50 µL of RNase free water was pipetted into the column and centrifuged for 1 minute in order to elute the purified RNA content. The concentration of RNA was measured by spectrophotometer.

Preparation of Complementary DNA (cDNA)

Complementary DNA (cDNA) of each tissue sample was prepared from its purified RNA solution using QuantiTect® Reverse Transcription kit (205311, Qiagen, Germany) in accordance to manufacturer's protocol. First, similar concentration of isolated RNA from each sample was incubated with 2 µL of gDNA wipeout buffer for 2 minutes at 42° C in order to remove any remaining genomic DNA content. Thus, the RNA sample was prepared for reverse transcription. After treatment with gDNA wipeout buffer, 0.5 µL of isolated RNA from each sample was kept in a separate tube for control PCR. Afterwards a master mix was prepared using Quantiscript reverse transcriptase, Quantiscript RT buffer and RT primer mix provided by the kit. Then purified RNA sample and the master mix was incubated at 42°C for 25 minutes then the reaction was inactivated by incubation at 95° C for 3 minutes. Thus, cDNA of each sample was prepared.

Control polymerase chain reaction (PCR)

Control PCR was performed using glyceraldehyde phosphate 3-dehydrogenase (GAPDH) primer. Primers were designed using Primer Express 3.0 software. Master mix was prepared using 10x buffer, deoxyribonucleotides (dNTPs), DNA polymerase enzyme, primers (forward and reverse) and RNAse free water. Then 0.5 µL of isolated RNA, 0.5 µL of isolated RNA treated with gDNA wipeout buffer and 0.5 µL of cDNA from each sample were mixed with 19.5 µL of master mix in three different tubes. Then the samples were put in the thermocycler and PCR was conducted involving 40 thermal cycles. RNAse free water was used as negative control in this process.

The volume distribution of component in each tube as followed-

Component	Volume
RNAse free water	16.78 µL
10x buffer	2 µL
dNTPs	0.4 µL

Forward primer Reverse primer	0.1 µL 0.1 µL
DNA polymerase enzyme	0.12 µL
isolated RNA/ isolated RNA treated with gDNA wipeout/ cDNA	0.5 µL

Quantitative PCR (qPCR)

Quantitative PCR was performed in order to quantify the mRNA expression for certain proteins in the tissue samples. Master mix was prepared using Taqman master mix (Thermo Fisher Scientific, Meerbusch, Germany), primers, and RNAse free water. Then the master mix was pipetted into the wells of the qPCR plate. After that cDNA was pipetted into each well and mixed properly. Then the plate was sealed with adhesive foil and qPCR was conducted using 7300 Real time PCR system.

The volume distribution of the components in each well as followed-

Component	Volume
Taqman master mix	10 µL
Primer	1µL
RNAse free water	8 µL
cDNA	1 µL
Total	20 µL

The thermal cycles of qPCR were conducted as followed-

Stage	Repetitions	Temperature	Time
1	1	95.0 °C	15:00
2	40	95.0 °C	00:15
		58.0 °C	00:30
		72.0 °C	00:30

		76.0 °C	00:34
3 (Dissociation)	1	95.0 °C	00:15
		60.0 °C	01:00
		95.0 °C	00:15
		60.0 °C	00:15

Analysis of qPCR results

The quantification of the PCR is based on calculation of the fluorescence threshold, also called threshold cycle or CT value. The CT value is the PCR cycle at which reporter fluorescence significantly exceeds background fluorescence. During the first cycles of the PCR reaction, only the background or background fluorescence is measured, since the reporter fluorescence is not detectable due to the low concentration of template in the reaction vessel. At CT value amplification of product occur exponentially and there are no limiting factors in this phase of the PCR reaction, such as primer or nucleotide deficiency, decreasing enzyme activity or inhibition of PCR reaction by generation of certain products.

To determine the relative expression of mRNA, the expression of target mRNA was normalized with the housekeeping gene GAPDH as double delta CT value. To obtain more statistically meaningful comparison double delta CT values of control were normalized to 1. Relative expression of mRNA was measured in arbitrary units.

All the Taqman primers were purchased from Applied Biosystems, Darmstadt, Germany.

Human Primer	Assay ID
GAPDH	Hs99999905_m1
TNF-α	Hs00174128_m1
IFN-γ	Hs00989291_m1
TGF	Hs00998133_m1
IL2	Hs00174114_m1
IL17a	Hs00936345_m1

Murine Primer	Assay ID
GAPDH	Mm99999915_g1
iNOS	Mm00440502_m1
MCP	Mm00441242_m1
IL-6	Mm00446190_m1
IL-1b	Mm00434228_m1
Il-12b	Mm00434174_m1
TNF-α	Mm00443258_m1
Cyclooxygenase 1	Mm00477214_m1
Cyclooxygenase 2	Mm03294838_g1
VCAM	Mm01320970_m1
ICAM1	Mm00516023_m1

Tissue fixation and paraffin embedding

After euthanasia, organs and tissues of the mice were collected and kept into 10% formalin solution overnight for fixation. Afterwards the organ and tissues were dehydrated with a series of incremental concentration of ethanol followed by 100% xylene solution. Later, fixed and dehydrated organs and tissues were carefully embedded on paraffin blocks and stored at room temperature.

Dewaxing and Hydration of FFPE

Since 2 µm stained tissue sections are more suitable for microscopic observation, each formalin fixed paraffin embedded (FFPE) tissue section was cut with a thickness of 2 µm. Later, the tissue sections were placed on glass slides and incubated overnight at 37° C. Afterwards, dewaxing and hydration of the tissue sections were performed in order to remove the paraffin from the tissue and make it suitable for the staining procedure. Tissue sections were dewaxed by xylene and hydrated by different concentration of ethanol. The steps of the procedure are as followed-

-10 minutes in 100% xylene.

-6 minutes in 100% ethanol

-3 mins in 96% ethanol

-3 mins in 80% ethanol

-3 mins in 70% ethanol

-5 minutes in Distilled water (2 times)

Sirius Red/Fast Green staining

The tissue samples were stained using Sirius Red/Fast Green Collagen Staining Kit (Chondrex™, Redmond, Washington, USA) in accordance with the manufacturer's protocol. After dewaxing and hydration, the slides were dried with paper and trapping on the desk without disrupting the tissue. Sample slides were placed in a humidity chamber and each tissue section was immersed by one drop of dye solution and incubated at room temperature for 30 minutes. The chamber was covered during the period in order to avoid evaporation of dye solution. After the incubation period, tissue sections were washed with distilled water Stained tissues were dried at room temperature, covered by mounting medium and sealed by cover slips. Afterwards, the stained tissues were analyzed under the microscope. Simple light microscope was used to analyze and digital camera was used to take 15-20 pictures of perivascular regions of each kidney section and 10x magnification of the microscope was used during the process Image J is an image processing software used to analyze the photos. It is an open-source software developed by the National Institutes of Health and the Laboratory for Optical and Computational Instrumentation (Schneider CA et al., 2012, Nat Methods). Freehand selection tool was used to select the area of the vascular lumen and area of the vascular wall to determine vascular wall hypertrophy as elaborated by Zhang et al 2005.

Vascular wall hypertrophy= area of the vessel wall/area of the lumen.

CD3 positive immune cell staining

CD3 represents cluster of differentiation 3 protein complex. It is a T cell co-receptor which involves in the interaction with T cell receptor. Thus, it is widely used as marker for T cells.

The tissue sections were dewaxed and hydrated as mentioned above. Then the tissue samples were incubated with TRIS/EDTA (TE) buffer (pH 9) at 98° C for 20 minutes in order to unmask the antigens of the sample. Then the samples were incubated in room temperature for 30 minutes. Later, the tissue samples were washed with distilled water and immersed in 3% H_2O_2 for 10 minutes in order to block the enzymes. Then each tissue sample was incubated

with one drop of normal horse serum (MP-7401, Vector Laboratories, Inc., Newark, USA) for 20 minutes at room temperature. Then the serum was removed from each sample just by tapping the slides on a tissue paper. Then CD3 primary antibody (IS503, Bio Rad Laboratories, USA) was added on each tissue sample and incubated for 1 hour at room temperature followed by washing with wash buffer. Afterwards each tissue sample was incubated with one drop of anti-rabbit secondary antibody (MP-7401, Vector Laboratories, Inc., Newark, USA) for 30 minutes at room temperature. Then the tissue samples were washed 3 times with wash buffer and stained with DAB chromogen (Dako, Jena, Germany) (diluted with substrate buffer) for 3.5 - 4 minutes at room temperature for visualization. For visualizing the nuclei, the tissue samples were shortly immersed in Mayer's Hemalum solution (Merck, Darmstadt, Germany) followed by washing with water. After that, stained tissues were dried at room temperature, covered by mounting medium and sealed by cover slips. Afterwards, the stained tissues were analyzed under the microscope and 15-20 pictures of perivascular regions of each kidney section were taken using light microscope and 10x magnification of the microscope was used during the process. Multipoint tool of image J software was used to count the CD3 positive cells surrounding the perivascular regions of the kidney.

Statistical Analysis

Graphpad Prism 6 (GraphPad Software, San Diego, CA) was used for statistical analysis and graphical representation of the data. Comparative analysis between two groups at one time point were determined using either t-test or Mann-Whitney test. Two-tailed test was used to test for a null hypothesis in any direction. One-tailed t test was used to determine whether there was a difference between the groups in a certain direction. When a Gaussian distribution was assumed, unpaired t-test was used while Mann Whitney test was used when non Gaussian distribution was assumed. Comparative analysis between more than two groups were performed using one way ANOVA followed by Bonferroni multiple comparison test. Two way ANOVA followed by Bonferroni multiple comparison test was used to compare two or more groups at different time points. Data were calculated as mean ± SEM. Grubbs' test was used to identify outliers that were later excluded. Degree of significance is the probability of rejecting a null hypothesis when it is true. A significant difference was considered when probability value or *P* value is <0.05 which indicates that there is only 5% or less probability that the difference in statistical data is based on assumption. If the *P* value is greater than the level of significance, then the difference between the statistical data is considered as coincidence.

4 Results

Successful engraftment of human T cells in a humanized mouse model after transfer of human peripheral mononuclear cells (PBMCs)

To investigate the pathophysiological role and molecular mechanism of human T cells in therapy resistant hypertension, we have established a humanized mouse model in which the murine immune system was replaced by human immune cells. For this purpose, we have used an immunodeficient humanized mouse model called NSG-(K^bD^b)^{null} mouse (NOD.Cg-Prkdcscid H2-K1tm1Bpe H2-D1tm1Bpe Il2rgtm1Wjl /SzJ) because it does not have murine adaptive immunity, MHC I molecules. Therefore, incidence of graft versus host disease in this mouse strain is very low, thus making it a perfect candidate for our study.

To ensure successful engraftment, $2x10e^6$ to $5x10e^6$ human PBMCs from healthy controls were injected intravenously into NSG-(K^bD^b) ^{null} mice. After 3 weeks, flow cytometry showed sufficient presence of human CD4 and CD8 positive T cells (Fig-7A) but no murine CD3 positive cells (Fig-7B) in peripheral blood of the mice injected with human PBMCs.

Moreover, after 2 weeks of Ang II infusion, flow cytometry analysis demonstrated significant amount of CD4 and CD8 positive T cells in the spleens (Fig-7C) and kidneys (Fig-7E) of the mice injected with human PBMCs but no murine CD3 positive cells was found both in spleen (Fig-7D) and in kidney (Fig-7F) of these mice. Furthermore, immunohistochemistry of kidney tissue showed accumulation of CD3 positive cells in the kidneys of Ang II infused mice injected with human PBMCs, thus indicating successful engraftment of human T cells (Fig-7G).

(A)

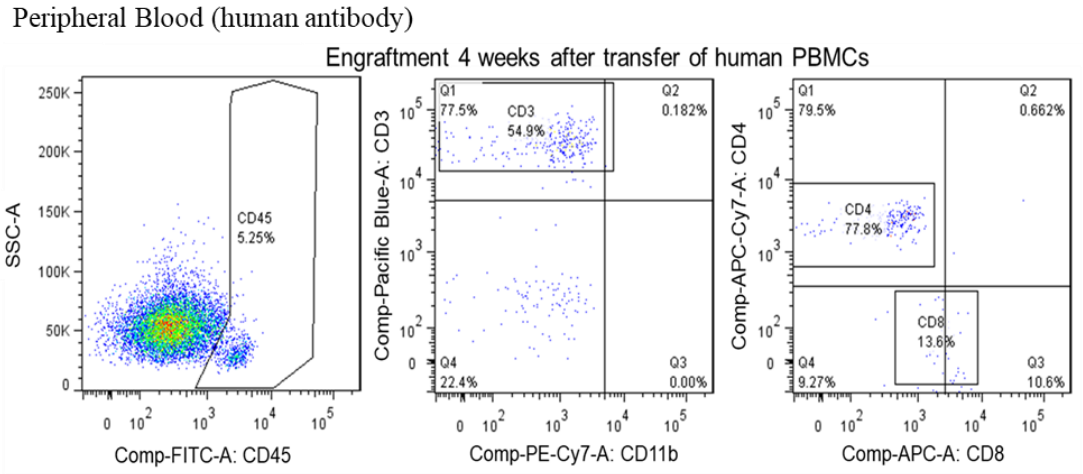

(B)

Peripheral Blood (mouse antibody)

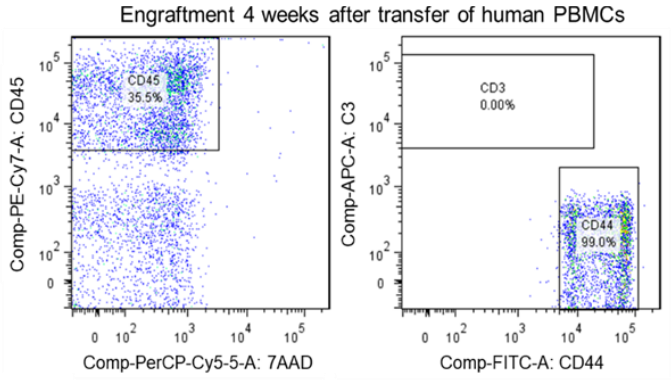

(C)

Spleen (human antibody)

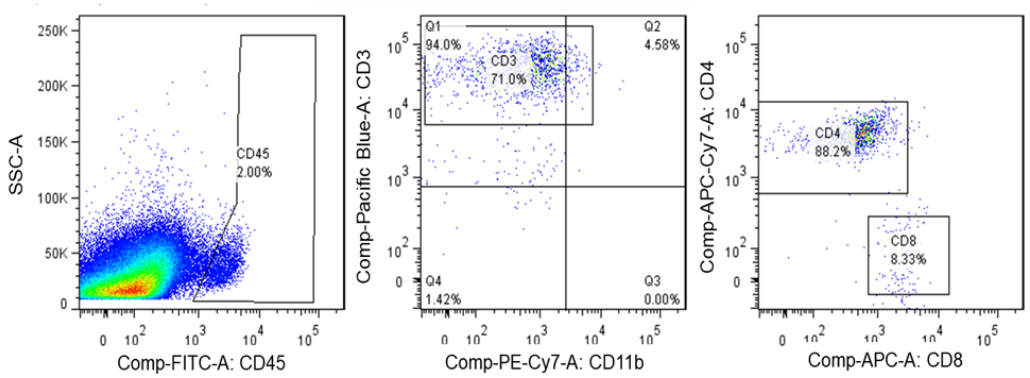

(D)

Spleen (mouse antibody)

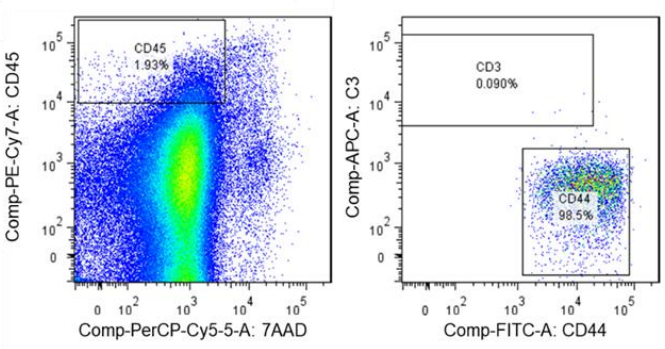

(E)

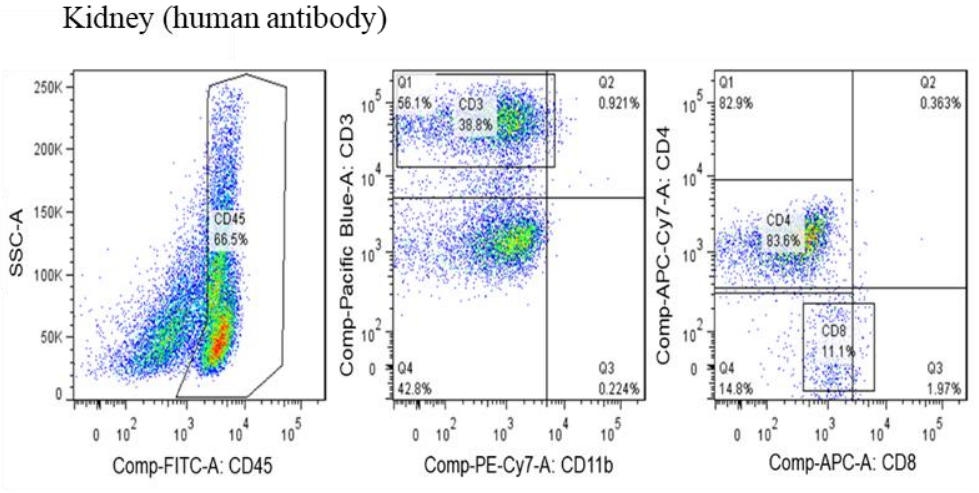
Kidney (human antibody)
SSC-A
CD45
66.5%
Comp-FITC-A: CD45
Comp-Pacific Blue-A: CD3
Q1
56.1%
CD3
38.8%
Q2
0.921%
Q4
42.8%
Q3
0.224%
Comp-PE-Cy7-A: CD11b
Comp-APC-Cy7-A: CD4
Q1
82.9%
Q2
0.363%
CD4
83.6%
CD8
11.1%
Q4
14.8%
Q3
1.97%
Comp-APC-A: CD8

(F)

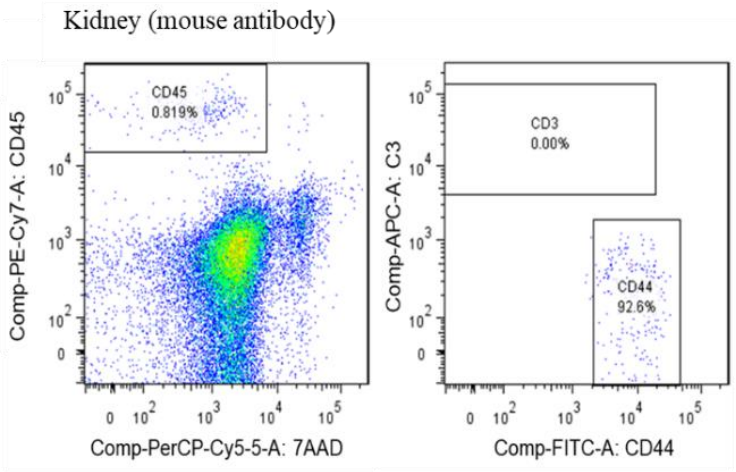
Kidney (mouse antibody)
Comp-PE-Cy7-A: CD45
CD45
0.819%
Comp-PerCP-Cy5-5-A: 7AAD
Comp-APC-A: C3
CD3
0.00%
CD44
92.6%
Comp-FITC-A: CD44

(G)

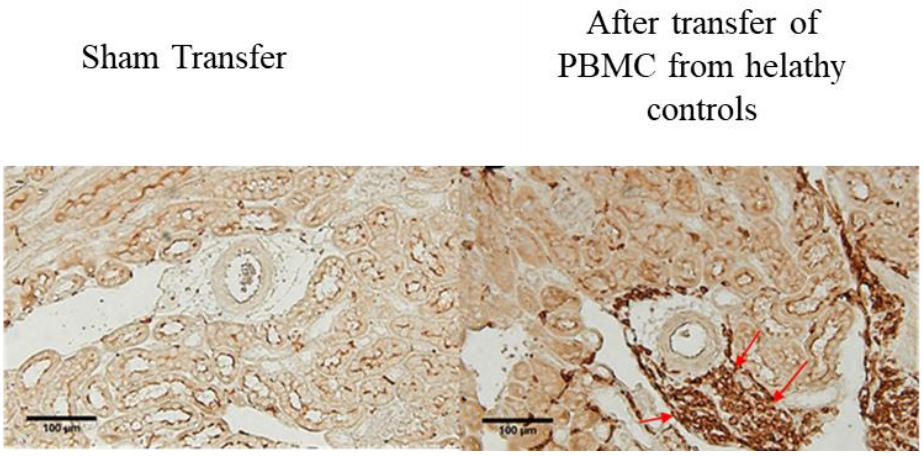
Sham Transfer
After transfer of PBMC from helathy controls
100 µm
100 µm

Figure 7: Representative-gaiting pictures showed human CD3, CD4 and CD8 positive cells in peripheral blood (Fig-7A) of the mice but no murine CD3 positive cells (Fig-7B) after 3 weeks of human PBMC injection. Moreover, representative gaiting showed presence of human CD3, CD4 and CD8 positive cells in the spleens (Fig-7C) and kidneys (Fig-7E) of humanized mice infused with Ang II for 14 days but no murine CD3 positive cells (Fig-7D and 7F). Representative pictures of immunohistological staining showed human CD3 positive cells in kidneys (Fig-7G) of angiotensin II infused NSG-(KbDb) ^{null} mice injected with human PBMCs.

Enhanced blood pressure and reduced renal endothelial dependent vasorelaxation in mice engrafted with PBMC

To investigate the role of T cell on blood pressure, systolic blood pressure was measured by tail cuff in mice engrafted with PBMC from healthy control (HC) and sham. In order to determine whether T cells influence Ang II dependent hypertension, Ang II (500 ng/kg per min) was infused in mice via osmotic minipumps for 14 days. At baseline, there is no difference in blood pressure but after infusion of Ang II, there is a rapid acceleration in blood pressure in both groups (119 ± 2 versus 115 ± 2 mmHg, P>0.05, n=5). After two weeks of Ang II infusion, there was a significant increase in systolic blood pressure in mice engrafted with healthy PBMC compared to sham (week 1, 147 ± 2 versus 130 ± 1 mmHg, P>0.05, n=5; week 2, 152 ± 2 versus 130 ±1 mmHg, *P<0.05, n=5) (Fig-8).

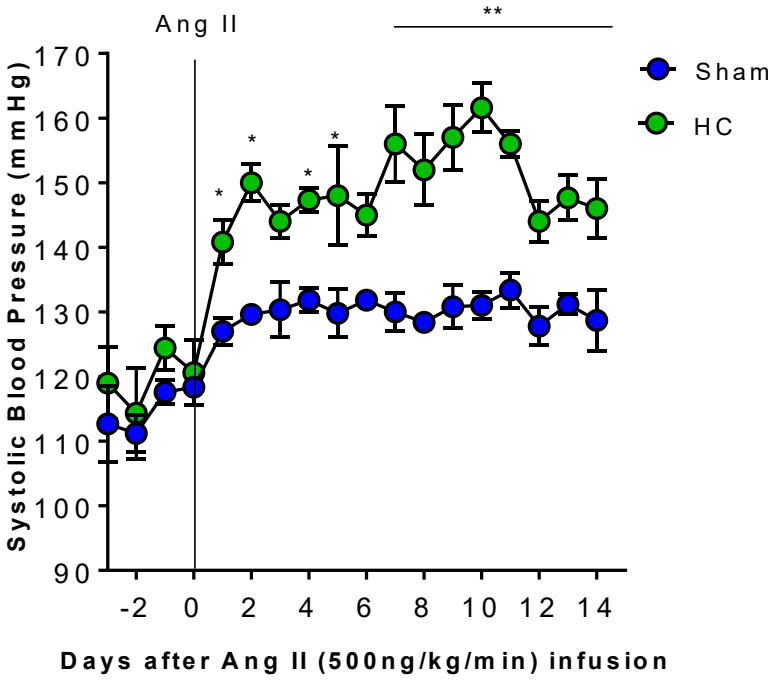

Figure 8: Increased systolic BP response during chronic Ang II infusion (Control versus Sham: baseline, 119 ± 2 versus 115 ± 2 mmHg, *P*>0.05, n=5; week 1, 147 ± 2 versus 130 ± 1 mmHg, *P*>0.05, n=5; week 2, 152 ± 2 versus 130 ± 1 mmHg, **P*<0.05, n=5 by Two-way ANOVA followed by Bonferroni multiple comparison test).

To investigate whether the accelerated blood pressure increase in mice engrafted with human PBMC affect renal endothelial function, vasorelaxation was determined *ex vivo* in isolated perfused kidneys model. Endothelial dependent vasorelaxation induced by carbachol was significantly impaired in the kidneys of the mice engrafted with healthy PBMC compared to sham indicating deteriorating effect of T cells on renal vascular function in hypertension (Fig-9).

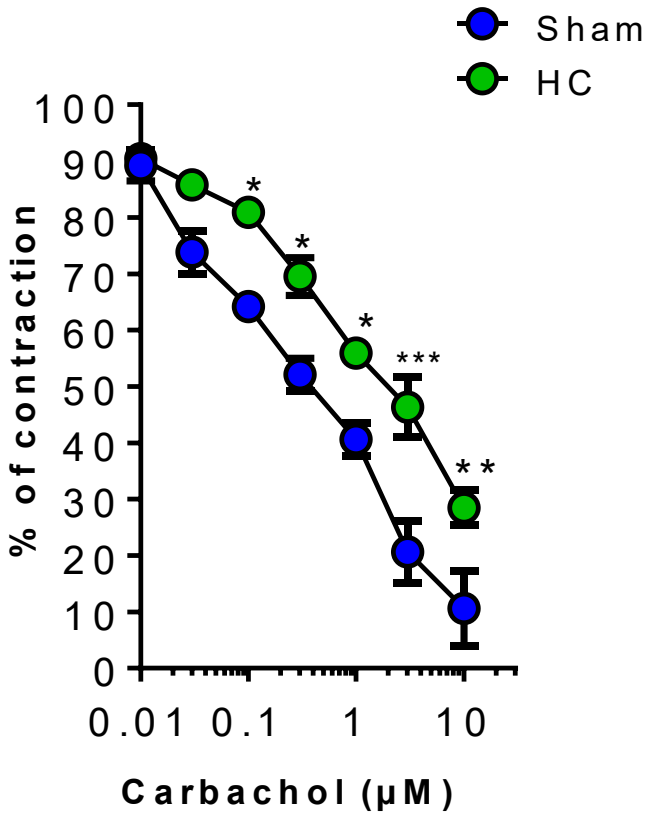

Figure 9: Endothelial-dependent renal vasorelaxation by carbachol was significantly reduced in isolated perfused kidneys of control mice (n=5) compared to Sham (n=6), **P*<0.05 by Two-way ANOVA followed by Bonferroni multiple comparison test.

Enhanced expression of pro-inflammatory cytokines by T cells activated by Angiotensin II

To check whether T cells were activated by Ang II, relative expression level of various T cell specific cytokines were measured in the kidneys of engrafted mice by real time PCR. Kidneys of successfully engrafted mice, which were infused with Ang II, have shown significantly increased mRNA expression levels of TNF-α (1.76 ± 0.6 vs 1.00 ± 0.1 A.U,*P<0.05), TGF ß (2.26 ± 0.34 vs 1.00 ± 0.12 A.U, *P<0.05) and IL-2 (3.8 ± 1.08 vs 1.00 ± 0.3 A.U,*P<0.05) and relatively higher expression of IFN-γ (3.03 ± 1.21 vs 1.00 ± 0.12 A.U, P=0.06) compared to the engrafted mice which were not treated with Ang II (Fig- 10). These results indicate that human T cells are activated by Ang II leading to increased production of these inflammatory cytokines.

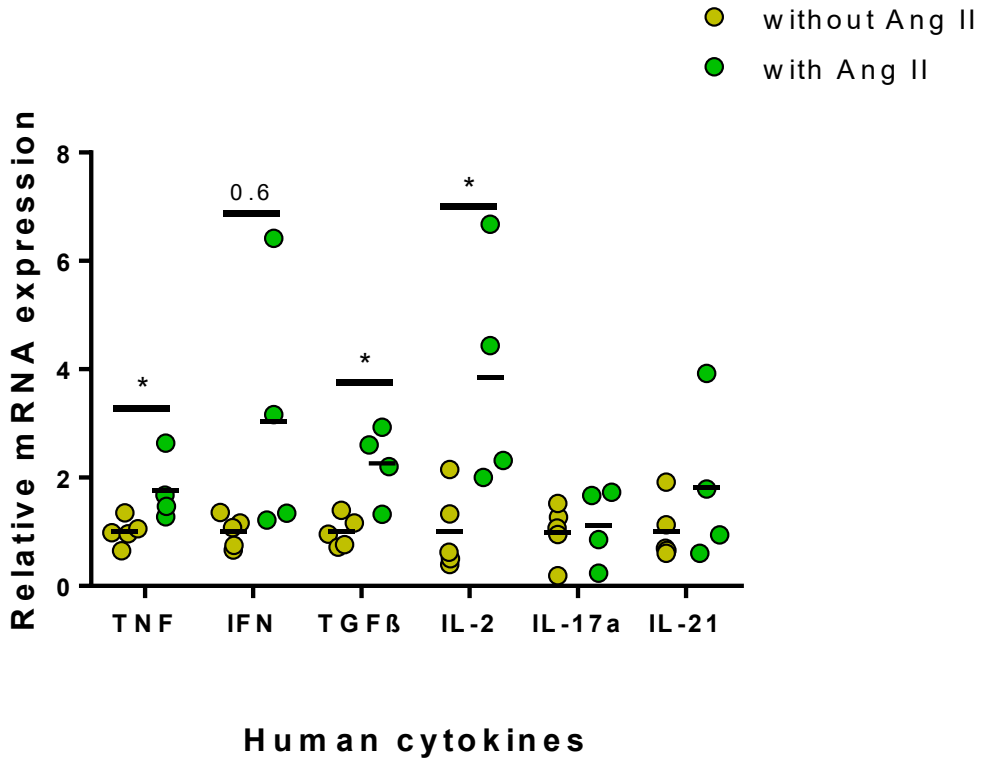

Figure 10: The relative abundance of mRNA of inflammatory cytokines in the kidney tissues of mice engrafted with human PBMC infused (n=4) and non-infused (n=4-5) with Ang II.*P<0.05 by unpaired t-test.

Influence of human T cells in renal damage in comparison to sham under hypertensive condition

To determine whether engraftment with human T cells deteriorate renal function, various parameters of renal damage were determined. The estimated glomerular filtration rate (GFR) was determined by plasma cystatin C. After two weeks of Ang II infusion, plasma cystatin C was significantly higher in HC compared to sham (Fig-11A) representing reduced estimated GFR. Moreover, renal vascular hypertrophy measured by wall to lumen ratio was significantly elevated in HC compared to sham (Fig-11B). In addition, immunohistochemical staining of CD3 positive cells showed that proportion of CD3 positive cell infiltration in the perivascular regions of the kidney was much higher in HC mice compared to sham. In HC mice, 60% of all renal perivascular regions of HC mice contained 5-19 CD3 positive cells and the remaining 40% of the renal perivascular regions of HC mice have more than 19 CD3+ cells. In contrast, 50% of the renal perivascular regions of sham mice had only 1-4 CD3 positive cell/s and remaining 50% of the renal perivascular regions did not have any CD3 positive cell at all (Fig-11C).

(A)

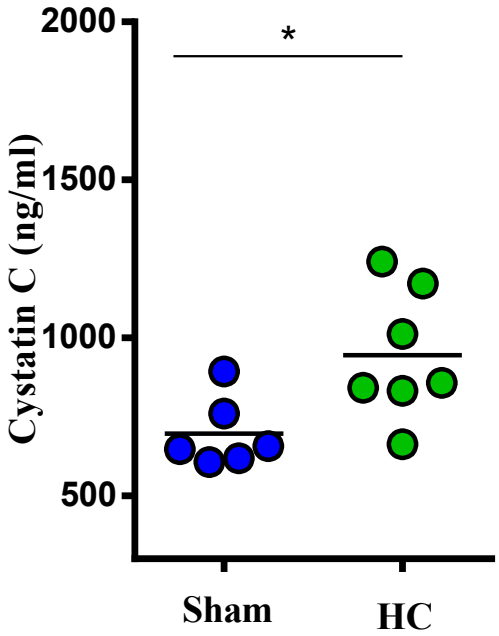

(B)

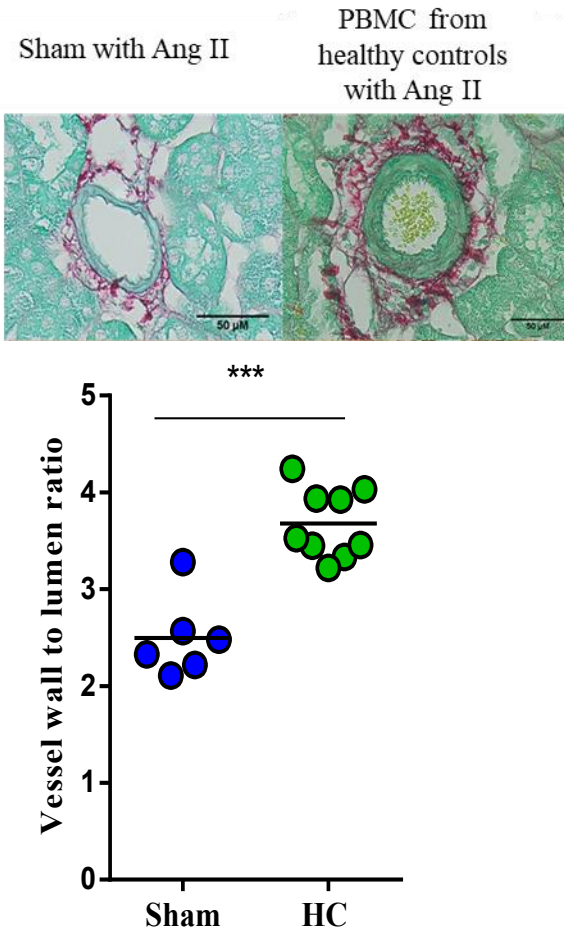

(C)

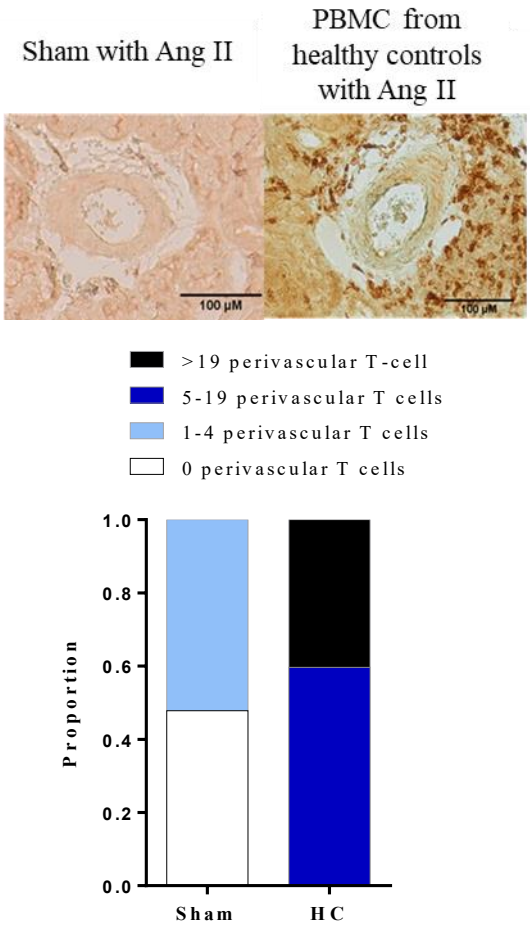

Figure 11: Engraftment with human T cells augmented renal damage during Ang II-dependent hypertension (Fig-11A) Significantly elevated plasma cystatin C in HC mice compared to sham (945 ± 77 versus 696 ± 44 ng/ml, **P*< 0.05, n=6-7 by unpaired t-test). (Fig-11B) wall/lumen ration analyzed by Sirius Red/ Fast green staining was significantly high in HC mice compared to sham (3.79 ± 0.13 versus 2.49 ± 0.17 A.U, ****P*< 0.001 n=6-7 by unpaired t-test). (Fig-11C) Increased infiltration of CD3 positive cells in the perivascular regions of the kidneys of the HC mice compared to sham.

Elevated blood pressure and reduced endothelial dependent vasorelaxation in mice engrafted with resistant hypertensive patient

After we have shown good T cell engraftment, we investigated whether T cells from resistant hypertensive patients play an important role in the blood pressure response to Ang II infusion. Therefore, mice were either engrafted with T cells from therapy resistant hypertensive patients (TRH) or T cells from healthy controls (HC) and blood pressure was measured continuously by

radiotelemetry catheter under baseline condition and during chronic Ang II infusion (500 ng/kg per min). At baseline no difference in systolic blood pressure was found between TRH and HC mice (130 ± 2 versus 131 ± 2 mmHg, $P>0.05$, n=6). On the first week of Ang II infusion, TRH mice showed significantly higher systolic blood pressure compared to HC mice (week 1, 161 ± 1 versus 135 ± 2 mmHg, *$P<0.05$, n=6; week 2, 156 ± 2 versus 140 ± 2 mmHg, $P>0.05$, n=6) (Fig- 12A). In addition, during chronic infusion of Ang II, there was no difference in heart rate between the groups (Fig-12B).

(A)

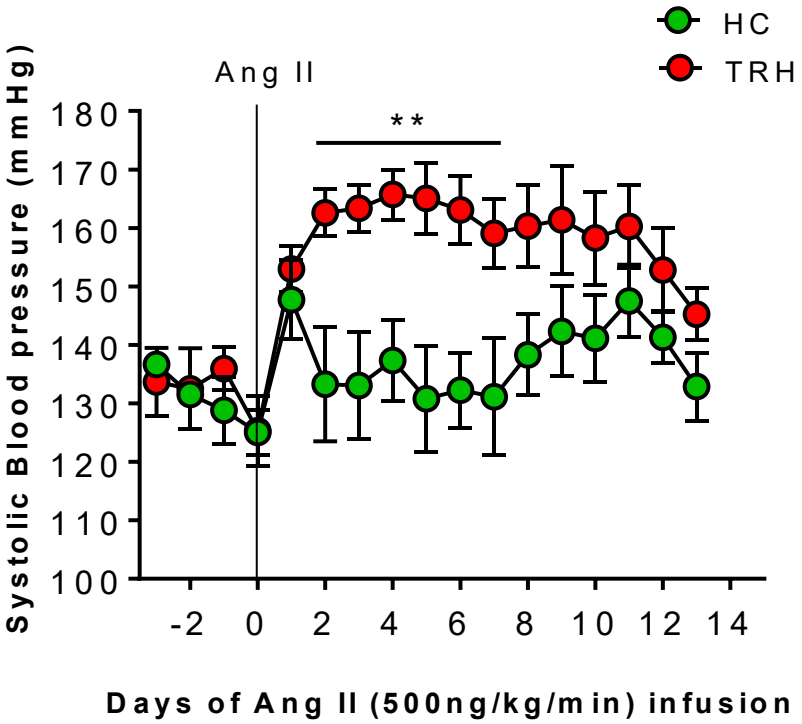

(B)

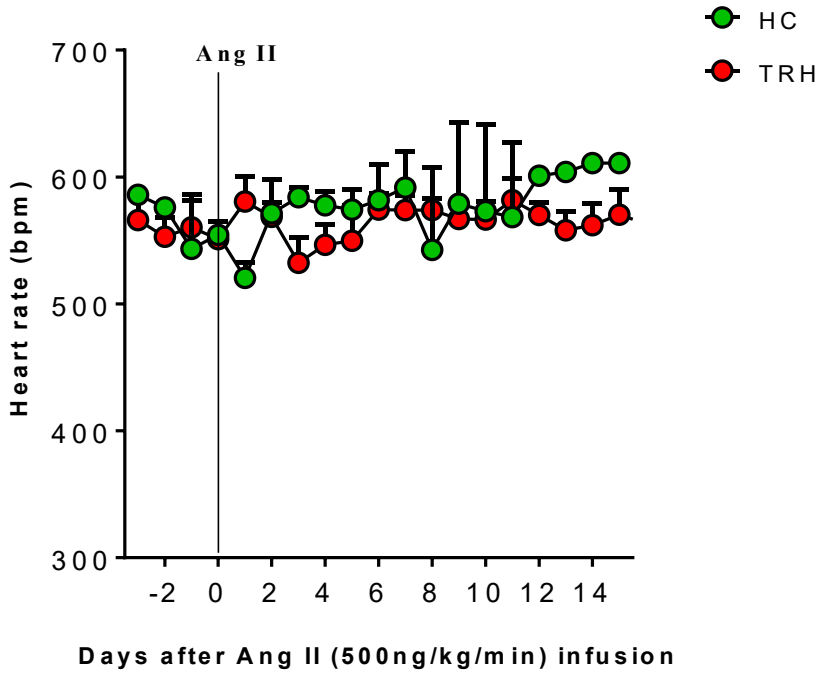

Figure 12: Exaggerated blood pressure response during chronic Ang II infusion. (Fig-12A) Systolic BP response (TRH versus HC: baseline, 130 ± 2 versus 131 ± 2 mmHg, *P*>0.05, n=6; week 1, 161 ±1 versus 135 ± 2 mmHg, **P*<0.05, n=6; week 2, 156 ± 2 versus 140 ± 2 mmHg, *P*>0.05, n=6). (Fig-12B) No change of heart rate during chronic infusion of Ang II (TRH versus HC: 563.5 ± 2.7 versus 576 ± 5.4 bpm, *P*>0.05, n=3-7) by Two-way ANOVA followed by Bonferroni multiple comparison test).

To evaluate the effect of hypertensive T cells on endothelial dependent renal vasorelaxation, *ex vivo* isolated kidneys of engrafted mice were pre-constricted by norepinephrine (1 µM). Compared with HC mice, endothelial dependent vasorelaxation induced by carbachol was significantly impaired in kidneys of TRH mice which suggests detrimental effect of T cells from resistant hypertensive patient on renal vascular function (Fig-13).

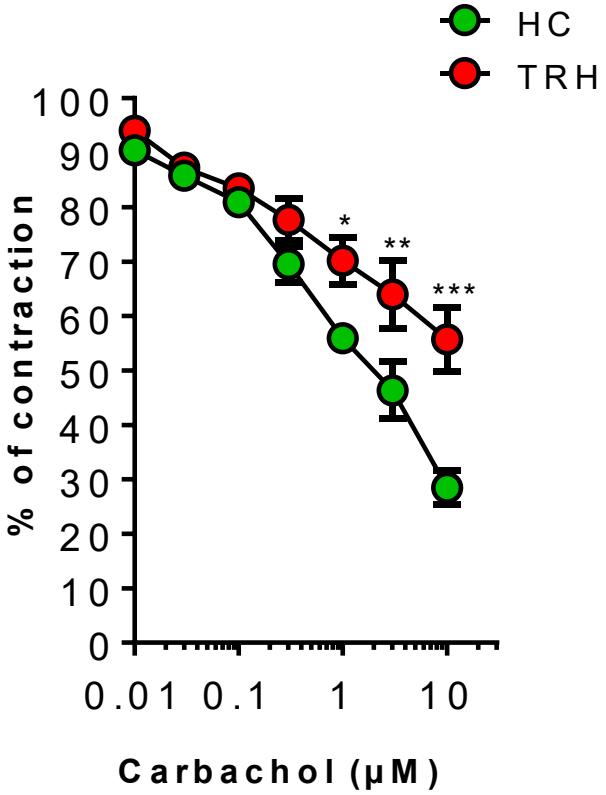

Figure 13: Endothelial-dependent renal vasorelaxation by carbachol was significantly reduced in isolated perfused kidneys of TRH mice (n=5) compared to HC mice (n=5), **P*<0.05, by Two-way ANOVA followed by Bonferroni multiple comparison test.

Increased renal infiltration of CD3+ T cell in TRH mice To investigate renal infiltration of immune cells, immunostaining of renal tissue of TRH and HC mice with anti-CD3 antibody confirmed that proportion of infiltrated CD3 positive cells was much higher in the perivascular regions of the kidneys of mice engrafted with T cells from patient indicating augmented renal damage compared to HC mice. In TRH mice, 70% of renal perivascular regions were infiltrated with >19 CD3 positive cells whereas in HC mice the proportion was only 40% (Fig-14).

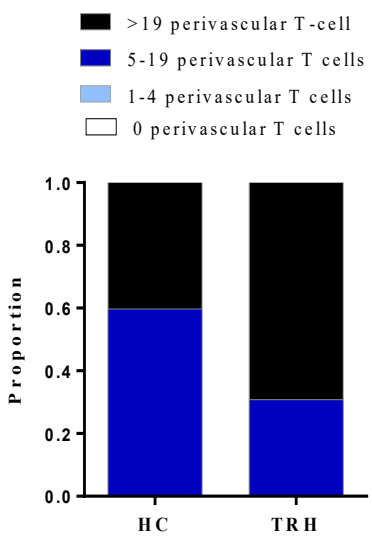

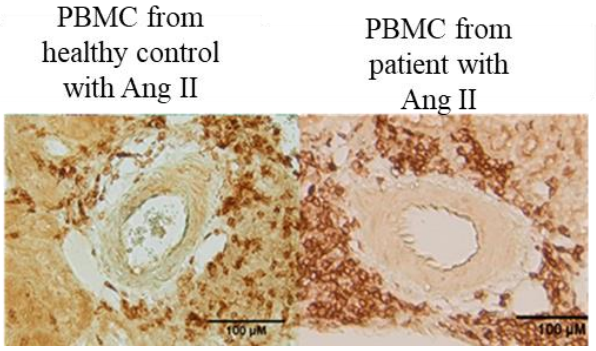

Figure 14: Increased infiltration of CD3 positive cells in the perivascular regions of the kidneys of the TRH mice compared to HC mice.

Increased splenic pro-inflammatory CD4+ T cell population in TRH mice

To find more evidence how T cells from TRH affect blood pressure and renal damage, we performed flow cytometry analysis of the spleen of the mice engrafted with T cells from patient and healthy controls under Ang II induced hypertensive condition. Flow cytometric assessment showed increased population of effector memory CD4 T-cells (CD45Ra+CCR7-) (Fig-15A) and reduced population of central memory CD4 T-cells (CD45Ra-CCR7+) (Fig-15B) in the spleen of TRH mice compared to HC mice. Moreover, Th17 subset of CD4 T-cells (CCR6+CXCR3-) (Fig-15C) were higher in the spleen of TRH mice compared to HC mice. However, no change was observed in Naïve CD4 (Fig-15D), effector CD4 (Fig-15E), Th1 (Fig-15F), Th2 (Fig-15G) and regulatory T cells (Fig-15H) subsets between two groups.

(A)

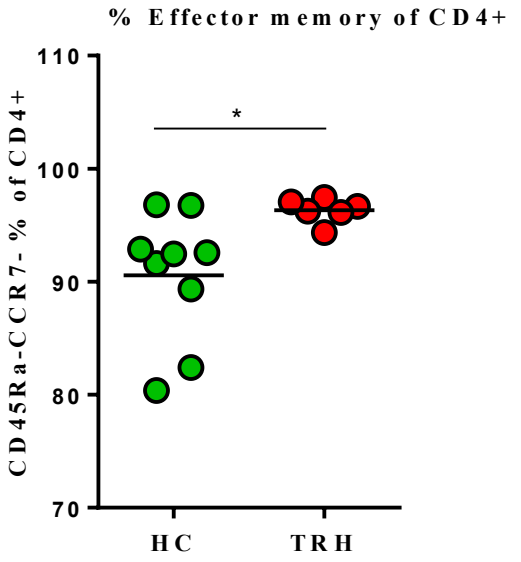
% Effector memory of CD4+
CD45Ra-CCR7- % of CD4+
110
100
90
80
70
*
HC
TRH

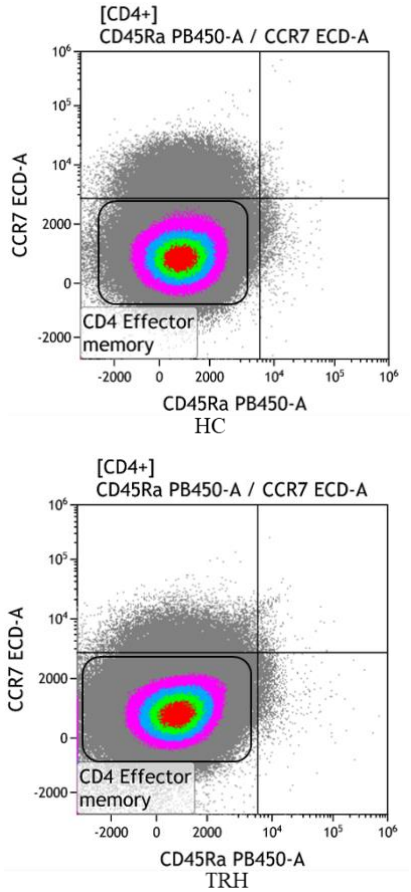
[CD4+]
CD45Ra PB450-A / CCR7 ECD-A
CCR7 ECD-A
CD45Ra PB450-A
CD4 Effector memory
HC
[CD4+]
CD45Ra PB450-A / CCR7 ECD-A
CCR7 ECD-A
CD45Ra PB450-A
CD4 Effector memory
TRH

(B)

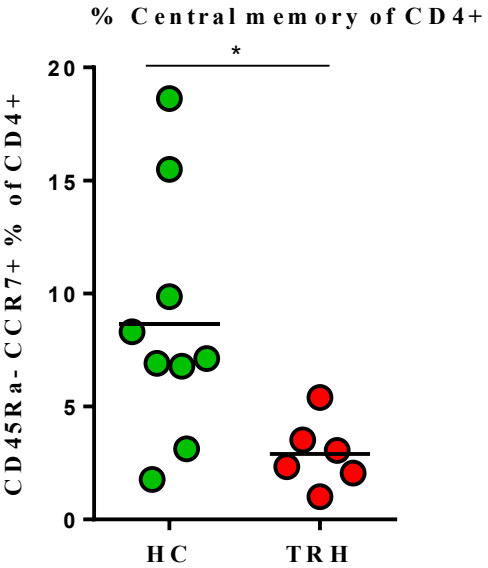
% Central memory of CD4+
CD45Ra-CCR7+ % of CD4+
20
15
10
5
0
*
HC
TRH

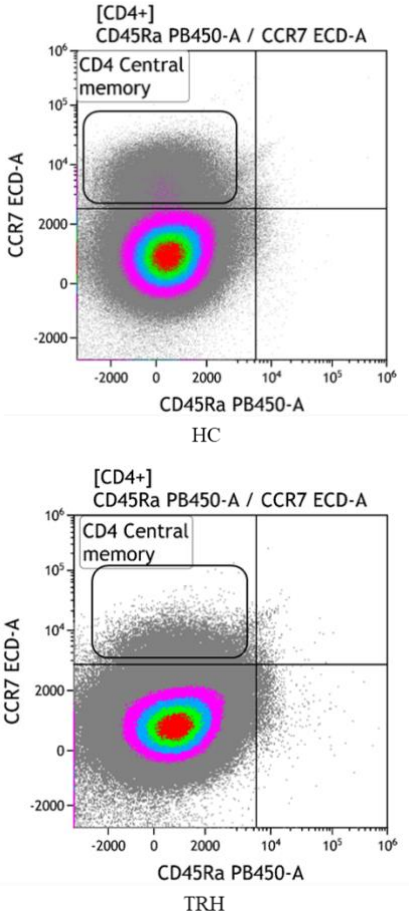
[CD4+]
CD45Ra PB450-A / CCR7 ECD-A
CD4 Central memory
CCR7 ECD-A
CD45Ra PB450-A
HC
[CD4+]
CD45Ra PB450-A / CCR7 ECD-A
CD4 Central memory
CCR7 ECD-A
CD45Ra PB450-A
TRH

(C)

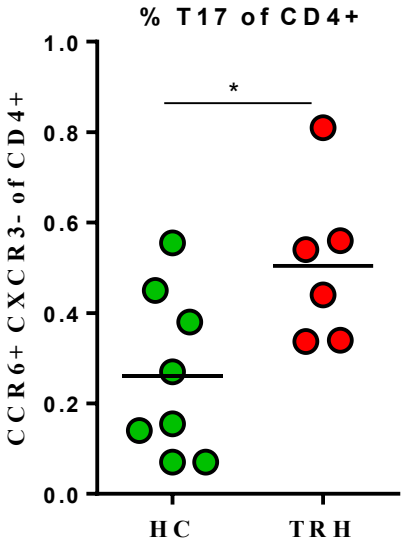
% T17 of CD4+
CCR6+ CXCR3- of CD4+
1.0
0.8
0.6
0.4
0.2
0.0
*
HC
TRH

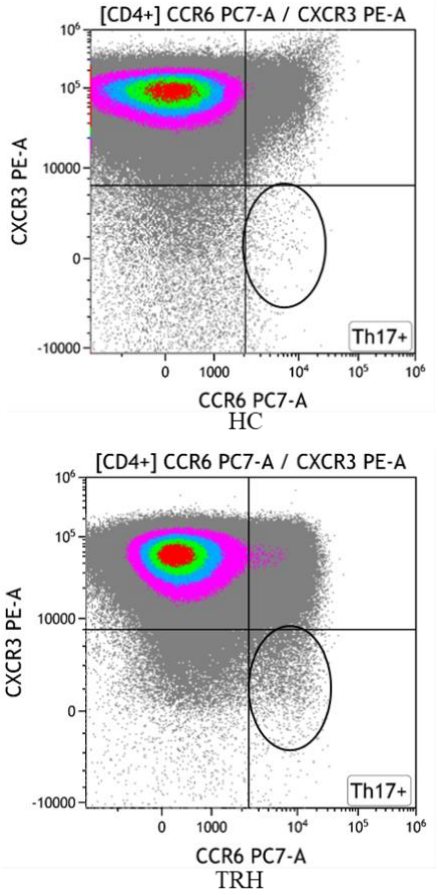
[CD4+] CCR6 PC7-A / CXCR3 PE-A
CXCR3 PE-A
CCR6 PC7-A
Th17+
HC
[CD4+] CCR6 PC7-A / CXCR3 PE-A
CXCR3 PE-A
CCR6 PC7-A
Th17+
TRH

(D)

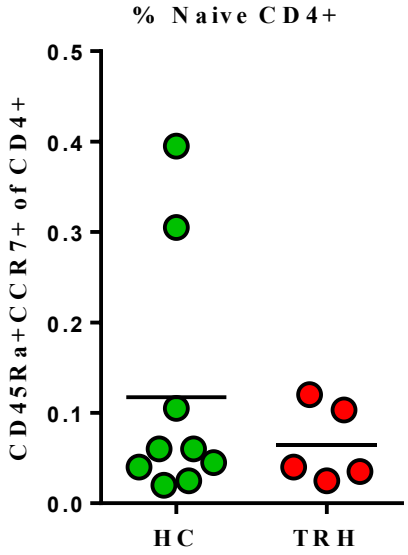
% Naive CD4+
CD45Ra+CCR7+ of CD4+
0.5
0.4
0.3
0.2
0.1
0.0
HC
TRH

(E)

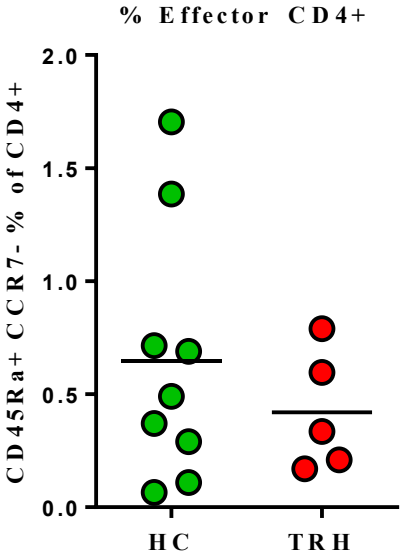
% Effector CD4+
CD45Ra+ CCR7- % of CD4+
2.0
1.5
1.0
0.5
0.0
HC
TRH

(F)

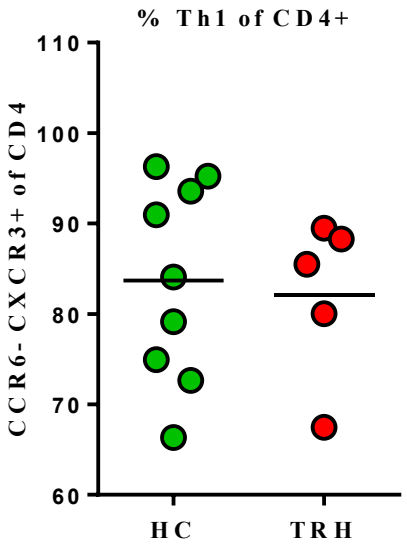

(G)

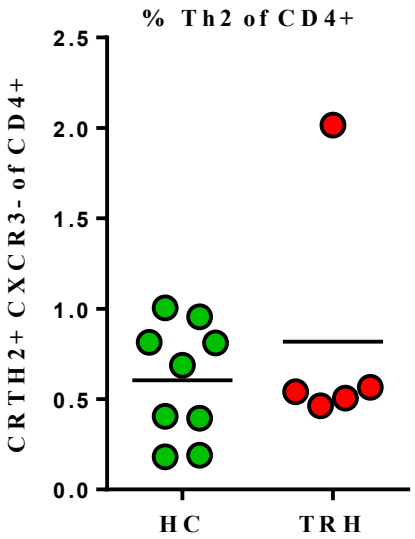

(H)

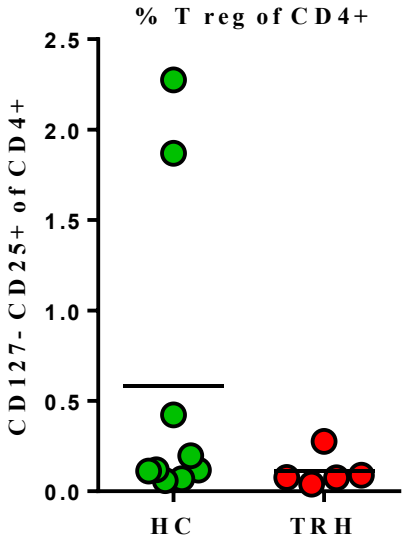

Figure 15: After 14 days of Ang II infusion, splenocytes were analyzed for effector memory (CD45Ra+CCR7-) (Fig-15A), central memory (CD45Ra-CCR7+) (Fig-15B), T helper 17 (CCR6+CXCR3-) (Fig-15C), naïve (CD45Ra+CCR7+) (Fig-15D), effector (CD45Ra+CCR7-) (Fig-15E) of CD4 T cell as well as T helper 1 (CCR6- CXCR3+) (Fig-15F), T helper 2 (CRTH2+CXCR3-) (Fig-15G) , regulatory T cell (CD127- CD25+) (Fig-15H) of CD4 subsets. HC n=9, TRH n=5-7; *P<0.05 by unpaired t-test.

No difference in splenic pro-inflammatory CD8+T cell population between HC and TRH mice

In addition, flow cytometry assessment also revelead different subpopulations of CD8 T cell in the spleen of TRH and HC mice. Astonishingly, no differences was found in the population of naïve (CD45Ra+CCR7+) (Fig-16A), effector (CD45Ra+CCR7-) (Fig-16B), effector memory (CD45Ra+CCR7-) (Fig-16C) and central memory (CD45Ra-CCR7+) (Fig-16D) CD8 T cells in the spleen of the TRH and HC mice.

(A)

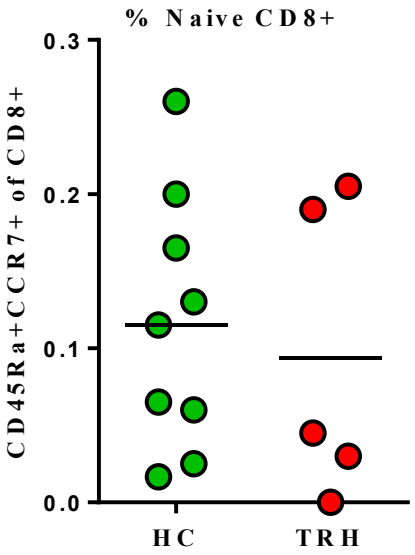

(B)

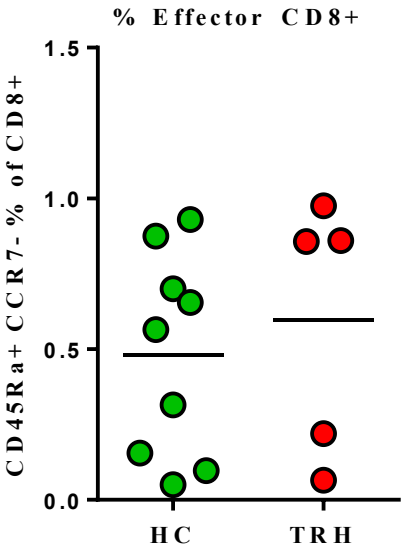

(C)

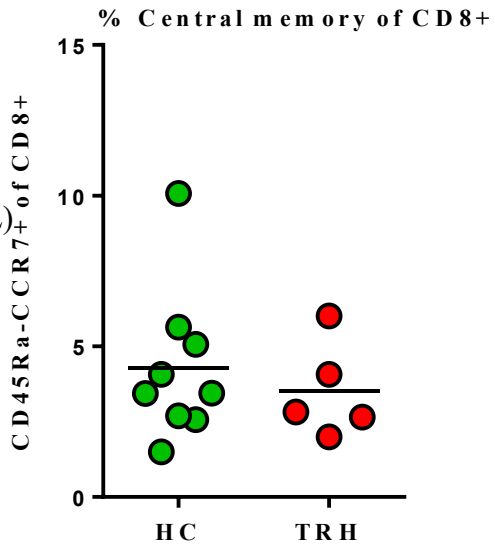

(D)

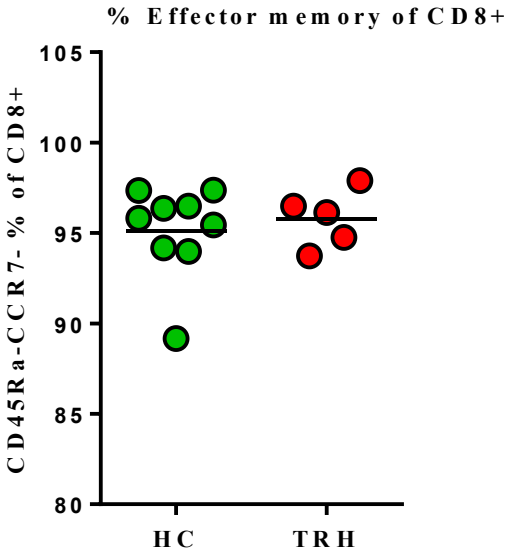

(L)

Figure 16: After 14 days of Ang II infusion, splenocytes were analyzed for naïve (CD45Ra+CCR7+) (Fig-16A), effector (CD45Ra+CCR7-) (Fig-16B), central memory (CD45Ra-CCR7+) (Fig-16C), effector memory (CD45Ra+CCR7-) (Fig-16D) of CD8 T cell. HC n=9, TRH n=5-7; *P*>0.05 by unpaired t-test.

Increased renal pro-inflammatory CD4+Tcell population in TRH mice

Since we have found increased accumulation of human CD3+ T cells in the kidneys of the mice, we performed flow cytometry analysis of the kidneys of the mice engrafted with T cells from TRH and healthy controls to investigate different subsets of T cells. After 14 days of Ang II infusion, effector memory CD4 T-cells (CD45Ra-CCR7-) (Fig-17A) increased significantly but central memory CD4 T-cell (CD45Ra-CCR7+) (Fig-17B) reduced significantly in the kidneys of mice engrafted with T cells from TRH compared to healthy controls. Flow cytometry analysis also showed increased subset of Th17 CD4 T-cells (CCR6+CXCR3-) (Fig-17C) in the kidneys of the mice engrafted with T cells from TRH compared to HC. Surprisingly, no difference in the population of naïve CD4 T cell (CD45Ra+CCR7+) (Fig-17D) and effector CD4 T cell (CD45Ra+CCR7-) (Fig-17E) as well as Th1 (CCR6-CXR3) (Fig-17F), Th2 (CRTH2+CXCR3) (Fig-17G), Treg (CD127-CD25+) (Fig-17H) CD4 T-cells were noticed in the kidneys of the mice engrafted with PBMCs from patient and healthy controls.

(A)

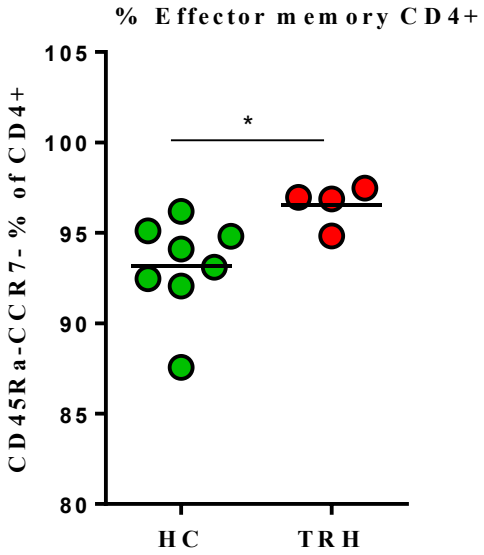

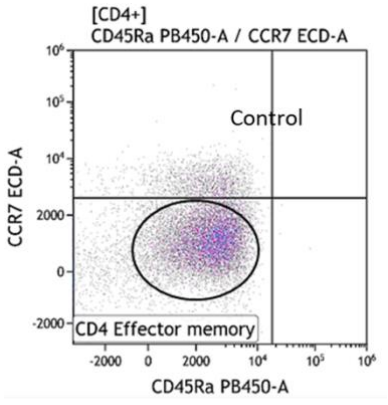

HC

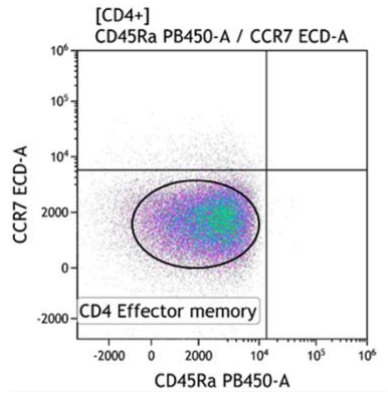

TRH

(B)

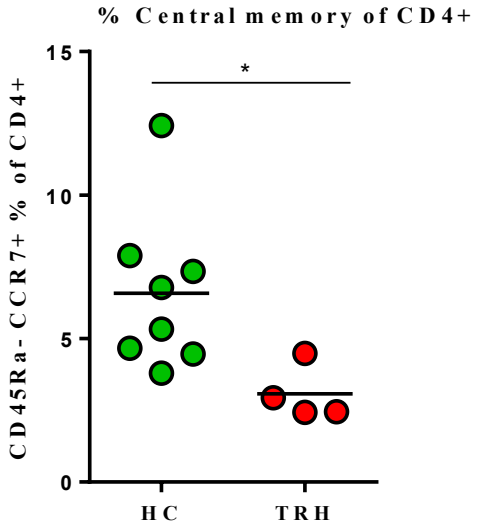

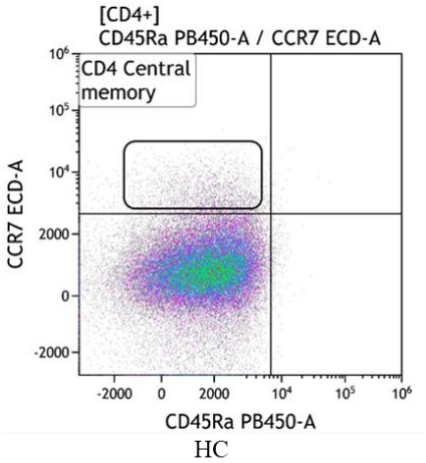

HC

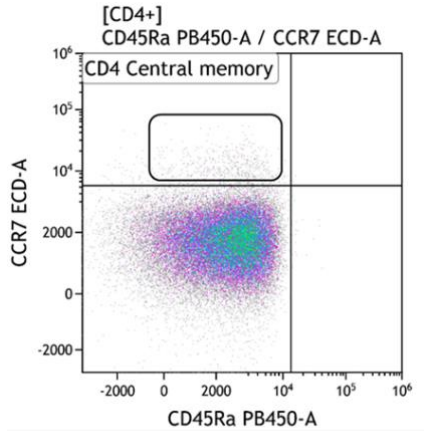

TRH

(C)

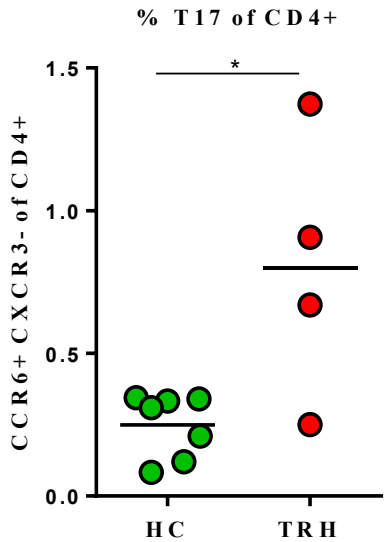

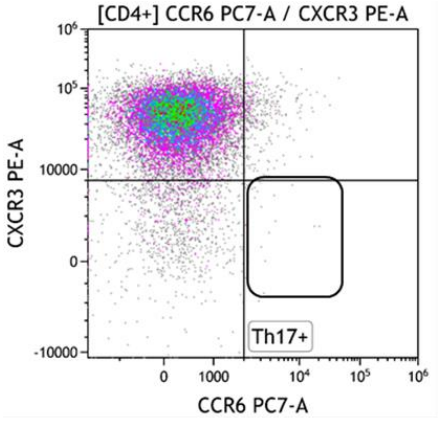

HC

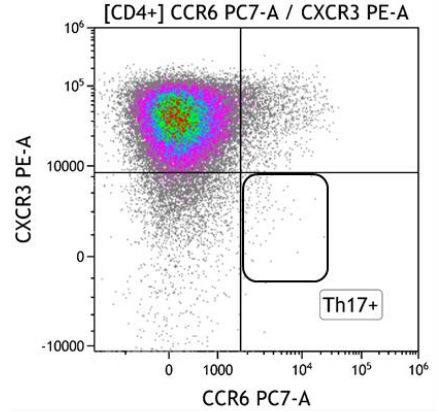

TRH

(D)

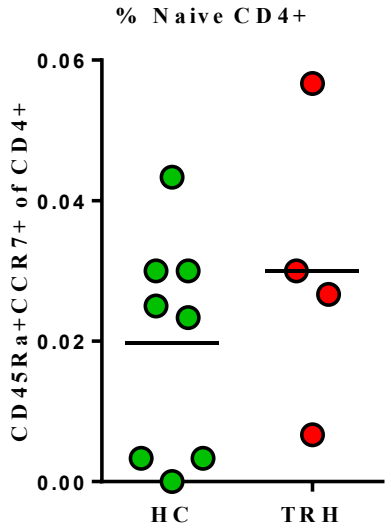
% Naive CD4+
CD45Ra+CCR7+ of CD4+
0.06
0.04
0.02
0.00
HC
TRH

(E)

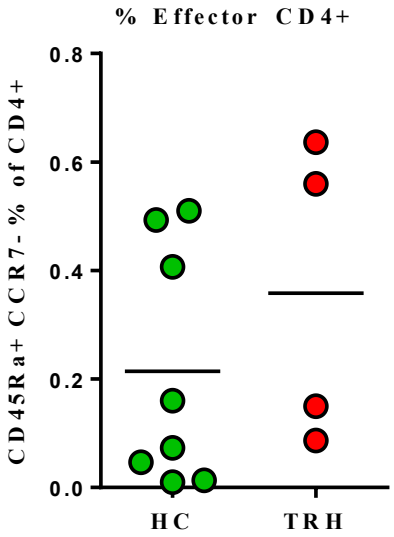
% Effector CD4+
CD45Ra+ CCR7- % of CD4+
0.8
0.6
0.4
0.2
0.0
HC
TRH

(F)

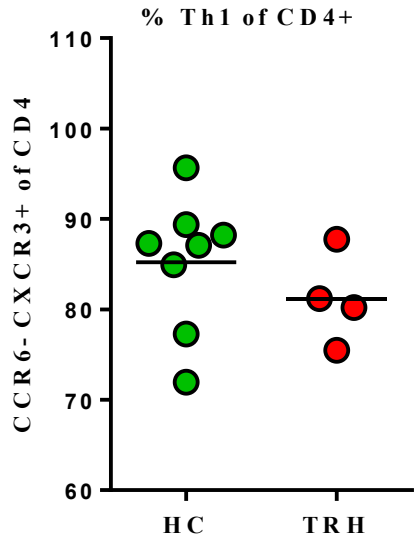
% Th1 of CD4+
CCR6- CXCR3+ of CD4
110
100
90
80
70
60
HC
TRH

(G)

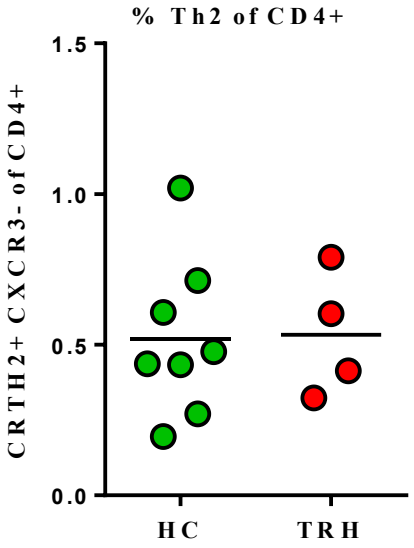
% Th2 of CD4+
CRTH2+ CXCR3- of CD4+
1.5
1.0
0.5
0.0
HC
TRH

(H)

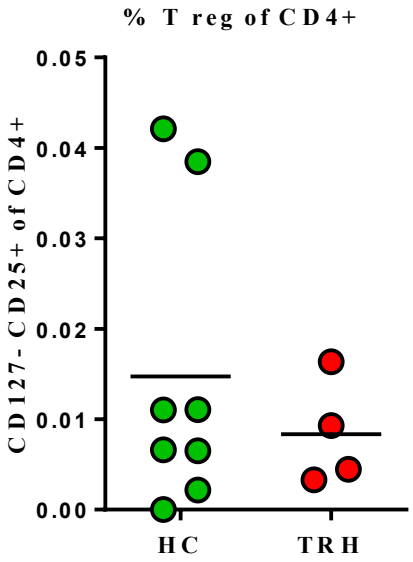

Figure 17: Flow cytometry was carried out using kidneys of TRH and HC mice to analyse effector memory (CD45Ra-CCR7-) (Fig-17A), central memory (CD45Ra-CCR7+) (Fig-17B), Th17 (CCR6+CXCR3-) (Fig-17C), naïve (CD45Ra+CCR7+) (Fig-17D), effector (CD45Ra+CCR7-) (Fig-17E), Th1 (CCR6-CXCR3+) (Fig-17F), Th2 (CRTH2+CXCR3-) (Fig-17G), Treg cell (CD127-CD25+) (Fig-17H) CD4 T cells. Control n=8, TRH n=4; **P*<0.05 by unpaired t-test.

Increased renal pro-inflammatory CD8+Tcell population in TRH mice

Moreover, flow cytometry analysis provide valuable data of CD8 T-cell populations in the kidneys of the mice engrafted with PBMC from TRH and healthy controls. After 14 days of Ang II infusion, effector memory CD8 T-cells (CD45Ra-CCR7-) (Fig-18A) increased significantly, whereas prominent decrease of central memory CD8 T-cells (CD45Ra-CCR7+) (Fig-18B) was found in the kidneys of the mice engrafted with T cells from TRH compared to healthy controls. However, no difference in the population of naïve CD8 T cell (CD45Ra+CCR7+) (Fig-18C) as well as effector CD8 T cell (CD45Ra+CCR7-) (Fig-18D) were found in the kidneys of the mice engrafted with TRH and healthy controls.

(A)

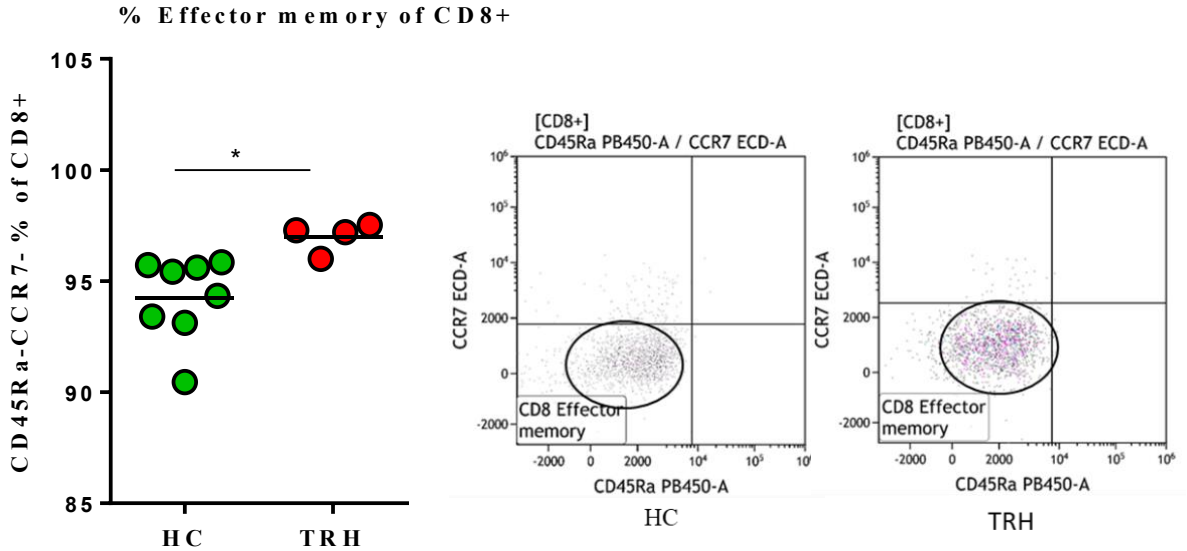

(B)

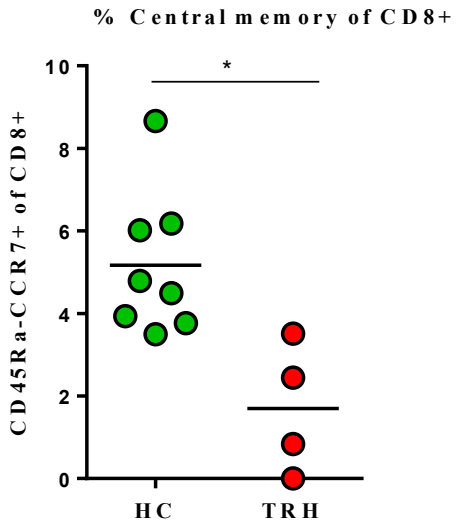
% Central memory of CD8+
CD45Ra-CCR7+ of CD8+
10
8
6
4
2
0
*
HC
TRH

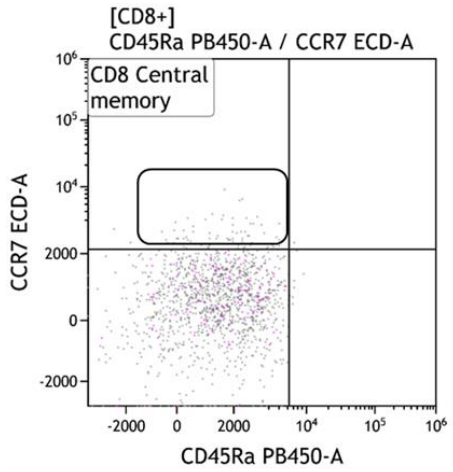
[CD8+]
CD45Ra PB450-A / CCR7 ECD-A
CD8 Central memory
CCR7 ECD-A
CD45Ra PB450-A

HC

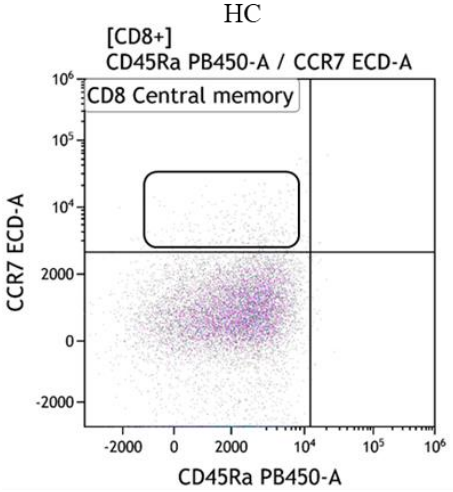
[CD8+]
CD45Ra PB450-A / CCR7 ECD-A
CD8 Central memory
CCR7 ECD-A
CD45Ra PB450-A

TRH

(C)

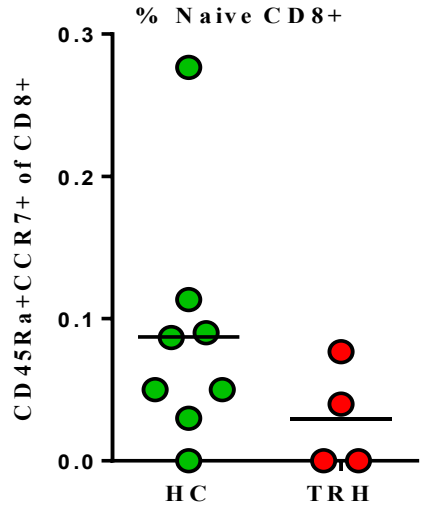
% Naive CD8+
CD45Ra+CCR7+ of CD8+
0.3
0.2
0.1
0.0
HC
TRH

(D)

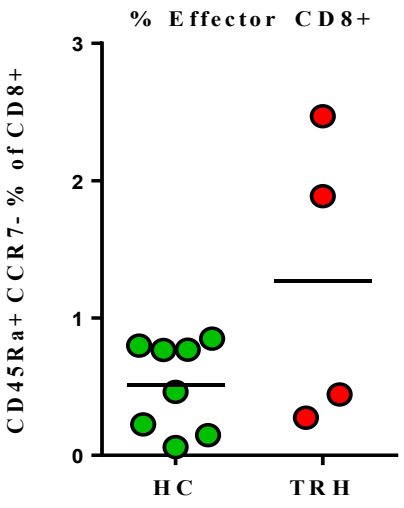
% Effector CD8+
CD45Ra+ CCR7- % of CD8+
3
2
1
0
HC
TRH

Figure 18: Flow cytometry was carried out using kidneys of TRH and HC mice to analyse effector memory (CD45Ra-CCR7-) (Fig-18A), central memory (CD45Ra-CCR7+) (Fig-18B), naïve (CD45Ra+CCR7+) (Fig-18C), effector (CD45Ra+CCR7-) (Fig- 18D) CD8 T cell. Control n=8, TRH n=4; *P<0.05 by unpaired t-test.

Increased pro-inflammation in the renal tissues of TRH mice

Since population of various human T cell subsets were higher in the kidneys of TRH mice, we assumed increased release of various pro-inflammatory cytokines by these T cell subsets in the kidneys of TRH mice. To test this hypothesis, relative abundance of various human inflammatory cytokines in the kidney tissue of the mice engrafted with PBMC from patient and healthy controls were assessed.

Relative

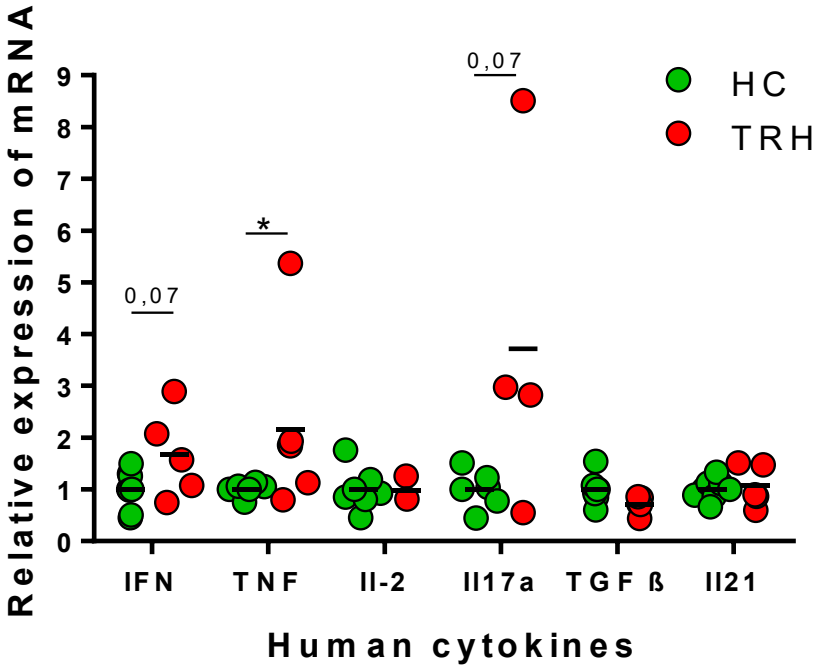

expression of pro-inflammatory cytokines such as TNF-α (1.51 ± 0.22 versus 1.00 ± 0.05 n=5-6, *P<0.05) was significantly higher in the mice engrafted with PBMC from patients compared to HC mice. Moreover, relative abundance of IFN-γ (1.67 ± 0.37 versus 1.00 ± 0.13 n=5-8, P>0.05) and IL-17a (3.71 ± 1.69 versus 1.00 ± 0.15, n=4-6, P>0.05) were relatively higher in renal tissue of TRH mice compared to HC mice. No differences in the relative abundance of IL-2, TGF ß, IL-21 were observed between the two groups (Fig-19). The elevated inflammatory cytokines in the kidneys of mice engrafted with patient PBMC represent enhanced renal inflammation due to increased number of certain pro-inflammatory T cell subsets.

Figure 19: Quantification of relative mRNA expression of inflammatory markers IFN-γ, TNF-α, IL-2, IL-17a, TGF ß, IL-21in the kidney tissue of mice engrafted with PBMC from patient and control. HC n=6-8, TRH n=3-5, *P<0.05 by unpaired t-test.

Influence of T cell from resistant hypertensive patient in exaggerated renal damage under hypertensive condition

Whether T cells from TRH exaggerate renal damage, renal function of the mice engraftment with T cells from TRH and healthy controls was determined. Plasma cystatin C was relatively higher in TRH mice indicating reduced renal function compared to HC mice (1379 ± 261 versus 945 ± 77 ng/ml, P>0.05, n=4-7 by unpaired t-test) (Fig-20B). In addition, vessel wall to lumen ratio representing renal vascular hypertrophy was significantly higher in TRH mice compared to HC mice (Fig-20A).

(A)

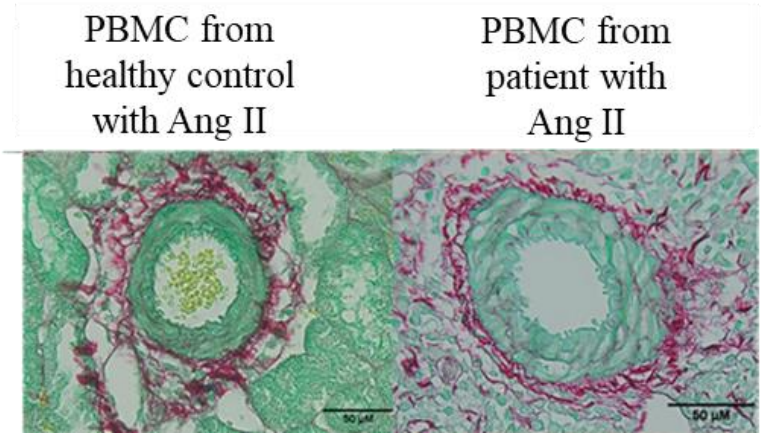

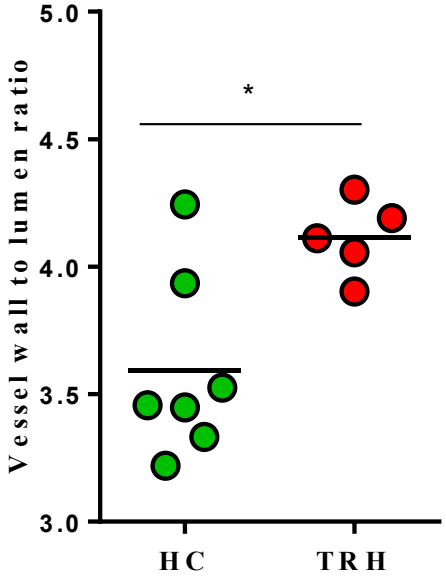

(B)

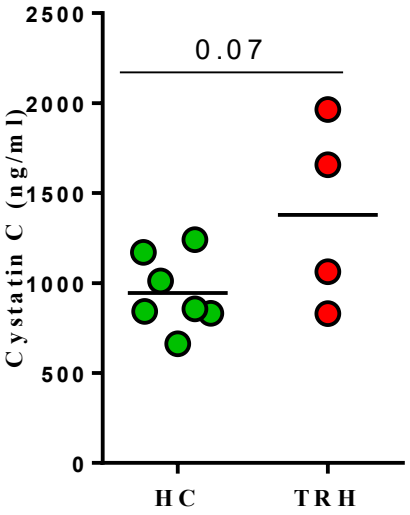

Figure 20: Engraftment with T cells from TRH exaggerated renal damage during Ang II-dependent hypertension. (Fig-20A) Renal vascular hypertrophy determined by wall to lumen ratio was significantly higher in TRH mice compared to HC mice (4.11 ± 0.06 versus 3.59 ± 0.13 A.U, **P*<0.05, n=5-7 by unpaired t-test). (Fig-20B) Plasma cystatin C was relatively higher in TRH mice compared to HC mice (1379 ± 261 versus 945 ± 77 ng/ml, *P*>0.05, n=4-7 by unpaired t-test).

Influence of human T cell on activation of murine macrophages

To check whether murine macrophages were activated differently due to engraftment of human PBMC, assessment of relative mRNA expression of various murine inflammatory cytokines were carried out in the kidneys of mice engrafted with PBMCs from patient and normotensive controls. Remarkably, no differences in relative abundance of iNOS (1.0 ± 0.1 versus 0.79 ± 0.09 A.U, *P*>0.05), MCP (1 ± 0.34 versus 0.42 ± 0.18 A.U, *P*>0.05) 1, IL-1b (1.0 ± 0.2 versus 1.7 ± 0.59 A.U, *P*>0.05), IL-6 (1.0 ± 0.38 versus 0.11 ± 0.04 A.U, *P*>0.05), TNF-α (0.912 ± 0.29 versus 2.9 ± 1.4 A.U, *P*>0.05), IL-12b (1.0 ± 0.91 versus 1.5 ± 0.67 A.U, *P*>0.05) were

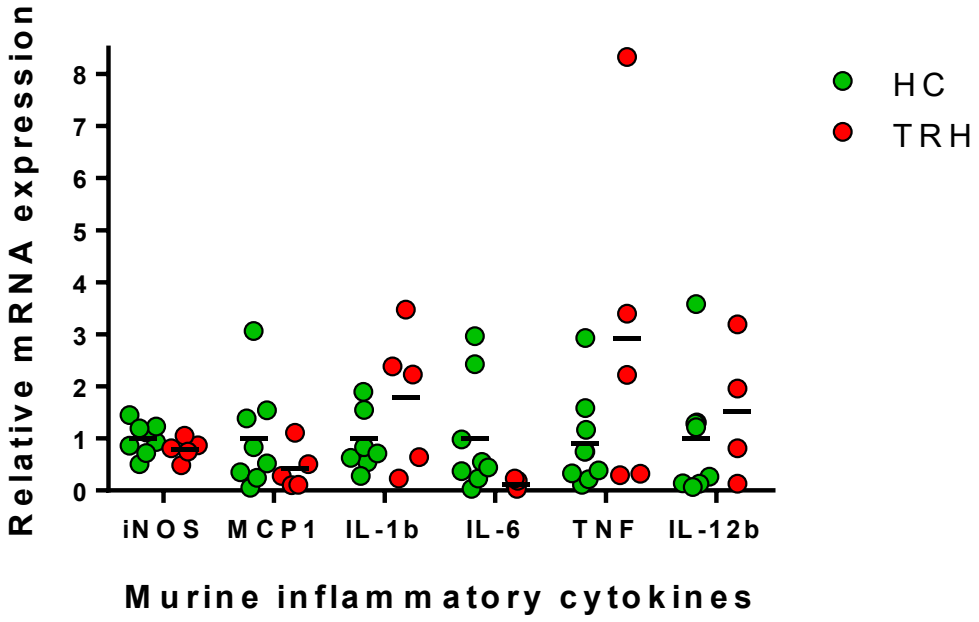

Figure 21: Relative abundance of mRNA of murine inflammatory cytokines in the kidney tissue of mice engrafted with patient and control PBMC. Control n=5-9; TRH n=3-5, *P*>0.05 by unpaired t-test.

detected between HC and TRH mice indicating human T cell did not play any role in the activation of murine macrophages (Fig-21).

Influence of human T cells in renal cyclooxygenase (COX) associated blood pressure modulation

As renal COX1 and COX 2 involve in natriuresis and blood pressure regulation, we have measured relative mRNA abundance of COX1 (1.0 ± 0.12 versus 0.87 ± 0.10 versus 0.88 ± 0.26 A.U, *P*>0.05) (Fig-22A) and COX 2 (1.0 ± 0.05 versus 2.66 ± 1.07 versus 1.18 ± 0.37 A.U, *P*>0.05) (Fig-22B) in the renal tissue of sham, HC and TRH mice, respectively. Interestingly, no change in the mRNA expression of COX 1 and COX 2 was detected among the groups.

(A)

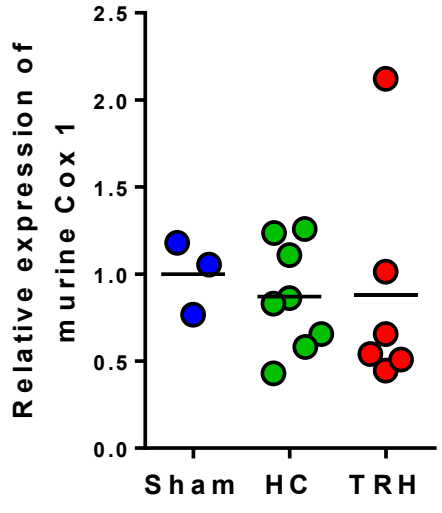

(B)

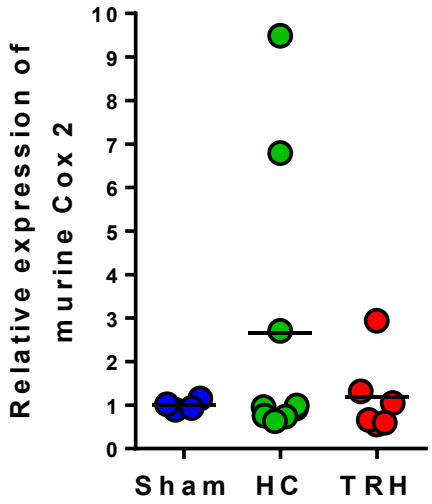

Figure 22: Relative mRNA expression of murine (Fig-22A) COX 1 and (Fig-22B) COX 2 in the kidney tissues of mice engrafted with PBMC from patient (TRH), normotensive controls and sham. Sham n=3-4, control n=8, THR n=5-6; *P*>0.05 by one way ANOVA followed by Bonferroni multiple comparison test.

Interaction between human cytokines and mouse renal tissue

To verify whether human cytokines interact with mouse renal tissue, we performed *in vitro* experiments in which mouse kidney slices were incubated with human TNF-α (0.1 ng/mL) for different periods of time. Mouse renal tissue treated with mouse TNF-α was used as positive control. Then assessment of relative abundance of various adhesion markers were carried out. After 6 hours of incubation, relative expression of mouse ICAM was significantly higher in the renal tissue of mice treated human TNF-α compared to sham (1.98 ± 0.21 versus 1.00 ± 0.1 A.U,**P*<0.05). Moreover, relative expression of VCAM was relatively higher in mouse tissue treated with human TNF-α compared to sham (1.67 ± 0.17 versus 1.00 ± 0.1 A.U, *P*>0.05). Furthermore, relative expression of both ICAM (2.70 ± 0.36 versus 1.00 ± 0.1 A.U, **P<0.05*) (Fig-23A) and VCAM (1.63 ± 0.02 versus 1.00 ± 0.1 A.U, **P*<0.05) (Fig-23A) were significantly higher in mouse tissue treated with mouse TNF-α compared to sham. No difference was observed in the expression of murine VCAM and ICAM between the tissues treated with mouse and human TNF-α. However, no changes in the expression of these markers were noticed at other time periods between the groups.

(A)

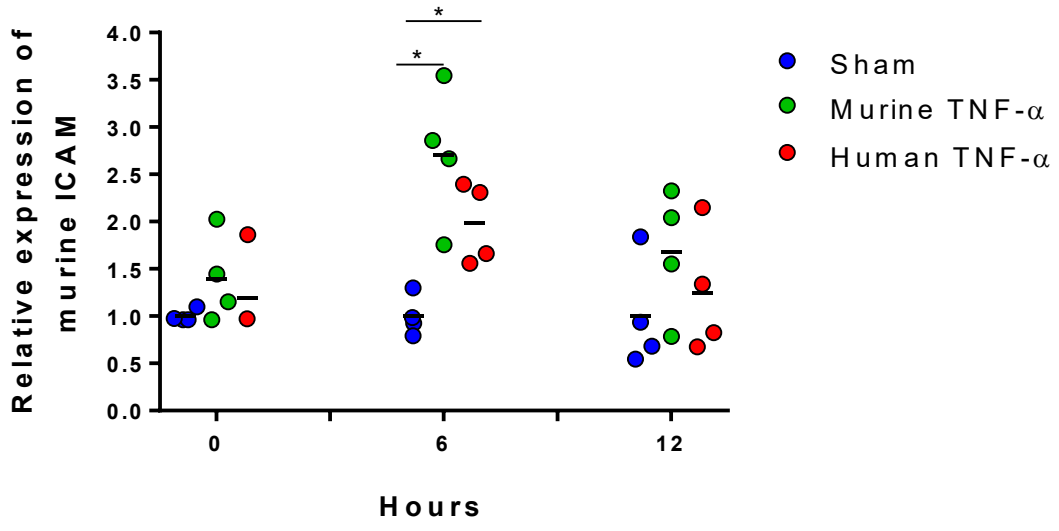

(B)

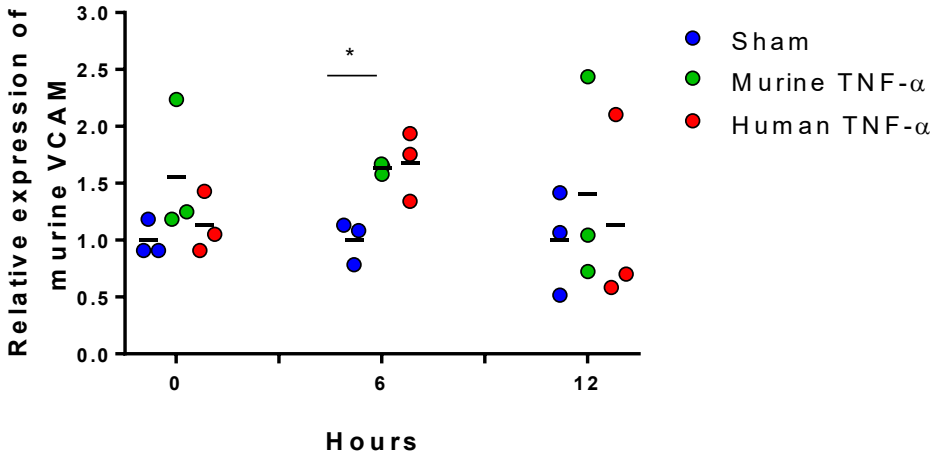

Figure 23: Relative abundance of mRNA of murine adhesion molecules ICAM (Fig-23A) and VCAM (Fig-23B) in the kidney tissues treated with saline, murine and human TNF-α, respectively at 0, 6 and 12 hours of intervals, *P<0.05; n=3-4 by Mann Whitney test.

To test whether human IFN-γ interacts with renal tissue of the mice, similar *in vitro* experiments were conducted where kidney slices were incubated with mouse and human IFN-γ at different time periods followed by assessment of relative abundance of interferon gamma induced protein 10 (CXCL10). After 12 hours of incubation, although relative expression of CXCL10 was higher in the tissues treated with human IFN-γ compared to sham, difference in relative abundance of CXCL10 between the groups was not statistically significant. (Fig-24).

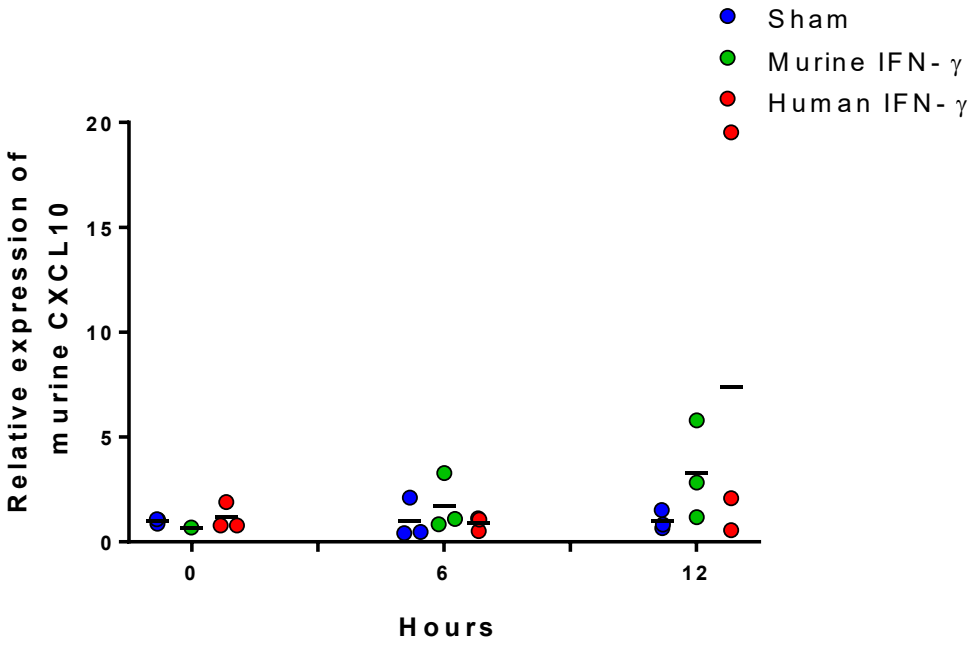

Figure 24: Quantification of relative abundance of mRNA of murine CXCL10 in kidney tissues treated with saline, murine IFN-γ (100 U/mL) and human IFN-γ (100 U/mL), respectively at 0, 6 and 12 hours of intervals. *P*>0.05; n=3 by Mann Whitney test.

No difference was observed in mRNA expression of CXCL10 at other time points between the groups (Fig-24).

In vitro treatment of murine aorta with human TNF-α leads to severe vascular dysfunction

Since human TNF-α interacts with mouse tissue, we assumed it might also affects vascular function of the mice. To test whether human TNF-α impede the vascular function of the mice, we incubated isolated thoracic aorta of the mice in human TNF-α (4 nM) for 22 hours and performed wire myography. Carbachol induced endothelial dependant vasorelaxation of the aorta treated with human TNF-α was significantly reduced compared to sham indicating effect of TNF-α on severe vascular impairment (Fig-25).

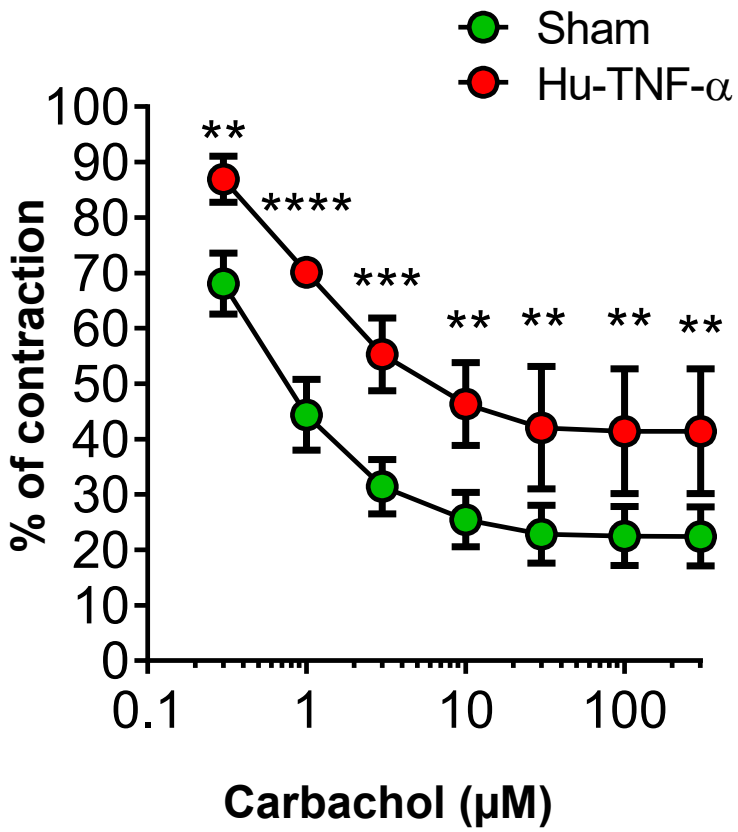

Figure 25: Cumulative concentration curve in response to carbachol (0.3-300 μM) in aortic rings treated with human TNF-α and sham for 22 hours. Endothelial dependent vasorelaxation was expressed as percentage of contraction induced by norepinephrine. Values are means ± SE; n=3-6; **P*<0.05, ***P*<0.01, ****P*<0.001. Two-way ANOVA followed by Bonferroni multiple comparison test.

Influence of human T cells in NO pathway associated blood pressure modulation

Since urinary excretion of NO2/NO3 directly associated with regulation of blood pressure, we analysed NO2/NO3 content in the urine of HC and TRH mice. No difference in urinary excretion of NO2/NO3 between HC and TRH was detected indicating human T cell did not interact with NO pathway to modulate blood pressure (Fig-26).

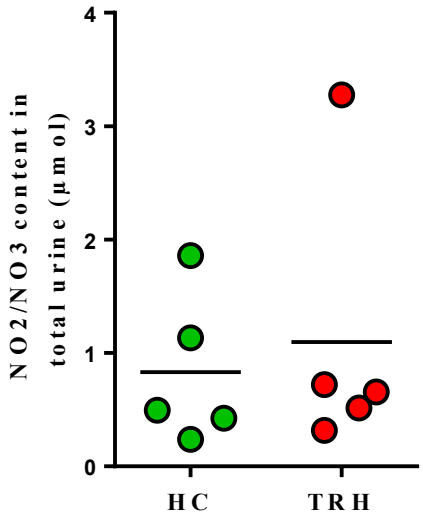

Figure 26: No difference in urinary excretion of NO2/NO3 content (HC versus TRH: 0.83 ± 0.29 versus 1.09 ± 0.54 μmol, n=5; *P*>0.05 by unpaired t-test).

TNF-α inhibitor, etanercept attenuates Ang II induced hypertension without affecting T-cell subpopulation

To test whether inhibition of human TNF-α reverses the aggravated hypertension in TRH mice, one group of TRH mice was treated with a TNF inhibitor, etanercept (0.8 mg/KG) (treated) whereas another group of TRH mice was treated with sham injection (non-treated). Etanercept binds with TNF and prevent its binding to its respective receptors thus inhibiting its biological function. At baseline, no difference in systolic BP (136 ± 2 versus 141 ± 1 mmHg, *P*>0.05,

n=6-7) was observed between the two groups but after initiation of Ang II infusion, blood pressure elevated rapidly in both groups of the mice. However, non-treated mice demonstrated continuous rise in blood pressure compared to treated mice. After 7 days of chronic Ang II infusion, systolic BP (week 1, 136 ± 2 versus 159 ± 4 mmHg, $P>0.05$, n=6; week 2, 130 ± 2 versus 163 ± 1 mmHg, $*P<0.05$, n=6) (Fig-27A) differ significantly between the groups indicating the prominent role of human TNF-α in Ang II dependent hypertension. However, no changes in heart rate were found between the groups (Fig-27B).

(A)

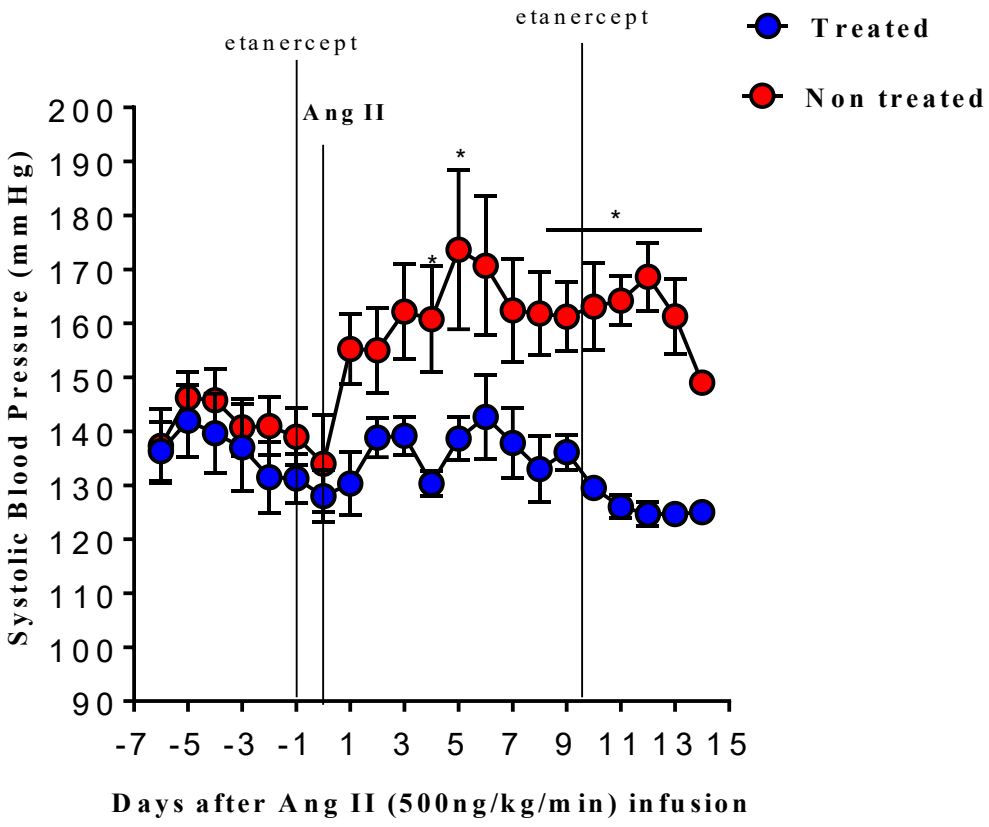

(B)

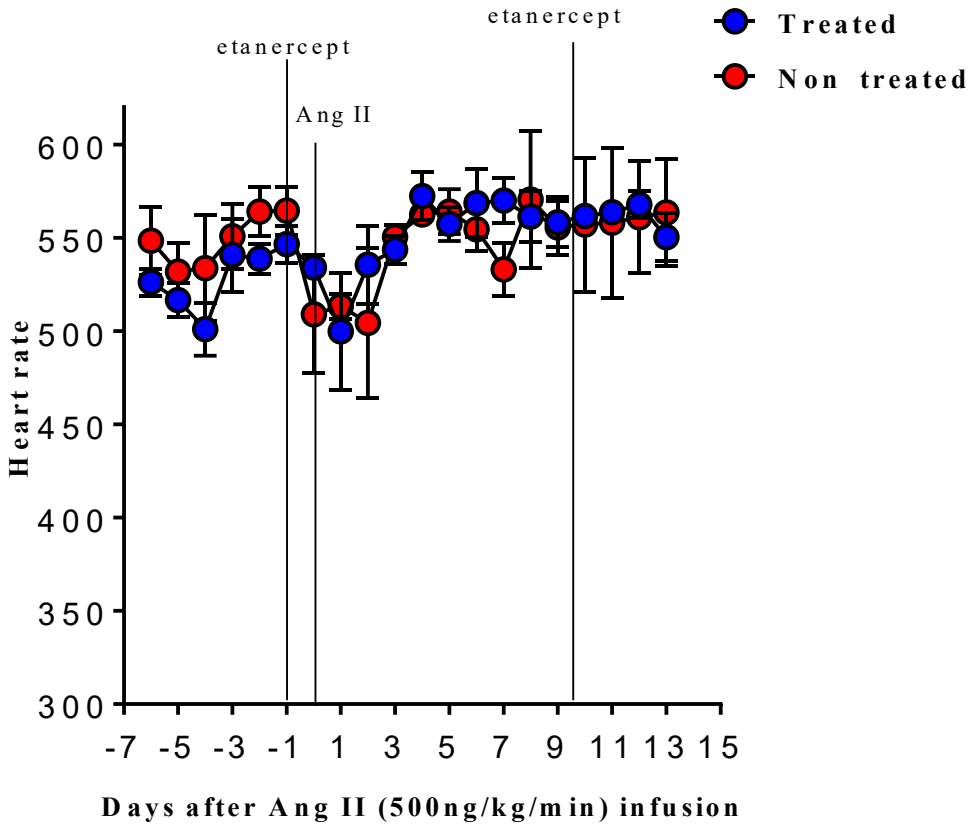

Figure 27: Etanercept attenuates Ang II dependent hypertension. (Fig-27A) Systolic BP response (treated versus non-treated: baseline, 136 ± 2 versus 141 ± 1 mmHg, *P*>0.05, n=6-7; week=1, 136 ± 2 versus 159 ± 4 mmHg, *P*>0.05, n=6; week 2, 130 ± 2 versus 163 ± 1 mmHg, **P*<0.05, n=6). (Fig-27B) After chronic infusion of Ang II, no changes in heart rate was found between the groups (treated versus non treated: 545 ± 4.8 versus 547 ± 4.9 bpm *P*>0.05, n=6-7) by Two-way ANOVA followed by Bonferroni multiple comparison test).

In order to check whether etanercept affects regulation of T-cell subsets, flow cytometry analysis was carried out using splenocytes of the TRH mice treated and non treated with etanercept. Surprisingly, no changes were detected in the subsets of CD4 as well as CD8 T-cell between the groups indicating etanercept reduces the blood pressure by inhibiting human TNF-α without interfering subpopulations of T cells. However, there was a tendency of downregulation of effector memory (Fig-28C), Th17 (Fig-28E) CD4 T cells and upregulation of central memory (Fig-28B), and Treg CD4 T (Fig-28H) cell subsets in the splenocytes of treated mice compared to non treated mice.

(A)

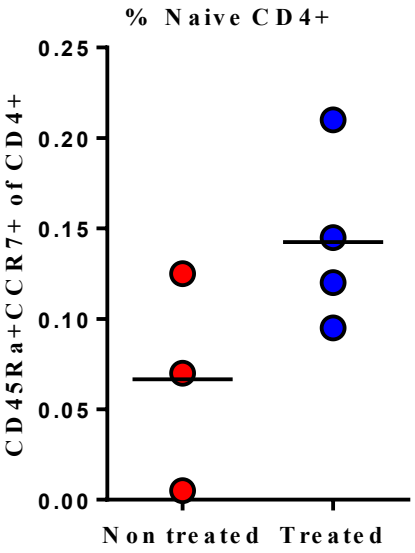

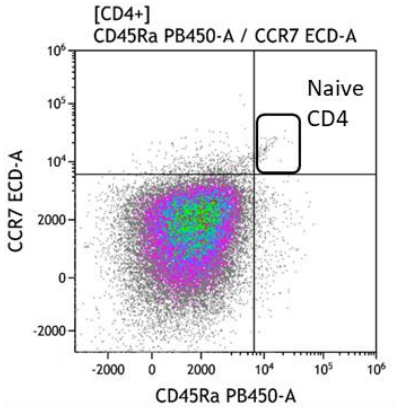

Treated

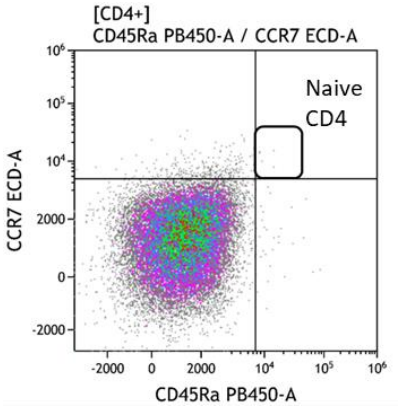

Non- treated

(B)

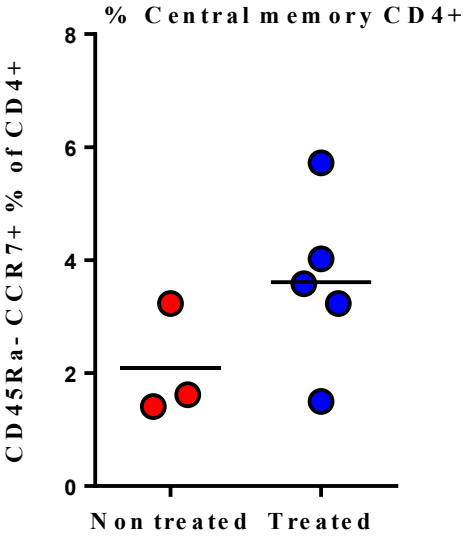

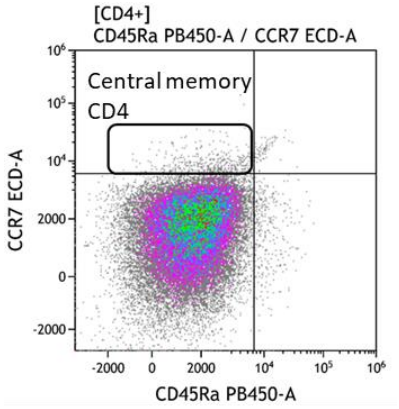

Treated

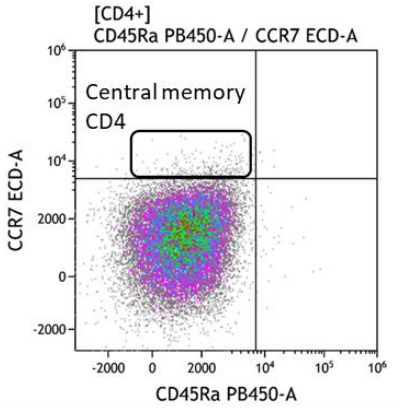

Non- treated

(C)

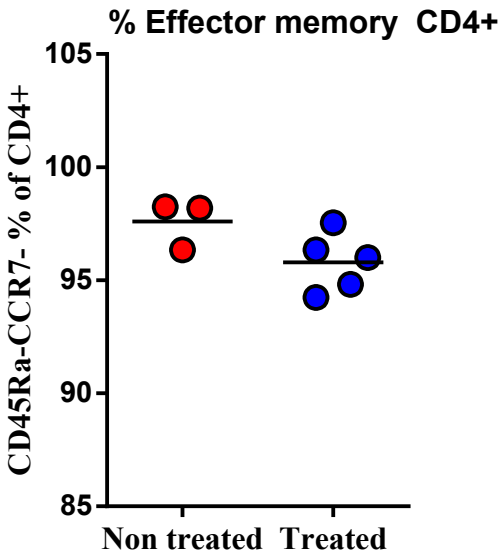

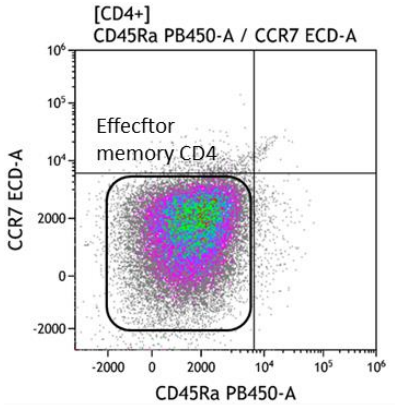

Treated

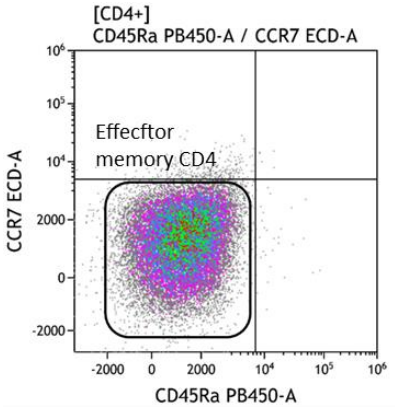

Non- treated

(D)

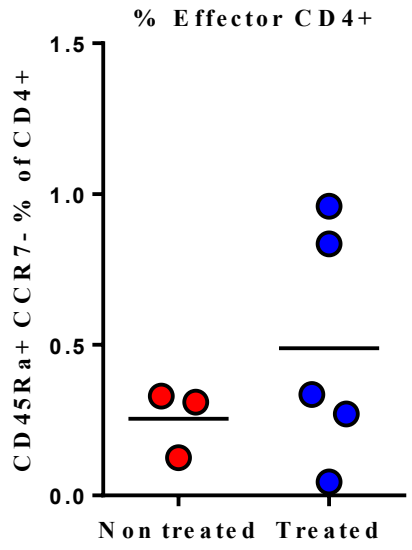

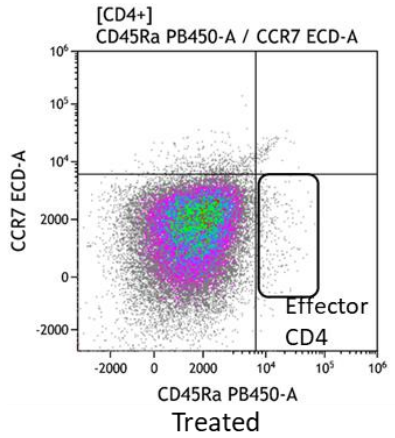

Treated

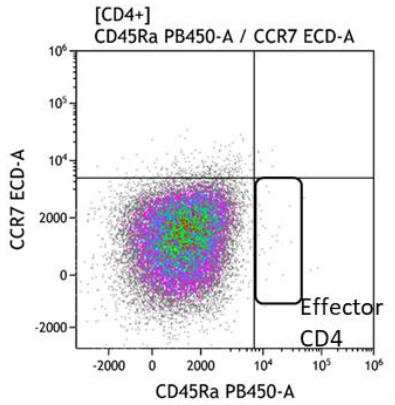

Non- treated

(E)

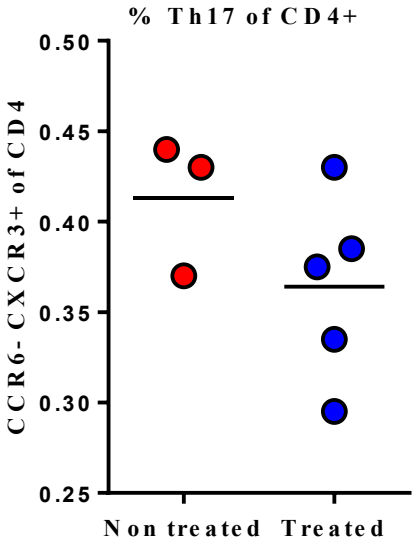

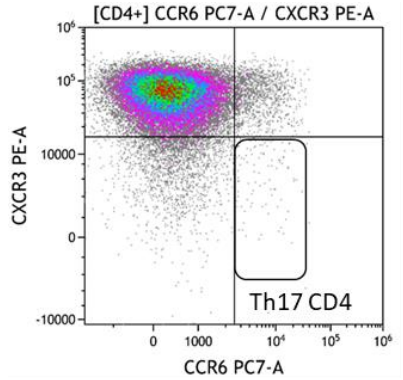

Treated

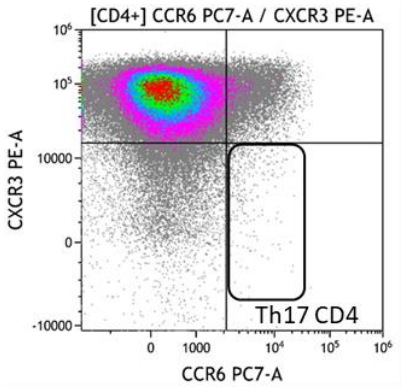

Non-treated

(F)

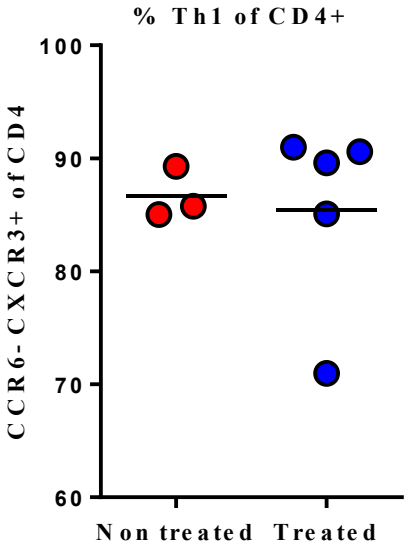

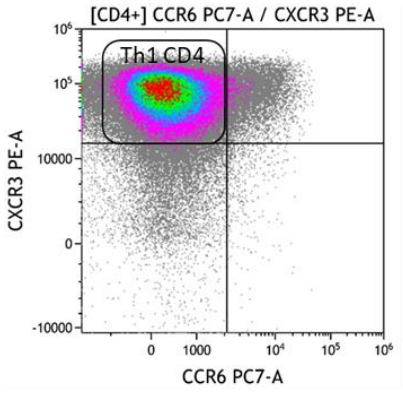

Treated

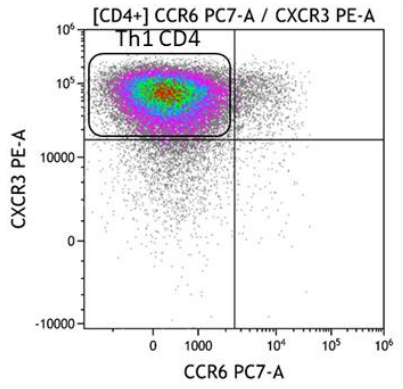

Non-treated

(G)

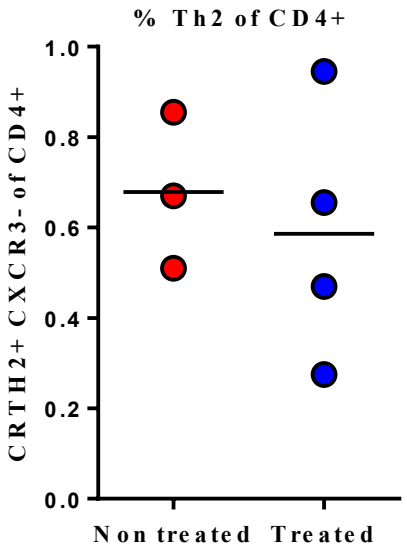

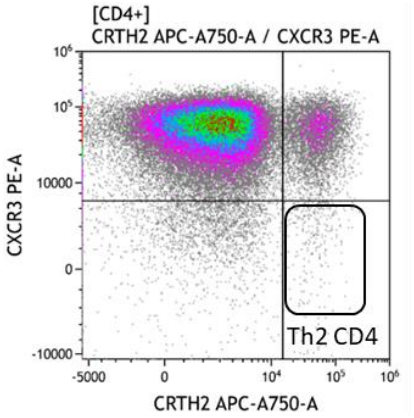

Treated

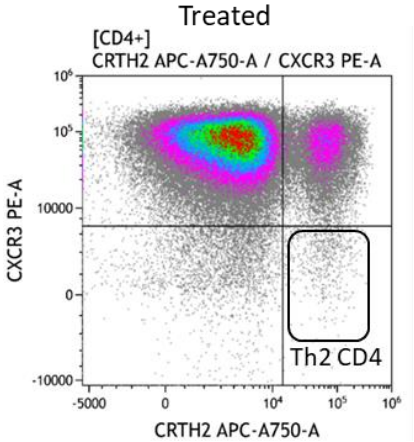

Non- treated

(H)

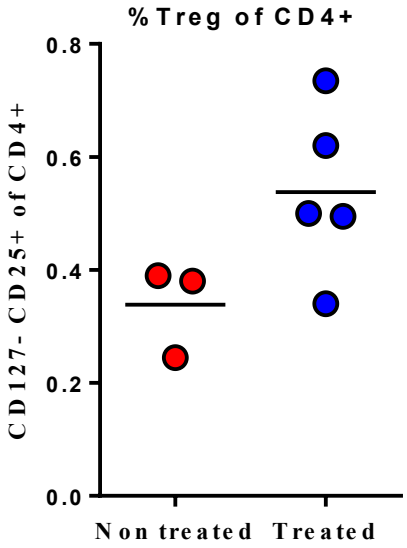

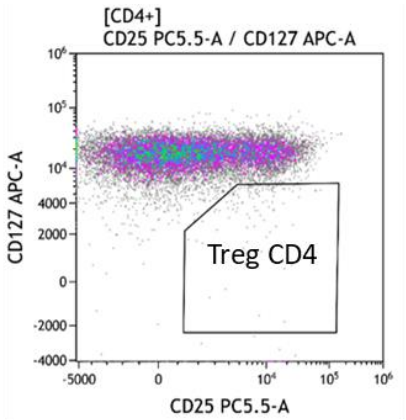

Treated

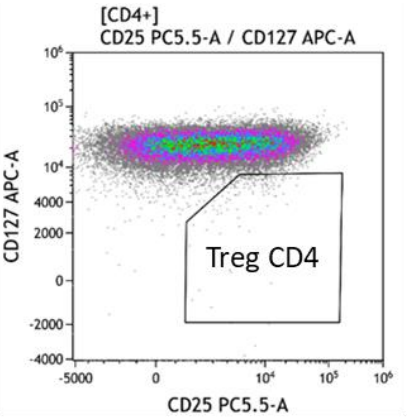

Non-treated

(I)

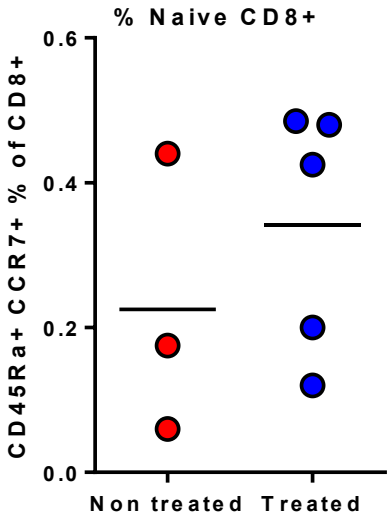
% Naive CD8+
CD45Ra+ CCR7+ % of CD8+
0.6
0.4
0.2
0.0
Non treated
Treated

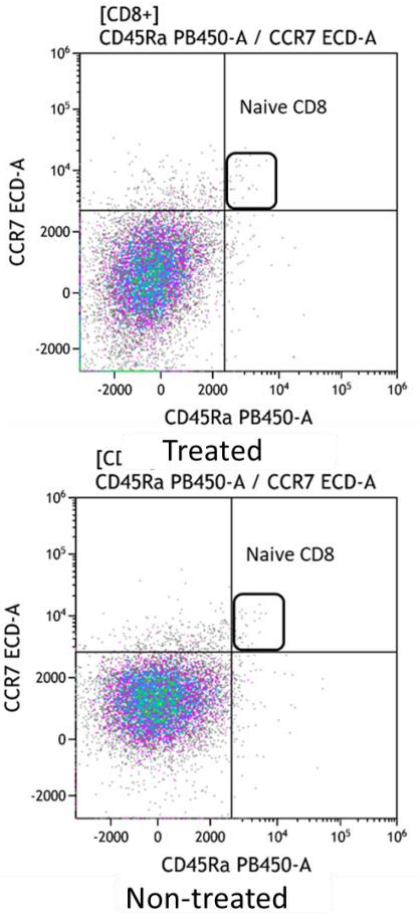
[CD8+]
CD45Ra PB450-A / CCR7 ECD-A
Naive CD8
CCR7 ECD-A
CD45Ra PB450-A
Treated
[CD8+]
CD45Ra PB450-A / CCR7 ECD-A
Naive CD8
CCR7 ECD-A
CD45Ra PB450-A
Non-treated

(J)

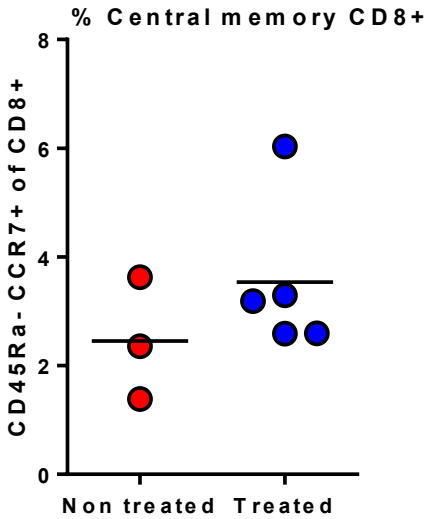
% Central memory CD8+
CD45Ra- CCR7+ of CD8+
8
6
4
2
0
Non treated
Treated

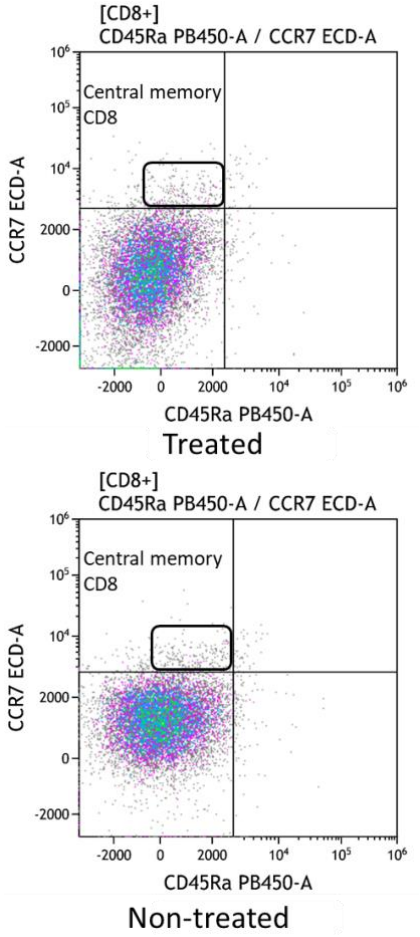
[CD8+]
CD45Ra PB450-A / CCR7 ECD-A
Central memory CD8
CCR7 ECD-A
CD45Ra PB450-A
Treated
[CD8+]
CD45Ra PB450-A / CCR7 ECD-A
Central memory CD8
CCR7 ECD-A
CD45Ra PB450-A
Non-treated

(K)

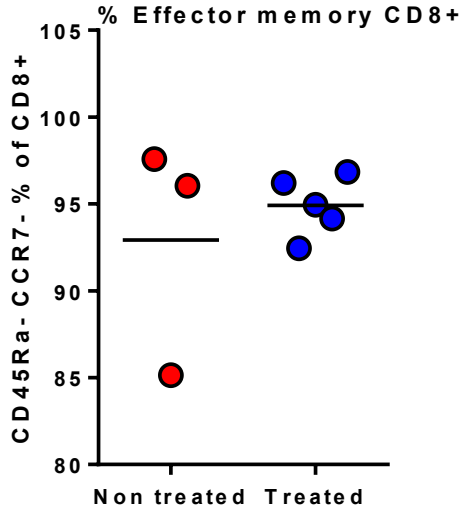

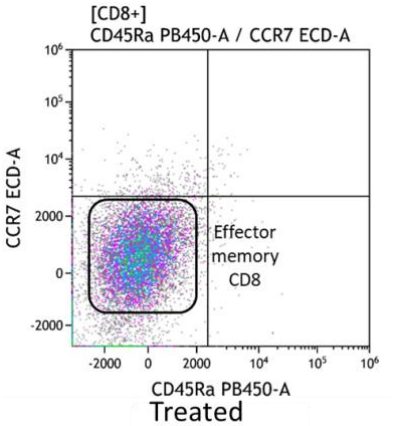

Treated

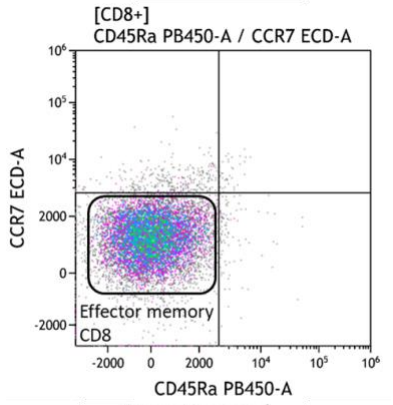

Non-treated

(L)

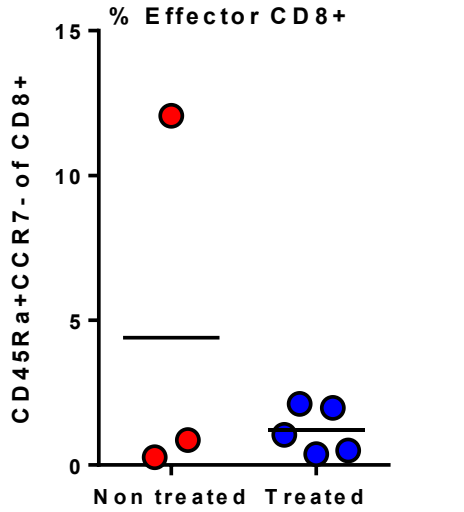

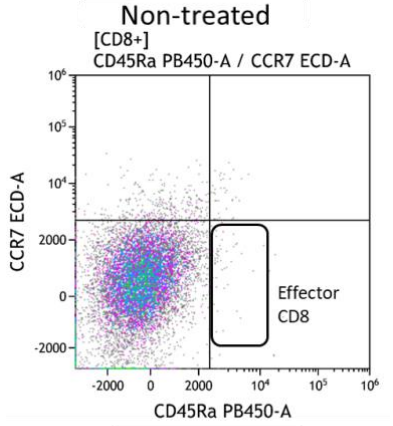

Treated

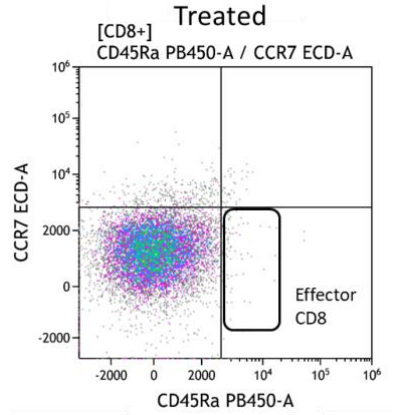

Non-treated

Figure 28: Flow cytometric quantification of splenocytes were analyzed for frequencies of various CD4 and CD8 subsets. Treated n=5, non treated n=3 $P>0.05$, by unpaired t-test.

5 Discussion

In the present study, we aimed to define the role of human T cells in experimental hypertension and associated renal damage. Three main objectives were accomplished in this study. First, we have successfully established a humanized mice model which enabled us to determine exclusive functions of human T cells under different pathological conditions. Second, we have shown that T cells from THR causes/exaggerated Ang II induced hypertension and renal damage. Third, we aimed to define the underlying mechanism of T cells in the development of experimental hypertension. Many animal studies have shown that adaptive immunity, particularly T cells influence the generation and progression of hypertension and kidney injury. However, here we demonstrated for the first time the pathophysiological role and underlying mechanism of T cells from therapy resistant hypertensive patients (TRH) in the development of hypertension and hypertensive renal damage.

Successful establishment of a humanized mouse model

Biomedical research on human immune system has multiple ethical and pragmatic restrictions, thus research in this field is highly limited to *in vitro* studies through which it is not possible to reflect various complex mechanisms of human physiology, such as interorgan communications. To overcome this limitation humanized mice were developed which can be defined as mice engrafted with functional human cells or tissue through which it is possible to investigate the development and function of human cells and tissues in a small animal. To develop a humanized mice model, we have used a special immunosuppressant mouse NSG-(KbDb) ^{null} mice (NOD.Cg-Prkdcscid H2-K1tm1Bpe H2-D1tm1Bpe Il2rgtm1Wjl/SzJ) (Covassin et al., 2013). NSG-(KbDb) ^{null} mouse strain has no mature T cell and B cell as well as no functional natural killer cell. Moreover, they are deficient in IL-2 cytokine signaling and do not express murine MHC I molecules which results in an attenuated graft versus host reaction, thus making it a suitable candidate for engraftment of human peripheral blood mononuclear cells (PBMCs). In our model, we treated the mice either with saline (sham) or with human PBMCs and later infused them with Ang II to induce blood pressure.

Three weeks after PBMC injection, flow cytometry analysis of peripheral blood of the mice treated with human PBMCs showed presence of human CD3+ T cells as well as CD4+ and CD8+ T cells (Fig-7A) but no murine CD3+ T cells (Fig-7B) were detected in these mice. Moreover, after two weeks of Ang II infusion, flow cytometry demonstrated substantial numbers of human CD3+, CD4+ and CD8+ T cells in the spleens (Fig-7C) and kidneys (Fig-

7E) of the mice treated with human PBMCs, however no murine CD3+ cell was found in these mice. These findings are similar to the previous observations by Guzik et al., where it has been demonstrated that human T cells accumulated in the kidneys of humanized mice with experimental hypertension (Itani et al., 2016). Furthermore, no human monocytes and macrophages were detected in the spleen and kidneys of these mice. In addition, immunohistochemistry showed massive infiltration of CD3+ cells in the kidney tissues of mice treated with human PBMCs. On the contrary, no such incidence was evident in the mice treated with saline (sham) (Fig-7G). Therefore, these results suggest that engraftment of T cell was successful in the mice which were treated with human PBMCs and these T cells are able to express exclusively human cytokines.

Guzik et al demonstrated that mice lacking B and T cells are resistant to blood pressure elevation and vascular dysfunction associated with impaired endothelium dependent vasodilatation under hypertensive stimuli such as Ang II but restoration of T cells by adoptive transfer in those mice re-established the Ang II induced hypertension and impaired endothelium dependent vasorelaxation (Guzik et al., 2007). In line with this observation, we have found that Ang II induced blood pressure is significantly lower in mice without human T cells (sham) compared to the mice engrafted with human T cells (Fig-8). Moreover, carbachol mediated vasorelaxation is significantly impaired in mice engrafted with human T cells compared to sham (Fig-9). Thus, these results indicate an important role of T cells in the development of augmented blood pressure and renal vascular dysfunction caused by Ang II.

Moreover, Ang II promotes T cell infiltration in the kidneys (Muller et al., 2002). Consistent with this, immunohistochemistry of renal tissue showed prominent infiltration of human CD3+ cells in the kidneys of mice engrafted with human T cells compared to sham (Fig-11C). T cells are activated by Ang II via AT1 receptors resulting in increased production of various pro-inflammatory cytokines. (Silva-Filho et al. 2016 & 2013; Coppo et al., 2008; Jurewicz et al., 2007). Analogue to this notion, we found increased expression of human pro-inflammatory cytokines such as human TNF-α, human IL-2 and human TFG-ß (Fig-10) in the kidneys of mice engrafted with human T cells and treated with Ang II compared to the mice only engrafted with human T cells but not infused with Ang II. Therefore, overexpression of these pro-inflammatory cytokines under Ang II infusion indicates activation of human T cell by Ang II in those mice. However, increased T cell activation and renal pro-inflammatory cytokines disrupt kidney function and promote kidney injury by multiple mechanisms (McMaster et al., 2015). In line with these findings, in our present study we observed that mice, which are

engrafted with human T cells, showed reduced glomerular filtration rate compared to sham (Fig-11A). Furthermore, Ang II stimulates vascular hypertrophy by increased deposition of extracellular matrix and proliferation of vascular smooth muscle cells (Sprague et al., 2009). Moreover, deletion or suppression of lymphocytes remarkably reduces Ang II induced vascular hypertrophy (Guzik et al., 2007). In parallel to this concept, we have found significantly reduced vascular wall hypertrophy in mice with no human T cells compared to mice engrafted with human T cells (Fig-11B).

Based on these evidence, we can conclude that we have successfully established a humanized mice model containing human T cells with its intrinsic functional characteristics.

T cells from TRH exaggerate hypertension and renal damage

To investigate whether T cells from TRH cause or exaggerate hypertension and impair renal endothelial function, we have successfully engrafted mice with T cells either from TRH or normotensive controls and infused them with Ang II to induce blood pressure. At baseline, blood pressure did not differ between the mice engrafted with T cells from normotensive control and TRH. During the first week of Ang II infusion, mice engrafted with T cells from TRH showed extravagant blood pressure increased to Ang II compared to the mice engrafted with T cells from normotensive controls (Fig-12A). Since, endothelial dysfunction is a commone feature of hypertension (Murray et al., 2021; Brandes et al., 2014, Konukoglu et al., 2017), we determined endothelium-dependent vasodilation of isolated perfused kidneys of the mice engrafted with T cells from TRH or normotensive controls under *ex vivo* condition. Remarkably, we found significantly impaired renal endothelial function in the mice engrafted with T cells from TRH compared to the mice engrafted with T cells from normotensive controls (Fig-13). In order to elucidate these unique and exaggerated influences of T cells on blood pressure and impaired renal function, we performed a series of investigations.

Immunostaining of the kidney tissues of our experimented mice with anti-CD3 antibody revealed that increased numbers of CD3+ cells are infiltrated into the kidneys and accumulated around the renal vessels of the mice engrafted with T cells from TRH compared to normotensive controls (Fig-14). In keeping with this notion, several studies suggested that infiltration of T cells in the kidney, specifically around the renal blood vessels play a significant role in the development of hypertension and renal injury under Ang II infusion. These accumulated T lymphocytes are associated with induction of pro-inflammatory cytokines and reactive oxygen species, extravagant aortic stiffness and vascular dysfunction leading to augmented blood

pressure and renal injury. (Zhang J et al., 2014 & 2015; Crowley et al., 2007; Muller et al., 2002).

To further investigate the cause of elevated blood pressure and impaired renal function in the mice engrafted with T cells from TRH, we analyzed different T cell subsets in the spleen and kidneys of the mice engrafted with T cells from TRH and normotensive controls via flow cytometry. Interestingly, we found significantly higher population of human CD4 effector memory T cells (TEM) in the spleens (Fig-15A) and both human CD4 TEM (Fig-17A) and CD8 TEM (Fig-18A) in the kidneys of the mice engrafted with T cells from TRH compared to the mice engrafted with T cells from normotensive controls. TEM are a type of memory T cells that produce effector molecules after rapid response to antigen/stimuli and are usually distributed in the blood, spleen and nonlymphoid tissue (Seder et al., 2003; Golubovskaya et al., 2016; Kaech et al., 2002). Upon re-stimulation, CD4 TEM and CD8 TEM can exert effector function of CD4 Th1 T cells (Stephens et al., 2010) and CD8 effector T cells, respectively and predominantly release TNF-α and IFN-γ. (Seder et al., 2003). However, analogue to our findings, Itani et al demonstrated that adoptive transfer of TEM from post hypertensive mice could induce hypertension in naïve mice upon hypertensive stimuli. Moreover, hypertensive mice showed increased accumulation of TEM in the kidneys and by reducing the migration of TEM in the kidneys through inhibition of TEM egression results attenuated blood pressure (Itani et al., 2016a; Itani et al., 2016b). Therefore, we can postulate that increased renal TEM and associated cytokines release might play a crucial role in Ang II induced hypertension and renal damage.

Furthermore, Th17 CD4 T cells are widely known for their pathogenic role on blood pressure and end organ damage both in humans and animals (Kamat et al., 2015 Cornelius et al., 2013; Madhur et al., 2010). Hypertensive patients show higher circulatory Th17 CD4 T cells compared to the healthy controls (Ji et al., 2017). Moreover, Tripton and colleagues demonstrated that spontaneously hypertensive rats (SHR) have increased renal infiltration of Th17 CD4 T cells and augmented blood pressure (Tipton et al., 2012). Consistent with these studies, our flow cytometric analysis data showed higher population of human Th17 CD4 T cells in the spleens (Fig-15C) and kidneys (Fig-17C) of the mice engrafted with T cells from THR compared to normotensive controls, signifying the role of human Th17 CD4 T cells in blood pressure elevation and renal damage in our mouse model.

Several studies suggested that renal infiltrated T cells cause renal inflammation by releasing pro-inflammatory cytokines which impair renal function and consecutively lead to hypertension

(Crowley et al., 2010; Rudemiller et al., 2014; Madhur et al., 2010 Marko et al., 2012 Singh et al., 2013). Since increased TEM and Th17 CD4 T cells are associated with pro-inflammatory conditions, we measured relative mRNA expression of different pro-inflammatory cytokines in the kidneys of our experimented mice. In our study, we found significantly higher renal mRNA expression of human TNF-α as well as relatively higher mRNA expression of human IFN-γ and human IL-17 in the mice engrafted with T cells from TRH compared to the mice engrafted with T cells from normotensive controls (Fig-19). These results indicate that T cells from TRH are responsible for exaggerated pro-inflammatory cytokines release and renal inflammation which is one of the hallmarks of hypertension. These observations comply with the previous studies where it has been shown that CD4 Th1 T cell specific cytokines TNF-α and IFN-γ as well as CD4 Th17 specific cytokine IL-17 involve in blood pressure regulation. Elmarakby et al. showed that inhibition of TNF-α by etanercept ameliorates blood pressure in hypertensive rats (Elmarakby et al., 2007 & 2008) whereas, Kamat and colleagues found that Ang II induced blood pressure is significantly blunted in IFN-γ knockout mice (Kamat et al., 2015). Moreover, IL-17 is the primary cytokine released by Th17 CD4 T cells (Chen et al., 2008; Marshall et al., 2018) and suppression of IL-17 leads to attenuated blood pressure under chronic Ang II infusion (Madhur et al., 2010; Kamat et al., 2015). Furthermore, clinical studies demonstrated that hypertensive patients have higher TNF-α, IFN-γ and IL-17 levels compared to healthy controls (Mirhafez et al., 2014; Ji et al., 2017).

Since TNF-α is responsible for damaging glomerular cell and preventing nephrin production in podocytes resulting in reduced renal function (Yamauchi et al., 2006), we determined glomerular filtration rate (GFR) by measuring plasma cystatin C level in our mouse model. Cystatin C is a small protein molecule produced by nucleated cells and easily filtered by kidney and removed from the blood stream (Hendrickson et al., 2020). Thus, it is a good marker for GFR and renal function. Plasma cystatin C level is inversely proportional to the glomerular filtration rate, thus increased plasma cystatin C represents reduced GFR and vice versa. Consistent with our hypothesis, we found higher plasma cystatin C level in the mice engrafted with T cells from TRH compared to the mice engrafted with T cells from normotensive controls (Fig-20B), thus demonstrating significantly reduced GFR and renal function in the mice with elevated renal human TNF-α level compared to the mice with lower renal human TNF-α level.

Furthermore, vascular hypertrophy is one of the common secondary outcomes of hypertension. Chronic blood pressure causes alteration of vascular structure such as increasing thickness of the medial wall or narrowing the diameter of the lumen resulting vascular hypertrophy which

further changes arterial pressure and exaggerates blood pressure (Mennuni et al., 2014). Nevertheless, TNF-α is directly associated with vascular hypertrophy because it promotes proliferation and migration of vascular smooth muscle cells (VSMCs) (Rastogi et al., 2012; Davis et al., 2012; Choi et al., 2016; Al Ghouleh et al., 2013). Therefore, we determined renal vascular hypertrophy by measuring the ratio of the diameter of the vascular wall and lumen. In parallel to the notion of the detrimental effect of TNF-α in vasculature, we found significantly higher renal vascular hypertrophy in the mice with augmented renal TNF-α levels compared to the mice with lower renal TNF-α level (Fig-20A).

Nonetheless, to ensure the augmented inflammatory response associated hypertension and renal damage is directly linked to cytokines released by human T cells, we measured relative abundance of murine pro-inflammatory cytokines in the kidneys of the mice engrafted with T cells from TRH and normotensive controls. We did not find any difference in renal mRNA expression of murine pro-inflammatory cytokines between the mice engrafted with T cells from TRH and mice engrafted with T cells from normotensive controls. These results represent that human pro-inflammatory cytokines such human TNF-α, human IFN-γ and human IL-17 released by human T cells are solely responsible for inflammation associated hypertension and renal damage in the mice engrafted with T cells from TRH (Fig-21).

In addition, cyclooxygenase (COX) enzyme produces prostanoids from arachidonic acid. Two isoforms of COX 1 and COX 2 regulate blood pressure by playing opposite role on renal function. COX 1 inhibition promotes natriuresis and reduces blood pressure while COX 2 inhibition increase sodium retention and elevate blood pressure (Drożdżal et al., 2021). Since COX plays a significant role on blood pressure regulation, we determined relative abundance of both murine COX 1 and murine COX 2 in the kidneys of the mice engrafted with T cells from TRH and from normotensive controls. Surprisingly, we did not detect any difference in the renal expression of murine COX 1 (Fig-22A) and murine COX 2 (Fig-22A) between the groups of mice, indicating that T cells from TRH and normotensive control do not influence COX pathway to modulate blood pressure in our mouse model.

Role of human TNF-α in vascular dysfunction and aggravated hypertension in our mouse model

To ensure whether human cytokines are interacting with mouse tissue in our mouse model and exert pathophysiological effect, we collected 2 μm slices of kidney from the mice and treated them *in vitro* with either human TNF-α or saline (sham) for different time intervals at optimum

conditions. After each time interval, relative abundances of different murine adhesion molecules were determined. In our study, we found significantly higher expression of murine intracellular adhesion molecules (ICAMs)-1 in the kidney slices of the mice treated with human TNF-α compared to sham (Fig-23A), thus confirming robust interaction of human TNF-α with murine renal tissue.

Similarly, to determine whether human IFN-γ interacts with murine tissue, we incubated kidney slices of mice either with human IFN-γ or saline for different time intervels at an optimun condition followed by determination of relative mRNA expression of interferone gamma induced protein 10 (CXCL10). Surprisingly, we did not detect any difference in the relative expression of CXCL10 in the renal tissue of the mice treated with human IFN-γ and saline. Thus, human IFN-γ does not interact with the renal tissue of our mouse model (Fig-24).

Endothelial dysfunction is a common phenomenon in hypertension (Brandes et al., 2014; Taddei et al., 2001) and many studies demonstrated impaired endothelium-dependent vasorelaxation in hypertensive animals (Calver et al. 1993; Luscher and Vanhoutte 1986; Dohi et al. 1990). In line with this concept, we found significantly impaired endothelium dependent renal vascular function in our hypertensive mice engrafted with T cells from TRH with elevated renal human TNF-α. T cells are one of the major sources of TNF-α which involves in blood pressure regulation (Ramseyer et al. 2013) and TNF-α levels are elevated predominately among hypertensive patients (Bautista et al., 2005; Cottone et al., 1998). Furthermore, TNF-α disrupts microvascular and macrovascular circulation both *in vitro* and *in vivo* (Zhang et al., 2009) and promotes impaired endothelium-dependent vascular function in various vascular beds of different animals (Gao et al., 2007; Picchi et al., 2006; Ahmad et al., 2002) via increased production of reactive oxygen species (ROS) and reducing bioavailability of NO. Therefore, to investigate whether human TNF-α impairing vascular function of our mice, we have carefully isolated thoracic aortas of our mice and treated them overnight with either human TNF-α or saline. Afterwards, we measured carbachol mediated endothelium-dependent vasorelaxation of these aortas via wire myography. Interestingly, we found a significantly reduced endothelium-dependent NO mediated vasorelaxation of the thoracic aorta treated with human TNF-α compared to sham (Fig-25). These results suggest that human TNF-α released by T cells from TRH interacts with renal vasculature of the mice causing endothelial dependent vascular dysfunction leading to vasoconstriction and exaggerated blood pressure in those mice.

Moreover, nitrate/ nitrite are the markers of NO (nitric oxide) formation. Since we found NO mediated renal endothelial dysfunction in the mice engrafted with T cells from TRH with

elevated renal human TNF-α, we measured and compared urinary content of nitrate/nitrite of the mice engrafted with T cells from TRH and normotensive controls. To our surprise, we did not notice any difference in the urinary content of nitrate/nitrite between the mice engrafted with T cells from TRH and normotensive controls (Fig-26), which is in contrast with findings of Smallwood et al., where it has been demonstrated that nitrate/nitrite excretion is directly associated with lower blood pressure (Smallwood et al., 2017). However, one of the possible explanations of this phenomenon is that total nitrate/nitrite content not only represents endothelial synthesis of NO but also various other factors such as diet, exercise etc. (Fujiwara et al., 2000). Thus, nitrate/nitrite excretion might not reflect the appropriate vascular endothelial function.

Nonetheless, previous studies suggested that TNF-α knockout mice show attenuated hypertensive response compared to wild type mice during chronic Ang II infusion. Sriramula and colleagues showed that transfer of murine TNF-α through recombinant therapy restore blood pressure induced by Ang II in those mice (Sriramula et al., 2008). Analogue to these studies, we conducted an experiment as a proof-of-concept to confirm that human TNF-α is exclusively responsible for elevated blood pressure in the mice engrafted with T cells from TRH. In this experiment, we used two groups of mice, both engrafted with T cells from TRH where one group was treated with saline but the other group was treated with TNF-α inhibitor, etanercept. Etanercept acts as a TNF-α inhibitor as it binds with TNF-α and prevents its binding with its respective receptors. After two weeks of Ang II infusion, the group of mice treated with etanercept demonstrated attenuated blood pressure compared to the mice treated with saline (Fig-27A). This finding is in parallel to the observation by Venegas-Pont & colleagues where it has been shown that inhibition of TNF-α by etanercept reduces blood pressure and improves renal function (Venegas-Pont et al., 2010). Moreover, flow cytometry analysis of splenocytes of these mice revealed that there is no difference in the population of human T cell subsets between the groups indicating etanercept does not influence proliferation or priming of T cells and inhibition of TNF-α is solely responsible for attenuated blood pressure in those mice. Hence, this proof-of-concept experiment confirms that human TNF-α is the main contributor of exaggerated blood pressure in mice engrafted with T cells from TRH.

Limitations

In the present study, we defined the role of T cells from TRH in hypertension and hypertensive renal damage in a humanized mouse model. Although our mouse model provides valuable informations about distinctive role and function of T cells in the pathogenesis of hypertension

and hypertensive renal damage, it might not reflect the exact clinical condition of a therapy resistant hypertensive patient as human T cells may act/react differently in a murine physiological system. Moreover, remaining murine immunity might also affect the re-constitution of human immune cells including activation, proliferation or priming of human T cells. However, our mouse model readily allows engraftment of human PBMCs and graft versus host disease is almost negligible in our model compared to other immunodeficient mouse strains. In this study, we established for the first time a humanized mice with T cells from TRH where human T cells are activated by Ang II and recapitulate their intrinsic function leading to hypertension. Moreover, T cell associated inflammation plays the vital role in the development of hypertension in our experimented animals and might be also indirectly implicated to human hypertension. Since our study provides new evidence that human T cells play a crucial role in the development of hypertension, our animal model can be used as a substitute for future investigation of hypertension in humans.

6 Conclusion

T cells from therapy resistant hypertensive patients contribute to the pathogenesis of hypertension. Since late 20th century, hypertension is the leading cause of cardiovascular morbidity and mortality (Kung et al., 2015). Therefore, further innovative and unique approaches are required to manage this problem. In our study, we have established a humanized mouse model for testing the effects of T cells on hypertension and hypertensive renal disease. Our data provide enough evidence to prostulate that T cells from patients with therapy resistant hypertension aggravate blood pressure response and renal vascular dysfunction to chronic Ang II infusion. The exaggerated blood pressure response is associated with certain pro-inflammatory T cell signatures. Furthermore, we could identify that TNF-α released by human T cells seem to mediate these effects. Thus, inhibition of TNF-α attenuates the blood pressure response to Ang II in mice engrafted with T cells from patients with therapy resistant hypertension. In this regard, modulating T cells and associated cytokines could be a promising therapeutical approach to treat patients with hypertension and hypertensive renal damage.

7 References

A

Ahmad, M., Zhang, Y., Zhang, Y., Papharalambus, C., & Alexander, R. W. (2002). Role of isoprenylcysteine carboxyl methyltransferase in tumor necrosis factor-alpha stimulation of expression of vascular cell adhesion molecule-1 in endothelial cells. *Arteriosclerosis, thrombosis, and vascular biology*, *22*(5), 759–764.

Al Ghouleh, I., Frazziano, G., Rodriguez, A. I., Csányi, G., Maniar, S., St Croix, C. M., Kelley, E. E., Egaña, L. A., Song, G. J., Bisello, A., Lee, Y. J., & Pagano, P. J. (2013). Aquaporin 1, Nox1, and Ask1 mediate oxidant-induced smooth muscle cell hypertrophy. *Cardiovascular research*, *97*(1), 134–142

Alsharari, R., Shantsila, E., Lip, G. Y. H., & Shantsila, A. (2022). Revisiting the diagnosis of 'resistant hypertension': what should we do nowadays'. Journal of human hypertension, 36(4), 337–340.

Amann, K., Rump, L. C., Simonaviciene, A., Oberhauser, V., Wessels, S., Orth, S. R., Gross, M. L., Koch, A., Bielenberg, G. W., VAN Kats, J. P., Ehmke, H., Mall, G., & Ritz, E. (2000). Effects of low dose sympathetic inhibition on glomerulosclerosis and albuminuria in subtotally nephrectomized rats. Journal of the American Society of Nephrology : JASN, 11(8), 1469–1478.

Azizi, M., Schmieder, R. E., Mahfoud, F., Weber, M. A., Daemen, J., Davies, J., Basile, J., Kirtane, A. J., Wang, Y., Lobo, M. D., Saxena, M., Feyz, L., Rader, F., Lurz, P., Sayer, J., Sapoval, M., Levy, T., Sanghvi, K., Abraham, J., Sharp, A. S. P., … RADIANCE-HTN Investigators (2018). Endovascular ultrasound renal denervation to treat hypertension (RADIANCE-HTN SOLO): a multicentre, international, single-blind, randomised, sham-controlled trial. Lancet (London, England), 391(10137), 2335–2345.

B

Baek, E. J., & Kim, S. (2021). Current Understanding of Pressure Natriuresis. *Electrolyte & blood pressure : E & BP*, *19*(2), 38–45.

Baudeau, C., Delarue, F., Hé, C. J., Nguyen, G., Adida, C., Peraldi, M. N., Sraer, J. D., & Rondeau, E. (1994). Induction of MHC class II molecules HLA-DR, -DP and -DQ and ICAM 1 in human podocytes by gamma-interferon. *Experimental nephrology*, *2*(5), 306–312.

Bellocchi, C., Carandina, A., Montinaro, B., Targetti, E., Furlan, L., Rodrigues, G. D., Tobaldini, E., & Montano, N. (2022). The Interplay between Autonomic Nervous System and Inflammation across Systemic Autoimmune Diseases. International journal of molecular sciences, 23(5), 2449.

Bomfim, G. F., Dos Santos, R. A., Oliveira, M. A., Giachini, F. R., Akamine, E. H., Tostes, R. C., Fortes, Z. B., Webb, R. C., & Carvalho, M. H. (2012). Toll-like receptor 4 contributes to blood pressure regulation and vascular contraction in spontaneously hypertensive rats. Clinical science (London, England : 1979), 122(11), 535–543.

Braam, B., Taler, S. J., Rahman, M., Fillaus, J. A., Greco, B. A., Forman, J. P., Reisin, E., Cohen, D. L., Saklayen, M. G., & Hedayati, S. S. (2017). Recognition and Management of Resistant Hypertension. Clinical journal of the American Society of Nephrology : CJASN, 12(3), 524–535.

Brandes R. P. (2014). Endothelial dysfunction and hypertension. Hypertension (Dallas, Tex. : 1979), 64(5), 924–928.

Brandes R. P. (2014). Endothelial dysfunction and hypertension. *Hypertension (Dallas, Tex. : 1979)*, *64*(5), 924–928.

Bush, E., Maeda, N., Kuziel, W. A., Dawson, T. C., Wilcox, J. N., DeLeon, H., & Taylor, W. R. (2000). CC chemokine receptor 2 is required for macrophage infiltration and vascular hypertrophy in angiotensin II-induced hypertension. *Hypertension (Dallas, Tex. : 1979)*, *36*(3), 360–363.

C

Caillon, A., Mian, M. O. R., Fraulob-Aquino, J. C., Huo, K. G., Barhoumi, T., Ouerd, S., Sinnaeve, P. R., Paradis, P., & Schiffrin, E. L. (2017). γδ T Cells Mediate Angiotensin II-Induced Hypertension and Vascular Injury. *Circulation*, *135*(22), 2155–2162.

Choi, H., Ettinger, N., Rohrbough, J., Dikalova, A., Nguyen, H. N., & Lamb, F. S. (2016). LRRC8A channels support TNFα-induced superoxide production by Nox1 which is required for receptor endocytosis. *Free radical biology & medicine*, *101*, 413–423.

Coers, W., Vos, J. T., Huitema, S., Dijk, F., & Weening, J. J. (1996). Biological alterations of rat podocytes cultured under basolateral hydrostatic pressure. *Pathobiology : journal of immunopathology, molecular and cellular biology*, *64*(4), 222–232.

Coppo, M., Boddi, M., Bandinelli, M., Degl'innocenti, D., Ramazzotti, M., Marra, F., Galastri, S., Abbate, R., Gensini, G. F., & Poggesi, L. (2008). Angiotensin II upregulates renin-angiotensin system in human isolated T lymphocytes. *Regulatory peptides*, *151*(1-3), 1–6

Cornelius, D. C., Hogg, J. P., Scott, J., Wallace, K., Herse, F., Moseley, J., Wallukat, G., Dechend, R., & LaMarca, B. (2013). Administration of interleukin-17 soluble receptor C suppresses TH17 cells, oxidative stress, and hypertension in response to placental ischemia during pregnancy. *Hypertension (Dallas, Tex. : 1979)*, *62*(6), 1068–1073.

Covassin, L., Jangalwe, S., Jouvet, N., Laning, J., Burzenski, L., Shultz, L. D., & Brehm, M. A. (2013). Human immune system development and survival of non-obese diabetic (NOD)-scid IL2rγ(null) (NSG) mice engrafted with human thymus and autologous haematopoietic stem cells. Clinical and experimental immunology, 174(3), 372–388.

Crowley, S. D., Song, Y. S., Lin, E. E., Griffiths, R., Kim, H. S., & Ruiz, P. (2010). Lymphocyte responses exacerbate angiotensin II-dependent hypertension. American journal of physiology. Regulatory, integrative and comparative physiology, 298(4), R1089–R1097.

D

Davis, R., Pillai, S., Lawrence, N., Sebti, S., & Chellappan, S. P. (2012). TNF-α-mediated proliferation of vascular smooth muscle cells involves Raf-1-mediated inactivation of Rb and transcription of E2F1-regulated genes. *Cell cycle (Georgetown, Tex.)*, *11*(1), 109–118.

De Ciuceis, C., Amiri, F., Brassard, P., Endemann, D. H., Touyz, R. M., & Schiffrin, E. L. (2005). Reduced vascular remodeling, endothelial dysfunction, and oxidative stress in resistance arteries of angiotensin II-infused macrophage colony-stimulating factor-deficient mice: evidence for a role in inflammation in angiotensin-induced vascular injury. *Arteriosclerosis, thrombosis, and vascular biology*, *25*(10), 2106–2113.

DiBona, G. F., & Kopp, U. C. (1997). Neural control of renal function. Physiological reviews, 77(1), 75–197.

Dimitrov, S., Lange, T., & Born, J. (2010). Selective mobilization of cytotoxic leukocytes by epinephrine. Journal of immunology (Baltimore, Md. : 1950), 184(1), 503–511.

Drożdżal, S., Lechowicz, K., Szostak, B., Rosik, J., Kotfis, K., Machoy-Mokrzyńska, A., Białecka, M., Ciechanowski, K., & Gawrońska-Szklarz, B. (2021). Kidney damage from nonsteroidal anti-inflammatory drugs-Myth or truth? Review of selected literature. *Pharmacology research & perspectives*, *9*(4), e00817.

Drummond, G. R., Vinh, A., Guzik, T. J., & Sobey, C. G. (2019). Immune mechanisms of hypertension. Nature reviews. Immunology, 19(8), 517–532.

E

Elmarakby, A. A., Quigley, J. E., Imig, J. D., Pollock, J. S., & Pollock, D. M. (2008). TNF-alpha inhibition reduces renal injury in DOCA-salt hypertensive rats. *American journal of physiology. Regulatory, integrative and comparative physiology*, *294*(1), R76–R83.

Elmarakby, A. A., Quigley, J. E., Olearczyk, J. J., Sridhar, A., Cook, A. K., Inscho, E. W., Pollock, D. M., & Imig, J. D. (2007). Chemokine receptor 2b inhibition provides renal protection in angiotensin II - salt hypertension. *Hypertension (Dallas, Tex. : 1979)*, *50*(6), 1069–1076.

Elmarakby, A. A., Quigley, J. E., Pollock, D. M., & Imig, J. D. (2006). Tumor necrosis factor alpha blockade increases renal Cyp2c23 expression and slows the progression of renal damage in salt-sensitive hypertension. Hypertension (Dallas, Tex. : 1979), 47(3), 557–562.

Elmarakby, A. A., Quigley, J. E., Pollock, D. M., & Imig, J. D. (2006). Tumor necrosis factor alpha blockade increases renal Cyp2c23 expression and slows the progression of renal damage in salt-sensitive hypertension. *Hypertension (Dallas, Tex. : 1979)*, *47*(3), 557–562.

F

Fanelli, C., Arias, S. C. A., Machado, F. G., Okuma, J. K., Malheiros, D. M. A. C., Azevedo, H., Moreira-Filho, C. A., Camara, N. O. S., Fujihara, C. K., & Zatz, R. (2017). Innate And Adaptive Immunity are Progressively Activated in Parallel with Renal Injury in the 5/6 Renal Ablation Model. Scientific reports, 7(1), 3192.

Fountain, J. H., Kaur, J., & Lappin, S. L. (2023). Physiology, Renin Angiotensin System. In StatPearls. StatPearls Publishing.

Fujiwara S. (2018). Humanized mice: A brief overview on their diverse applications in biomedical research. *Journal of cellular physiology*, *233*(4), 2889–2901.

Fujiwara, N., Osanai, T., Kamada, T., Katoh, T., Takahashi, K., & Okumura, K. (2000). Study on the relationship between plasma nitrite and nitrate level and salt sensitivity in human hypertension : modulation of nitric oxide synthesis by salt intake. *Circulation*, *101*(8), 856–861.

G

Ganta, C. K., Lu, N., Helwig, B. G., Blecha, F., Ganta, R. R., Zheng, L., Ross, C. R., Musch, T. I., Fels, R. J., & Kenney, M. J. (2005). Central angiotensin II-enhanced splenic cytokine gene expression is mediated by the sympathetic nervous system. American journal of physiology. Heart and circulatory physiology, 289(4), H1683–H1691.

Gao, X., Belmadani, S., Picchi, A., Xu, X., Potter, B. J., Tewari-Singh, N., Capobianco, S., Chilian, W. M., & Zhang, C. (2007). Tumor necrosis factor-alpha induces endothelial dysfunction in Lepr(db) mice. *Circulation*, *115*(2), 245–254.

GBD 2016 Risk Factors Collaborators (2017). Global, regional, and national comparative risk assessment of 84 behavioural, environmental and occupational, and metabolic risks or clusters of risks, 1990-2016: a systematic analysis for the Global Burden of Disease Study 2016. Lancet (London, England), 390(10100), 1345–1422.

GBD 2019 Risk Factors Collaborators (2020). Global burden of 87 risk factors in 204 countries and territories, 1990-2019: a systematic analysis for the Global Burden of Disease Study 2019. Lancet (London, England), 396(10258), 1223–1249.

Grassi, G., & Ram, V. S. (2016). Evidence for a critical role of the sympathetic nervous system in hypertension. *Journal of the American Society of Hypertension : JASH*, *10*(5), 457–466.

Grassi, G., Mark, A., & Esler, M. (2015). The sympathetic nervous system alterations in human hypertension. *Circulation research*, *116*(6), 976–990.

Grisk, O., & Rettig, R. (2004). Interactions between the sympathetic nervous system and the kidneys in arterial hypertension. Cardiovascular research, 61(2), 238–246.

Guzik, T. J., Hoch, N. E., Brown, K. A., McCann, L. A., Rahman, A., Dikalov, S., Goronzy, J., Weyand, C., & Harrison, D. G. (2007). Role of the T cell in the genesis of angiotensin II induced hypertension and vascular dysfunction. The Journal of experimental medicine, 204(10), 2449–2460.

H

Hamrahian, S. M., & Falkner, B. (2017). Hypertension in Chronic Kidney Disease. Advances in experimental medicine and biology, 956, 307–325.

Hendrickson, C. M., Kwong, Y. D., Belzer, A. G., Shlipak, M. G., Matthay, M. A., & Liu, K. D. (2020). Higher plasma cystatin C is associated with mortality after acute respiratory distress

syndrome: findings from a Fluid and Catheter Treatment Trial (FACTT) substudy. *Critical care (London, England)*, *24*(1), 416.

I

Ishibashi, M., Hiasa, K., Zhao, Q., Inoue, S., Ohtani, K., Kitamoto, S., Tsuchihashi, M., Sugaya, T., Charo, I. F., Kura, S., Tsuzuki, T., Ishibashi, T., Takeshita, A., & Egashira, K. (2004). Critical role of monocyte chemoattractant protein-1 receptor CCR2 on monocytes in hypertension-induced vascular inflammation and remodeling. *Circulation research*, *94*(9), 1203–1210.

Itani HA, Xiao L, Saleh MA, Wu J, Pilkinton MA, Dale BL, Barbaro NR, Foss JD, Kirabo A, Montaniel KR, Norlander AE, Chen W, Sato R, Navar LG, Mallal SA, Madhur MS, Bernstein KE, Harrison DG(2016). CD70 Exacerbates Blood Pressure Elevation and Renal Damage in Response to Repeated Hypertensive Stimuli. Circ Res.118(8) 1233-1243.

Itani, H. A., & Evans, L. C. (2023). Editorial: Inflammation in hypertensive disorders. *Frontiers in physiology*, *13*, 1085856.

Itani, H. A., McMaster, W. G., Jr, Saleh, M. A., Nazarewicz, R. R., Mikolajczyk, T. P., Kaszuba, A. M., Konior, A., Prejbisz, A., Januszewicz, A., Norlander, A. E., Chen, W., Bonami, R. H., Marshall, A. F., Poffenberger, G., Weyand, C. M., Madhur, M. S., Moore, D. J., Harrison, D. G., & Guzik, T. J. (2016). Activation of Human T Cells in Hypertension: Studies of Humanized Mice and Hypertensive Humans. *Hypertension (Dallas, Tex. : 1979)*, *68*(1), 123–132.

Itani, M. M., Jarrah, H., Maaliki, D., Radwan, Z., Farhat, R., & Itani, H. A. (2022). Sphingosine 1 phosphate promotes hypertension specific memory T cell trafficking in response to repeated hypertensive challenges. *Frontiers in physiology*, *13*, 930487.

Ivy, J. R., & Bailey, M. A. (2014). Pressure natriuresis and the renal control of arterial blood pressure. The Journal of physiology, 592(18), 3955–3967.

J

Ji, Q., Cheng, G., Ma, N., Huang, Y., Lin, Y., Zhou, Q., Que, B., Dong, J., Zhou, Y., & Nie, S. (2017). Circulating Th1, Th2, and Th17 Levels in Hypertensive Patients. Disease markers, 2017, 7146290

Jurewicz, M., McDermott, D. H., Sechler, J. M., Tinckam, K., Takakura, A., Carpenter, C. B., Milford, E., & Abdi, R. (2007). Human T and natural killer cells possess a functional renin-angiotensin system: further mechanisms of angiotensin II-induced inflammation. *Journal of the American Society of Nephrology : JASN*, *18*(4), 1093–1102.

K

Kaech, S. M., Wherry, E. J., & Ahmed, R. (2002). Effector and memory T-cell differentiation: implications for vaccine development. *Nature reviews. Immunology*, *2*(4), 251–262.

Kamat, N. V., Thabet, S. R., Xiao, L., Saleh, M. A., Kirabo, A., Madhur, M. S., Delpire, E., Harrison, D. G., & McDonough, A. A. (2015). Renal transporter activation during angiotensin-II hypertension is blunted in interferon-γ-/- and interleukin-17A-/- mice. Hypertension (Dallas, Tex. : 1979), 65(3), 569–576.

Kasal, D. A., Barhoumi, T., Li, M. W., Yamamoto, N., Zdanovich, E., Rehman, A., Neves, M. F., Laurant, P., Paradis, P., & Schiffrin, E. L. (2012). T regulatory lymphocytes prevent aldosterone-induced vascular injury. Hypertension (Dallas, Tex. : 1979), 59(2), 324–330.

Khraibi A. A. (2002). Renal interstitial hydrostatic pressure and sodium excretion in hypertension and pregnancy. Journal of hypertension. Supplement : official journal of the International Society of Hypertension, 20(3), S21–S27.

Kim, J., & Padanilam, B. J. (2013). Renal nerves drive interstitial fibrogenesis in obstructive nephropathy. Journal of the American Society of Nephrology : JASN, 24(2), 229–242.

Konukoglu, D., & Uzun, H. (2017). Endothelial Dysfunction and Hypertension. Advances in experimental medicine and biology, 956, 511–540.

Kung, H. C., & Xu, J. (2015). Hypertension-related Mortality in the United States, 2000-2013. NCHS data brief, (193), 1–8.

L

Leong, P. K., Yang, L. E., Landon, C. S., McDonough, A. A., & Yip, K. P. (2006). Phenol injury-induced hypertension stimulates proximal tubule Na+/H+ exchanger activity. American journal of physiology. Renal physiology, 290(6), F1543–F1550.

Liu, Y., Rafferty, T. M., Rhee, S. W., Webber, J. S., Song, L., Ko, B., Hoover, R. S., He, B., & Mu, S. (2017). $CD8^+$ T cells stimulate Na-Cl co-transporter NCC in distal convoluted tubules leading to salt-sensitive hypertension. Nature communications, 8, 14037.

M

Madhur, M. S., Lob, H. E., McCann, L. A., Iwakura, Y., Blinder, Y., Guzik, T. J., & Harrison, D. G. (2010). Interleukin 17 promotes angiotensin II-induced hypertension and vascular dysfunction. Hypertension (Dallas, Tex. : 1979), 55(2), 500–507.

Mahfoud, F., Ukena, C., Schmieder, R. E., Cremers, B., Rump, L. C., Vonend, O., Weil, J., Schmidt, M., Hoppe, U. C., Zeller, T., Bauer, A., Ott, C., Blessing, E., Sobotka, P. A., Krum, H., Schlaich, M., Esler, M., & Böhm, M. (2013). Ambulatory blood pressure changes after renal sympathetic denervation in patients with resistant hypertension. Circulation, 128(2), 132–140.

Manrique, C., Lastra, G., Gardner, M., & Sowers, J. R. (2009). The renin angiotensin aldosterone system in hypertension: roles of insulin resistance and oxidative stress. *The Medical clinics of North America*, *93*(3), 569–582.

Mattson, D. L., Lund, H., Guo, C., Rudemiller, N., Geurts, A. M., & Jacob, H. (2013). Genetic mutation of recombination activating gene 1 in Dahl salt-sensitive rats attenuates hypertension and renal damage. American journal of physiology. Regulatory, integrative and comparative physiology, 304(6), R407–R414.

McDonough A. A. (2010). Mechanisms of proximal tubule sodium transport regulation that link extracellular fluid volume and blood pressure. American journal of physiology. Regulatory, integrative and comparative physiology, 298(4), R851–R861.

McMaster, W. G., Kirabo, A., Madhur, M. S., & Harrison, D. G. (2015). Inflammation, immunity, and hypertensive end-organ damage. *Circulation research*, *116*(6), 1022–1033.

Mennuni, S., Rubattu, S., Pierelli, G., Tocci, G., Fofi, C., & Volpe, M. (2014). Hypertension and kidneys: unraveling complex molecular mechanisms underlying hypertensive renal damage. Journal of human hypertension, 28(2), 74–79.

Mervaala, E. M., Müller, D. N., Park, J. K., Schmidt, F., Löhn, M., Breu, V., Dragun, D., Ganten, D., Haller, H., & Luft, F. C. (1999). Monocyte infiltration and adhesion molecules in a rat model of high human renin hypertension. *Hypertension (Dallas, Tex. : 1979)*, *33*(1 Pt 2), 389–395.

Mian, M. O., Barhoumi, T., Briet, M., Paradis, P., & Schiffrin, E. L. (2016). Deficiency of T-regulatory cells exaggerates angiotensin II-induced microvascular injury by enhancing immune responses. Journal of hypertension, 34(1), 97–108.

Mirhafez, S. R., Mohebati, M., Feiz Disfani, M., Saberi Karimian, M., Ebrahimi, M., Avan, A., Eslami, S., Pasdar, A., Rooki, H., Esmaeili, H., Ferns, G. A., & Ghayour-Mobarhan, M. (2014). An imbalance in serum concentrations of inflammatory and anti-inflammatory cytokines in hypertension. Journal of the American Society of Hypertension : JASH, 8(9), 614–623

Muller, D. N., Shagdarsuren, E., Park, J. K., Dechend, R., Mervaala, E., Hampich, F., Fiebeler, A., Ju, X., Finckenberg, P., Theuer, J., Viedt, C., Kreuzer, J., Heidecke, H., Haller, H., Zenke, M., & Luft, F. C. (2002). Immunosuppressive treatment protects against angiotensin II-induced renal damage. The American journal of pathology, 161(5), 1679–1693.

Murray, E. C., Nosalski, R., MacRitchie, N., Tomaszewski, M., Maffia, P., Harrison, D. G., & Guzik, T. J. (2021). Therapeutic targeting of inflammation in hypertension: from novel mechanisms to translational perspective. Cardiovascular research, 117(13), 2589–2609.

N

Nguyen, T. N., & Chow, C. K. (2021). Global and national high blood pressure burden and control. Lancet (London, England), 398(10304), 932–933.

Norlander, A. E., Saleh, M. A., Kamat, N. V., Ko, B., Gnecco, J., Zhu, L., Dale, B. L., Iwakura, Y., Hoover, R. S., McDonough, A. A., & Madhur, M. S. (2016). Interleukin-17A Regulates Renal Sodium Transporters and Renal Injury in Angiotensin II-Induced Hypertension. Hypertension (Dallas, Tex. : 1979), 68(1), 167–174.

P

Patel, S., Rauf, A., Khan, H., & Abu-Izneid, T. (2017). Renin-angiotensin-aldosterone (RAAS): The ubiquitous system for homeostasis and pathologies. Biomedicine & pharmacotherapy = Biomedecine & pharmacotherapie, 94, 317–325.

Picchi, A., Gao, X., Belmadani, S., Potter, B. J., Focardi, M., Chilian, W. M., & Zhang, C. (2006). Tumor necrosis factor-alpha induces endothelial dysfunction in the prediabetic metabolic syndrome. *Circulation research*, *99*(1), 69–77.

Przybyl, L., Ibrahim, T., Haase, N., Golic, M., Rugor, J., Luft, F. C., Bendix, I., Serdar, M., Wallukat, G., Staff, A. C., Müller, D. N., Hünig, T., Felderhoff-Müser, U., Herse, F., LaMarca, B., & Dechend, R. (2015). Regulatory T cells ameliorate intrauterine growth retardation in a transgenic rat model for preeclampsia. Hypertension (Dallas, Tex. : 1979), 65(6), 1298–1306.

Q

Qi, H. M., Cao, Q., & Liu, Q. (2021). TLR4 regulates vascular smooth muscle cell proliferation in hypertension via modulation of the NLRP3 inflammasome. American journal of translational research, 13(1), 314–325.

R

Ramseyer, V. D., & Garvin, J. L. (2013). Tumor necrosis factor-α: regulation of renal function and blood pressure. *American journal of physiology. Renal physiology*, *304*(10), F1231–F1242.

Rastogi, S., Rizwani, W., Joshi, B., Kunigal, S., & Chellappan, S. P. (2012). TNF-α response of vascular endothelial and vascular smooth muscle cells involve differential utilization of ASK1 kinase and p73. *Cell death and differentiation*, *19*(2), 274–283.

Ribot, J. C., Lopes, N., & Silva-Santos, B. (2021). γδ T cells in tissue physiology and surveillance. *Nature reviews. Immunology*, *21*(4), 221–232.

Rodriguez-Iturbe, B., Pons, H., & Johnson, R. J. (2017). Role of the Immune System in Hypertension. Physiological reviews, 97(3), 1127–1164.

Romero, C. A., Orias, M., & Weir, M. R. (2015). Novel RAAS agonists and antagonists: clinical applications and controversies. Nature reviews. Endocrinology, 11(4), 242–252.

Rump, L. C., Bohmann, C., Schaible, U., Schultze-Seemann, W., & Schollmeyer, P. J. (1995). Beta-adrenergic, angiotensin II, and bradykinin receptors enhance neurotransmission in human kidney. Hypertension (Dallas, Tex. : 1979), 26(3), 445–451.

S

Sallusto, F., Geginat, J., & Lanzavecchia, A. (2004). Central memory and effector memory T cell subsets: function, generation, and maintenance. *Annual review of immunology*, *22*, 745–763.

Sanders V. M. (2012). The beta2-adrenergic receptor on T and B lymphocytes: do we understand it yet?. Brain, behavior, and immunity, 26(2), 195–200.

Sarafidis, P. A., Georgianos, P., & Bakris, G. L. (2013). Resistant hypertension--its identification and epidemiology. Nature reviews. Nephrology, 9(1), 51–58.

Savoia, C., D'Agostino, M., Lauri, F., & Volpe, M. (2011). Angiotensin type 2 receptor in hypertensive cardiovascular disease. Current opinion in nephrology and hypertension, 20(2), 125–132.

Schweda F. (2015). Salt feedback on the renin-angiotensin-aldosterone system. Pflugers Archiv : European journal of physiology, 467(3), 565–576.

Seder, R. A., & Ahmed, R. (2003). Similarities and differences in CD4+ and CD8+ effector and memory T cell generation. *Nature immunology*, *4*(9), 835–842.

Shao, J., Nangaku, M., Miyata, T., Inagi, R., Yamada, K., Kurokawa, K., & Fujita, T. (2003). Imbalance of T-cell subsets in angiotensin II-infused hypertensive rats with kidney injury. Hypertension (Dallas, Tex. : 1979), 42(1), 31–38.

Silva-Filho, J. L., Souza, M. C., Ferreira-Dasilva, C. T., Silva, L. S., Costa, M. F., Padua, T. A., Henriques, M.d, Morrot, A., Savino, W., Caruso-Neves, C., & Pinheiro, A. A. (2013). Angiotensin II is a new component involved in splenic T lymphocyte responses during Plasmodium berghei ANKA infection. *PloS one*, *8*(4), e62999.

Silva-Filho, J. L., Souza, M. C., Henriques, M.d, Morrot, A., Savino, W., Nunes, M. P., Caruso-Neves, C., & Pinheiro, A. A. (2011). AT1 receptor-mediated angiotensin II activation and chemotaxis of T lymphocytes. *Molecular immunology*, *48*(15-16), 1835–1843.

Silva-Filho, J., Caruso-Neves, C. & Pinheiro, A. (2016). Angiotensin II type-1 receptor (AT_1R) regulates expansion, differentiation, and functional capacity of antigen-specific $CD8^+$ T cells. *Sci Rep* **6**, 35997

Singh, M. V., Chapleau, M. W., Harwani, S. C., & Abboud, F. M. (2014). The immune system and hypertension. Immunologic research, 59(1-3), 243–253.

Smallwood, M. J., Ble, A., Melzer, D., Winyard, P. G., Benjamin, N., Shore, A. C., & Gilchrist, M. (2017). Relationship Between Urinary Nitrate Excretion and Blood Pressure in the InChianti Cohort. *American journal of hypertension*, *30*(7), 707–712.

Sparks, M. A., Crowley, S. D., Gurley, S. B., Mirotsou, M., & Coffman, T. M. (2014). Classical Renin-Angiotensin system in kidney physiology. Comprehensive Physiology, 4(3), 1201–1228

Sprague, A. H., & Khalil, R. A. (2009). Inflammatory cytokines in vascular dysfunction and vascular disease. *Biochemical pharmacology*, *78*(6), 539–552.

Sprague, A. H., & Khalil, R. A. (2009). Inflammatory cytokines in vascular dysfunction and vascular disease. *Biochemical pharmacology*, *78*(6), 539–552.

Sriramula, S., Haque, M., Majid, D. S., & Francis, J. (2008). Involvement of tumor necrosis factor-alpha in angiotensin II-mediated effects on salt appetite, hypertension, and cardiac hypertrophy. Hypertension (Dallas, Tex. : 1979), 51(5), 1345–1351.

Stegbauer, J., Lee, D. H., Seubert, S., Ellrichmann, G., Manzel, A., Kvakan, H., Muller, D. N., Gaupp, S., Rump, L. C., Gold, R., & Linker, R. A. (2009). Role of the renin-angiotensin system in autoimmune inflammation of the central nervous system. Proceedings of the National Academy of Sciences of the United States of America, 106(35), 14942–14947.

Stegbauer, J., Vonend, O., Habbel, S., Quack, I., Sellin, L., Gross, V., & Rump, L. C. (2005). Angiotensin II modulates renal sympathetic neurotransmission through nitric oxide in AT2 receptor knockout mice. Journal of hypertension, 23(9), 1691–1698

Stephens, R., & Langhorne, J. (2010). Effector memory Th1 CD4 T cells are maintained in a mouse model of chronic malaria. *PLoS pathogens*, *6*(11), e1001208.

T

Tipton, A. J., Baban, B., & Sullivan, J. C. (2012). Female spontaneously hypertensive rats have greater renal anti-inflammatory T lymphocyte infiltration than males. *American journal of physiology. Regulatory, integrative and comparative physiology*, *303*(4), R359–R367.

Trott, D. W., Thabet, S. R., Kirabo, A., Saleh, M. A., Itani, H., Norlander, A. E., Wu, J., Goldstein, A., Arendshorst, W. J., Madhur, M. S., Chen, W., Li, C. I., Shyr, Y., & Harrison, D. G. (2014). Oligoclonal CD8+ T cells play a critical role in the development of hypertension. Hypertension (Dallas, Tex. : 1979), 64(5), 1108–1115.

V

Van Beusecum, J., & Inscho, E. W. (2015). Regulation of renal function and blood pressure control by P2 purinoceptors in the kidney. Current opinion in pharmacology, 21, 82–88.

W

Wadei, H. M., & Textor, S. C. (2012). The role of the kidney in regulating arterial blood pressure. Nature reviews. Nephrology, 8(10), 602–609.

Wirth, T., Westendorf, A. M., Bloemker, D., Wildmann, J., Engler, H., Mollerus, S., Wadwa, M., Schäfer, M. K., Schedlowski, M., & del Rey, A. (2014). The sympathetic nervous system modulates CD4(+)Foxp3(+) regulatory T cells via noradrenaline-dependent apoptosis in a murine model of lymphoproliferative disease. Brain, behavior, and immunity, 38, 100–110.

Yamauchi, K., Takano, Y., Kasai, A., Hayakawa, K., Hiramatsu, N., Enomoto, N., Yao, J., & Kitamura, M. (2006). Screening and identification of substances that regulate nephrin gene expression using engineered reporter podocytes. *Kidney international*, *70*(5), 892–900.

Z

Zaika, O., Mamenko, M., Staruschenko, A., & Pochynyuk, O. (2013). Direct activation of ENaC by angiotensin II: recent advances and new insights. *Current hypertension reports*, *15*(1), 17–24.

Zhang, H., Park, Y., Wu, J., Chen, X.p, Lee, S., Yang, J., Dellsperger, K. C., & Zhang, C. (2009). Role of TNF-alpha in vascular dysfunction. *Clinical science (London, England : 1979)*, *116*(3), 219–230.

Zhang, J. D., Patel, M. B., Griffiths, R., Dolber, P. C., Ruiz, P., Sparks, M. A., Stegbauer, J., Jin, H., Gomez, J. A., Buckley, A. F., Lefler, W. S., Chen, D., & Crowley, S. D. (2014). Type 1 angiotensin receptors on macrophages ameliorate IL-1 receptor-mediated kidney fibrosis. The Journal of clinical investigation, 124(5), 2198–2203.

Zhang, J., & Crowley, S. D. (2015). Role of T lymphocytes in hypertension. Current opinion in pharmacology, 21, 14–19.

Zhang, J., Patel, M. B., Griffiths, R., Mao, A., Song, Y. S., Karlovich, N. S., Sparks, M. A., Jin, H., Wu, M., Lin, E. E., & Crowley, S. D. (2014). Tumor necrosis factor-α produced in the kidney contributes to angiotensin II-dependent hypertension. Hypertension (Dallas, Tex. : 1979), 64(6), 1275–1281.

Zhang, Y., Peng, W., Ao, X., Dai, H., Yuan, L., Huang, X., & Zhou, Q. (2015). TAK-242, a Toll-Like Receptor 4 Antagonist, Protects against Aldosterone-Induced Cardiac and Renal Injury. PloS one, 10(11), e0142456.

Zhou, L., Lopes, J. E., Chong, M. M., Ivanov, I. I., Min, R., Victora, G. D., Shen, Y., Du, J., Rubtsov, Y. P., Rudensky, A. Y., Ziegler, S. F., & Littman, D. R. (2008). TGF-beta-induced Foxp3 inhibits T(H)17 cell differentiation by antagonizing RORgammat function. Nature, 453(7192), 236–240.

Zhu, J., & Paul, W. E. (2008). CD4 T cells: fates, functions, and faults. Blood, 112(5), 1557–1569.

8 Acknowledgment

First and foremost, I would like to show my full gratitude and appreciation to Professor Dr Johannes Stegbauer, who has been always supportive through all the steps of my doctoral research. I have learned a lot from him. Despite his huge responsibilities, he was never bothered by me asking for advice at any time. He encouraged me to learn many techniques, attend conferences and courses. Without his support nothing would be possible.

My profound gratitude goes to Ms Christina Schwandt, Ms Blanka Duvnjak, and Ms Nicola Kuhr for their outstanding technical support. I am extremely thankful to all my colleagues in my laboratory, especially, Dr Mina Yakoub, Dr Lydia Hering and Dr Sacha Höges. I had a great time working with them.

Finally, I would like to thank my mentor Professor Eckhard Lammert and Prof Dr Lars Christian Rump for their counseling.